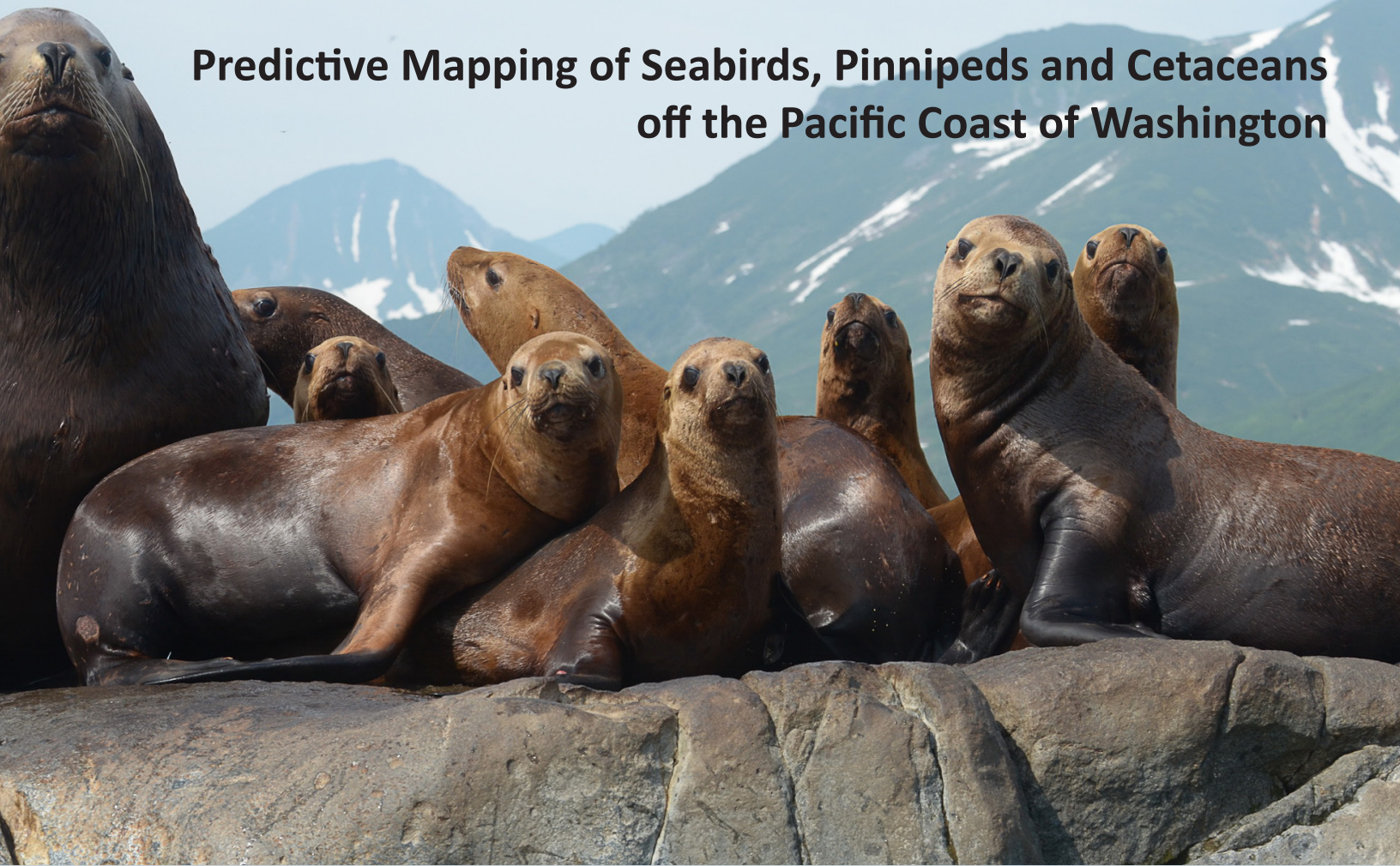
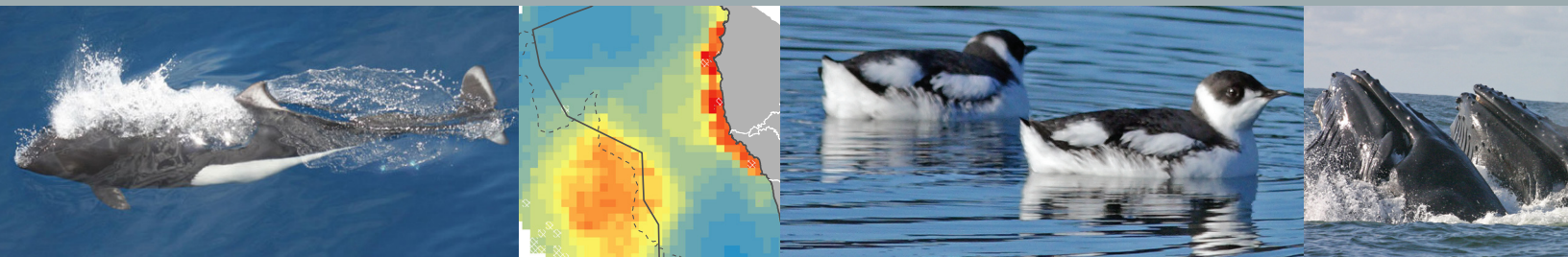


Predictive Mapping of Seabirds, Pinnipeds and Cetaceans off the Pacific Coast of Washington



A collaborative investigation by
NOAA's National Ocean Service and National Marine Fisheries Service
U.S. Geological Survey
Bureau of Ocean Energy Management
Washington State Department of Fish and Wildlife
Cascadia Research Collective



March 2016

NOAA TECHNICAL MEMORANDUM NOS NCCOS 210

NOAA NCCOS Center for Coastal Monitoring and Assessment



Citation for Report

Menza, C., J. Leirness, T. White, A. Winship, B. Kinlan, L. Kracker, J. E. Zamon, L. Ballance, E. Becker, K. A. Forney, J. Barlow, J. Adams, D. Pereksta, S. Pearson, J. Pierce, S. Jeffries, J. Calambokidis, A. Douglas, B. Hanson, S. R. Benson and L. Antrim. 2016. Predictive Mapping of Seabirds, Pinnipeds and Cetaceans off the Pacific Coast of Washington. NOAA Technical Memorandum NOS NCCOS 210. Silver Spring, MD. 96 pp.

Acknowledgements

We are thankful to the scientists, seabird and marine mammal observers, ship crews, and coastal managers who contributed data and advice. In particular, we thank Jeff Laake for contributing the Harbor Porpoise survey data, Rob Suryan and Jarrod Santora for providing the frequency of chlorophyll peaks index predictor data, and Nancy Wright for contributing sanctuary seabird and mammal observations. We are also thankful to Bill Peterson for providing valuable advice on climate indices, Jonathan Scordino and Kevin McMahon for reviewing this report, Sarah Hile for producing this document, and Katrina Lassiter and Jennifer Hennessey who provided valuable guidance on Washington State's marine spatial plan, facilitated contact with state natural resources agencies and reviewed early versions of spatial models.

This research was funded by a contract with the state of Washington Department of Natural Resources (MOA-2013-038(Annex 002)/8963) and a discretionary grant from the National Centers for Coastal Ocean Science. CSS-Dynamac employees were supported under NOAA Contract No. EA133C-14-NC-1384 with CSS-Dynamac.

The covers for this document were designed and created by Gini Kennedy (NOAA); document design and layout completed by Sarah D. Hile. Front cover photos were provided by Vladimir Burkanov (Steller sea lion, NOAA NMF/AFSC/NMML), NOAA NMFS/SWFSC/PRD (Dall's porpoise), David Pereksta (Marbled Murrelet, BOEM) and Cornelia Odekoven (humpback whales, NOAA NOS/ONMS/OCNMS). Back cover photos were provided by David Pereksta (Tufted Puffin juvenile, BOEM), Vladimir Burkanov (Steller sea lion, WDFW), Paul Blake (gray whale, NOAA NOS/ONMS/OCNMS) and David Pereksta (Pink-footed Shearwater, BOEM).

Mention of trade names or commercial products does not constitute endorsement or recommendation for their use by the United States government.

Predictive Mapping of Seabirds, Pinnipeds and Cetaceans off the Pacific Coast of Washington

Authors

Charles Menza¹, Jeffery Leirness^{1,2}, Tim White^{1,2}, Arliss Winship^{1,2}, Brian Kinlan¹, Laura Kracker¹, Jeannette E. Zamon³, Lisa Ballance⁴, Elizabeth Becker⁴, Karin A. Forney⁴, Jay Barlow⁴, Josh Adams⁵, David Pereksta⁶, Scott Pearson⁷, John Pierce⁷, Steven Jeffries⁷, John Calambokidis⁸, Annie Douglas⁸, Brad Hanson⁹, Scott R. Benson¹⁰ and Liam Antrim¹¹

March 2016

Address for Correspondence

NOAA National Centers for Coastal Ocean Science (NCCOS)
1305 East West Highway, SSMC4, N/SCI-1
Silver Spring, MD 20910

Contributor Affiliations

- ¹ National Centers for Coastal Ocean Science, NOAA/NOS
- ² CSS-Dynamac
- ³ Point Adams Research Station, NOAA/NMFS/NWFSC
- ⁴ Marine Mammal and Turtle Division, NOAA/NMFS/SWFSC
- ⁵ Western Ecological Research Center, Santa Cruz Field Station, USGS
- ⁶ Pacific OCS Region, Bureau of Ocean Energy Management
- ⁷ Wildlife Science Division, Washington Department of Fish and Wildlife
- ⁸ Cascadia Research Collective
- ⁹ Marine Mammal and Seabird Ecology Program, NOAA/NMFS/NWFSC
- ¹⁰ Marine Turtle Ecology and Assessment Program, NOAA/NMFS/SWFSC
- ¹¹ Olympic Coast National Marine Sanctuary, NOAA/NOS



NOAA Technical Memorandum NOS NCCOS 210

United States Department
of Commerce

National Oceanic and
Atmospheric Administration

National
Ocean Service

Penny Pritzker
Secretary

Kathryn Sullivan
Administrator

Russell Callender
Assistant Administrator

About This Report

This report supports Washington-led marine spatial planning and responsible stewardship of natural and cultural resources by the Olympic Coast National Marine Sanctuary. Washington state agencies and the sanctuary continually seek the best available science to improve management of marine uses and stewardship of resources (Etheridge et al., 2010; Washington Department of Fish and Wildlife, 2015a). This report and associated data provide new, state- and sanctuary-requested information on seabird, pinniped, and cetacean distributions. Through spatial planning, information on species distributions can help to identify high-value conservation areas, minimize adverse effects of ocean uses and mitigate impacts of coastal hazards. Correspondingly, the Washington Department of Fish and Wildlife has already begun to use the maps of predicted relative density presented in this report to identify ecologically important areas off the Pacific Coast of Washington and apply this information to plan for offshore renewable energy development.

This is the culmination of three years of work to compile information on seabirds, pinnipeds, and cetaceans, and advance a modeling framework that can integrate data sets and develop accurate predictions of relative density for important species off the Pacific Coast of Washington. Previous reports, which evaluated existing datasets of at-sea observations (Menza et al., 2014; Kracker and Menza, 2015) and presented superseded versions of seabird models (Menza et al., 2015), provided base information for this report. In addition to the maps in this published report, all new seabird, pinniped and cetacean predictions will be made publicly available as digital geospatial data through the National Centers for Environmental Information.

This research supports the National Oceanic and Atmospheric Administration (NOAA) Coastal Zone Management Program, a voluntary partnership between the federal government and U.S. coastal and Great Lakes states and territories authorized by the Coastal Zone Management Act (CZMA) of 1972 to address national coastal issues. The act provides the basis for protecting, restoring, and responsibly developing our nation's diverse coastal communities and resources. To meet the goals of the CZMA, the national program takes a comprehensive approach to coastal resource management – balancing the often competing and occasionally conflicting demands of coastal resource use, economic development, and conservation. A wide range of issues are addressed through the program, including coastal development, water quality, public access, habitat protection, energy facility siting, ocean governance and planning, coastal hazards, and climate change. Accurate maps of seabird and marine mammal distributions are an important tool for making informed management decisions that affect all of these issues.

The National Centers for Coastal Ocean Science (NCCOS) provides coastal managers the information and tools they need to balance society's environmental, social, and economic goals. NCCOS is the primary coastal science arm within NOAA's National Ocean Service. NCCOS works directly with managers, industry, regulators, and scientists to deliver relevant, timely, and accurate scientific information and tools.

For more information contact:

Charles Menza
National Centers for Coastal Ocean Science
Center for Coastal Monitoring and Assessment
240-533-0372
charles.menza@noaa.gov

Jeffery Leirness
National Centers for Coastal Ocean Science
Center for Coastal Monitoring and Assessment
jeffery.leirness@noaa.gov

Table of Contents

Executive Summary	i
Background	1
Methods	3
Species of interest	3
Study area	5
Species sightings data	5
Predictive modeling framework	10
Predictor variables	10
Predictive modeling process	14
<i>Likelihoods and model components</i>	14
<i>Base-learners</i>	14
<i>Effort offset</i>	15
<i>Stochastic gradient boosting</i>	15
<i>Boosting “offsets”</i>	15
<i>Tuning of shrinkage rate and number of boosting iterations</i>	15
<i>Model performance and selection</i>	16
<i>Bootstrapping</i>	16
<i>Spatial prediction</i>	17
<i>Implementation</i>	17
<i>Review</i>	17
Predictive modeling products	17
<i>Maps</i>	17
<i>Variable importance</i>	18
Results and Discussion	19
Distribution of survey effort	19
Predicted spatial distributions	22
Predictive model performance	58
Uses of models and maps	60
Information gaps	61
Next steps	61
References	63
Appendices	68

List of Table and Figures

Table 1.	List of seabird, pinniped and cetacean species chosen for modeling, conservation status, and frequency of sightings.	3
Table 2.	Distribution of survey effort from each survey program used to model species distributions in the summer (April to October) and winter (November to March) seasons	6
Table 3.	Segment strip widths and estimated effective strip widths in meters by platform type.	9
Table 4.	Predictor variables used in the models.	11
Table 5.	Pairwise Spearman’s rank correlation coefficients (ρ) for spatial predictor variables used in seabird models for the months of April to October and November to March	13
Table 6.	Pairwise Spearman’s rank correlation coefficients (ρ) for spatial predictor variables used in pinniped and cetacean models for the months of April to October.	13
Table 7.	Base-learners employed in the boosted generalized additive modeling framework	14
Table 8.	Model performance metrics and corresponding quality levels.	16
Table 9.	Performance metrics for the final selected model of each species-season combination.	59
Figure 1.	Map of the study area (red line) used to model seabird, pinniped and cetacean distributions	4
Figure 2.	Spatial distribution of survey programs used to model species distributions	7
Figure 3.	Schematic of the segmentation process used to partition animal observations along transects.	8
Figure 4.	Distribution of survey effort by month and year in the data set used to model seabird, pinniped and cetacean distributions	20
Figure 5.	Spatial distribution of survey effort (sq. km) for summer (April to October) seabird (a), winter (November to March) seabird (b), and summer pinniped (c) and cetacean (d) models within the study area	21
Figure 6.	Long-term relative density (individuals per sq. km) prediction map for Marbled Murrelet (<i>Brachyramphus marmoratus</i>).	24
Figure 7.	Long-term relative density (individuals per sq. km) prediction maps for Marbled Murrelet (<i>Brachyramphus marmoratus</i>) during the months of April to October: a) 50% quantile of bootstrap (median), b) coefficient of variation, c) 5% quantile of bootstrap, d) 95% quantile of bootstrap	25
Figure 8.	Long-term relative density (individuals per sq. km) prediction map for Rhinoceros Auklet (<i>Cerorhinca monocerata</i>) during the months of April to October	26
Figure 9.	Long-term relative density (individuals per sq. km) prediction maps for Rhinoceros Auklet (<i>Cerorhinca monocerata</i>) during the months of April to October: a) 50% quantile of bootstrap (median), b) coefficient of variation, c) 5% quantile of bootstrap, d) 95% quantile of bootstrap	27
Figure 10.	Long-term relative density (individuals per sq. km) prediction map for Rhinoceros Auklet (<i>Cerorhinca monocerata</i>) during the months of November to March	28
Figure 11.	Long-term relative density (individuals per sq. km) prediction maps for Rhinoceros Auklet (<i>Cerorhinca monocerata</i>) during the months of November to March: a) 50% quantile of bootstrap (median), b) coefficient of variation, c) 5% quantile of bootstrap, d) 95% quantile of bootstrap	29
Figure 12.	Long-term relative density (individuals per sq. km) prediction map for Tufted Puffin (<i>Fratercula cirrhata</i>) during the months of April to October	30
Figure 13.	Long-term relative density (individuals per sq. km) prediction maps for Tufted Puffin (<i>Fratercula cirrhata</i>) during the months of April to October: a) 50% quantile of bootstrap (median), b) coefficient of variation, c) 5% quantile of bootstrap, d) 95% quantile of bootstrap	31
Figure 14.	Long-term relative density (individuals per sq. km) prediction map for Common Murre (<i>Uria aalge</i>) during the months of April to October	32
Figure 15.	Long-term relative density (individuals per sq. km) prediction maps for Common Murre (<i>Uria aalge</i>) during the months of April to October: a) 50% quantile of bootstrap (median), b) coefficient of variation, c) 5% quantile of bootstrap, d) 95% quantile of bootstrap	33

Figure 16.	Long-term relative density (individuals per sq. km) prediction map for Common Murre (<i>Uria aalge</i>) during the months of November to March	34
Figure 17.	Long-term relative density (individuals per sq. km) prediction maps for Common Murre (<i>Uria aalge</i>) during the months of November to March: a) 50% quantile of bootstrap (median), b) coefficient of variation, c) 5% quantile of bootstrap, d) 95% quantile of bootstrap	35
Figure 18.	Long-term relative density (individuals per sq. km) prediction map for Black-footed Albatross (<i>Phoebastria nigripes</i>) during the months of April to October	36
Figure 19.	Long-term relative density (individuals per sq. km) prediction maps for Black-footed Albatross (<i>Phoebastria nigripes</i>) during the months of April to October: a) 50% quantile of bootstrap (median), b) coefficient of variation, c) 5% quantile of bootstrap, d) 95% quantile of bootstrap	37
Figure 20.	Long-term relative density (individuals per sq. km) prediction map for Black-footed Albatross (<i>Phoebastria nigripes</i>) during the months of November to March	38
Figure 21.	Long-term relative density (individuals per sq. km) prediction maps for Black-footed Albatross (<i>Phoebastria nigripes</i>) during the months of November to March: a) 50% quantile of bootstrap (median), b) coefficient of variation, c) 5% quantile of bootstrap, d) 95% quantile of bootstrap	39
Figure 22.	Long-term relative density (individuals per sq. km) prediction map for Northern Fulmar (<i>Fulmarus glacialis</i>) during the months of April to October	40
Figure 23.	Long-term relative density (individuals per sq. km) prediction maps for Northern Fulmar (<i>Fulmarus glacialis</i>) during the months of April to October: a) 50% quantile of bootstrap (median), b) coefficient of variation, c) 5% quantile of bootstrap, d) 95% quantile of bootstrap	41
Figure 24.	Long-term relative density (individuals per sq. km) prediction map for Pink-footed Shearwater (<i>Puffinus creatopus</i>) during the months of April to October	42
Figure 25.	Long-term relative density (individuals per sq. km) prediction maps for Pink-footed Shearwater (<i>Puffinus creatopus</i>) during the months of April to October: a) 50% quantile of bootstrap (median), b) coefficient of variation, c) 5% quantile of bootstrap, d) 95% quantile of bootstrap	43
Figure 26.	Long-term relative density (individuals per sq. km) prediction map for Sooty Shearwater (<i>Puffinus griseus</i>) during the months of April to October	44
Figure 27.	Long-term relative density (individuals per sq. km) prediction maps for Sooty Shearwater (<i>Puffinus griseus</i>) during the months of April to October: a) 50% quantile of bootstrap (median), b) coefficient of variation, c) 5% quantile of bootstrap, d) 95% quantile of bootstrap	45
Figure 28.	Long-term relative density (individuals per sq. km) prediction map for Steller sea lion (<i>Eumetopias jubatus</i>) during the months of April to October	46
Figure 29.	Long-term relative density (individuals per sq. km) prediction maps for Steller sea lion (<i>Eumetopias jubatus</i>) during the months of April to October: a) 50% quantile of bootstrap (median), b) coefficient of variation, c) 5% quantile of bootstrap, d) 95% quantile of bootstrap	47
Figure 30.	Long-term relative density (individuals per sq. km) prediction map for harbor seal (<i>Phoca vitulina</i>) during the months of April to October	48
Figure 31.	Long-term relative density (individuals per sq. km) prediction maps for harbor seal (<i>Phoca vitulina</i>) during the months of April to October: a) 50% quantile of bootstrap (median), b) coefficient of variation, c) 5% quantile of bootstrap, d) 95% quantile of bootstrap	49
Figure 32.	Long-term relative density (individuals per sq. km) prediction map for humpback whale (<i>Megaptera novaeangliae</i>) during the months of April to October	50
Figure 33.	Long-term relative density (individuals per sq. km) prediction maps for humpback whale (<i>Megaptera novaeangliae</i>) during the months of April to October: a) 50% quantile of bootstrap (median), b) coefficient of variation, c) 5% quantile of bootstrap, d) 95% quantile of bootstrap	51
Figure 34.	Long-term relative density (individuals per sq. km) prediction map for gray whale (<i>Eschrichtius robustus</i>) during the months of April to October	52
Figure 35.	Long-term relative density (individuals per sq. km) prediction maps for gray whale (<i>Eschrichtius robustus</i>) during the months of April to October: a) 50% quantile of bootstrap (median), b) coefficient of variation, c) 5% quantile of bootstrap, d) 95% quantile of bootstrap	53

Figure 36.	Long-term relative density (individuals per sq. km) prediction map for harbor porpoise (<i>Phocoena phocoena</i>) during the months of April to October	54
Figure 37.	Long-term relative density (individuals per sq. km) prediction maps for harbor porpoise (<i>Phocoena phocoena</i>) during the months of April to October: a) 50% quantile of bootstrap (median), b) coefficient of variation, c) 5% quantile of bootstrap, d) 95% quantile of bootstrap	55
Figure 38.	Long-term relative density (individuals per sq. km) prediction map for Dall's porpoise (<i>Phocoenoides dalli</i>) during the months of April to October	56
Figure 39.	Long-term relative density (individuals per sq. km) prediction maps for Dall's porpoise (<i>Phocoenoides dalli</i>) during the months of April to October: a) 50% quantile of bootstrap (median), b) coefficient of variation, c) 5% quantile of bootstrap, d) 95% quantile of bootstrap	57
Figure D1.	Marginal and residual plots for Marbled Murrelet (<i>Brachyramphus marmoratus</i>) during the months of April to October.	75
Figure D2.	Marginal and residual plots for Rhinoceros Auklet (<i>Cerorhinca monocerata</i>) during the months of April to October.	76
Figure D3.	Marginal and residual plots for Rhinoceros Auklet (<i>Cerorhinca monocerata</i>) during the months of November to March.	77
Figure D4.	Marginal and residual plots for Tufted Puffin (<i>Fratercula cirrhata</i>) during the months of April to October.	78
Figure D5.	Marginal and residual plots for Common Murre (<i>Uria aalge</i>) during the months of April to October.	79
Figure D6.	Marginal and residual plots for Common Murre (<i>Uria aalge</i>) during the months of November to March.	80
Figure D7.	Marginal and residual plots for Black-footed Albatross (<i>Phoebastria nigripes</i>) during the months of April to October.	81
Figure D8.	Marginal and residual plots for Black-footed Albatross (<i>Phoebastria nigripes</i>) during the months of November to March.	82
Figure D9.	Marginal and residual plots for Northern Fulmar (<i>Fulmarus glacialis</i>) during the months of April to October.	83
Figure D10.	Marginal and residual plots for Pink-footed Shearwater (<i>Puffinus creatopus</i>) during the months of April to October.	84
Figure D11.	Marginal and residual plots for Sooty Shearwater (<i>Puffinus griseus</i>) during the months of April to October.	85
Figure D12.	Marginal and residual plots for Steller sea lion (<i>Eumetopias jubatus</i>) during the months of April to October.	86
Figure D13.	Marginal and residual plots for harbor seal (<i>Phoca vitulina</i>) during the months of April to October	87
Figure D14.	Marginal and residual plots for humpback whale (<i>Megaptera novaeangliae</i>) during the months of April to October.	88
Figure D15.	Marginal and residual plots for gray whale (<i>Eschrichtius robustus</i>) during the months of April to October.	89
Figure D16.	Marginal and residual plots for harbor porpoise (<i>Phocoena phocoena</i>) during the months of April to October.	90
Figure D17.	Marginal and residual plots for Dall's porpoise (<i>Phocoenoides dalli</i>) during the months of April to October.	91
Figure E1.	Mean relative importance of predictor variables for seabird species in the months of April to October and November to March, calculated by averaging across species within the zero-inflation (p) and count (μ) components of the selected models.	92
Figure E2.	Mean relative importance of predictor variables for pinniped species in the months of April to October, calculated by averaging across species within the zero-inflation (p) and count (μ) components of the selected models.	92
Figure E3.	Mean relative importance of predictor variables for cetacean species in the months of April to October, calculated by averaging across species within the zero-inflation (p) and count (μ) components of the selected models.	93
Figure E4.	Relative importance of predictor variables for the selected model of each seabird species during the months of April to October	94
Figure E5.	Relative importance of predictor variables for the selected model of each seabird species during the months of November to March	95
Figure E6.	Relative importance of predictor variables for the selected model of each pinniped and cetacean species during the months of April to October	96

Executive Summary

This report presents long-term seasonal distribution maps of selected seabird, pinniped and cetacean species off the Pacific coast of Washington. The maps were created to support state-led marine spatial planning and responsible stewardship of natural resources by the Olympic Coast National Marine Sanctuary. They are intended to distinguish persistent areas of high relative density from areas of low relative density, and are useful for identifying ecologically important areas, recognizing and mitigating impacts from human uses and coastal hazards, and improving our understanding of marine environments.

Predicted relative density distribution maps were constructed using associative models linking at-sea species observations with environmental covariates. Associative models relied on species observations compiled from federal, state, and non-governmental monitoring programs with data between 1995 and 2014. Environmental variables, such as depth, sea surface temperature, and indices of primary productivity, were processed from long-term archival satellite, oceanographic, and hydrographic databases.

The compilation of at-sea species observations represents the first attempt to combine eleven selected survey programs, and is a substantial combination of nearshore and offshore survey effort. As far as we are aware, the compilation prepared for this report is the largest synthesis of recent seabird, pinniped, and cetacean observations in the study area, in terms of both number of observations and number of programs combined.

A boosted generalized additive modeling framework was applied to associate seabird and environmental covariate data sets and develop contiguous, accurate predictions of relative density. To improve model performance, the modeling framework allowed for flexible relationships and multi-way interactions between environmental variables while accounting for sampling heterogeneity between and within datasets.

Model performance was assessed using cross validation and a range of model fit and bias diagnostics. All models showed good performance based on model performance diagnostics, and expert reviewers agreed all maps were valuable representations of species distributions. Reviewers included ecologists, coastal resource managers, and modelers from multiple agencies and organizations.

These maps represent an important step towards improving our understanding of the long-term spatial distributions of selected seabirds, pinnipeds, and cetaceans, identifying persistent hotspots of relative densities, and more effectively planning offshore human activities. The seabird, pinniped, and cetacean predictions are already being used by the Washington Department of Fish and Wildlife to identify ecologically important areas off the Pacific Coast of Washington, and they intend to utilize this information in planning for offshore renewable energy development.

The Pacific Northwest depends on a healthy coastal and marine ecosystem to maintain thriving economies and vibrant communities. Marine ecosystems support critical habitats for wildlife and a growing number of ocean activities such as fishing, transportation, aquaculture, recreation, and energy production. Planners, policy makers, and resource managers are being challenged to sustainably balance multiple ocean uses and environmental conservation mandates in a finite space and with limited information. This balancing act is being supported by spatial planning.

Marine spatial planning is a planning process that enables integrated, forward-looking, and consistent decision making on the human uses which occur in the oceans and along coasts (Ehler and Douvère, 2009). It can improve marine resource management by planning for human uses in locations that reduce conflict among different activities, and supports a balance among social, economic, and ecological benefits received from ocean resources.

Forward-looking coastal states such as Washington are investing in and assuming marine spatial planning as an integral part of managing human uses and activities in the marine environment. In March 2010, the Washington state legislature enacted a marine spatial planning law (RCW §43.372) to address resource use conflicts in waters off Washington. In 2011, a report to the legislature and a workshop on human use data provided guidance for the marine spatial planning process. In 2012, the governor amended the existing law to focus funding on mapping and ecosystem assessments for Washington's Pacific coast and the legislature provided \$3.7 million in the 2013-15 fiscal year biennium to begin marine spatial planning off Washington's coast. The funds were appropriated through the Washington Department of Natural Resources Marine Resources Stewardship Account with coordination among the State Ocean Caucus, the four Coastal Treaty Tribes, four coastal Marine Resource Committees and the Washington Coastal Marine Advisory Council. This project was initiated to support Washington's marine spatial plan.



Ruby Beach along Washington's coast. Source: Jane Chavey (WADNR).

Background

NOAA shares responsibility for managing ecological and cultural resources off the Pacific Coast of Washington with the state of Washington, as well as the Hoh, Makah, and Quileute tribes and the Quinault Indian Nation. The Olympic Coast National Marine Sanctuary spans 2,408 square nautical miles (8,259 square kilometers [sq. km]) of marine waters off Washington's Olympic Peninsula coast, and approximately 17% of the sanctuary is located within Washington state waters. The Olympic Coast National Marine Sanctuary is managed using a collaborative framework to coordinate management and stewardship of resources and is driven by ecosystem-based management informed by scientific research, monitoring, and characterization. Key objectives in the sanctuary's management plan (Office of National Marine Sanctuaries, 2011) are to characterize and map the sanctuary's species and habitats, and facilitate wise and sustainable use of sanctuary resources. The sanctuary's management framework, goals and objectives are inherently a marine spatial planning process.

Seabirds, pinnipeds, and cetaceans are conspicuous and ecologically important components of the marine ecosystem off Washington. These taxa are typically long-lived, move over broad spatial ranges, and are consumers of production at most trophic levels (Bowen, 1997; Schreiber and Burger, 2001). As such, they are responsive to changes in the marine and coastal environments, and can be useful integrative indicators of environmental change (Furness and Camphuysen, 1997). Seabirds, pinnipeds and cetaceans are also important to coastal economies and cultures. They provide direct eco-tourism benefits to coastal communities through recreational bird and marine mammal watching opportunities (Hoyt, 2001; U.S. Fish and Wildlife Service, 2013), and they are central to the cultures of coastal peoples.

Many seabird, pinniped, and cetacean populations are under threat from ongoing human activities including coastal development, fishing, shipping, resource extraction, and renewable energy development (Croxall et al., 2012; Carretta et al., 2013; Paleczny et al., 2015). Given changes in population numbers and their economic and ecological importance, all seabirds and marine mammals off Washington are subject to conservation requirements under the Migratory Bird Treaty Act and the Marine Mammal Protection Act, respectively. Some species are also protected under the U.S. Endangered Species Act or are listed in Washington State's list of species of concern (Washington Department of Fish and Wildlife, 2015b).

SPECIES OF INTEREST

There are nearly one hundred different species of marine birds and shorebirds, five species of pinnipeds, and twenty-three species of cetaceans off the Pacific coast of Washington (Office of National Marine Sanctuaries, 2008). This report focuses on developing maps for eight seabird, two pinniped and four cetacean species frequently sighted in the study area (Table 1, Figure 1). Selected seabird species are the Marbled Murrelet (*Brachyramphus marmoratus*), Rhinoceros Auklet (*Cerorhinca monocerata*), Tufted Puffin (*Fratercula cirrhata*), Common Murre (*Uria aalge*), Black-footed Albatross (*Phoebastria nigripes*), Northern Fulmar (*Fulmarus glacialis*), Pink-footed Shearwater (*Puffinus creatopus*) and Sooty Shearwater (*Puffinus griseus*). Selected pinniped species are the Steller sea lion (*Eumetopias jubatus*) and harbor seal (*Phoca vitulina*), and selected cetacean species are the humpback whale (*Megaptera novaeangliae*), gray whale (*Eschrichtius robustus*), harbor porpoise (*Phocoena phocoena*) and Dall's porpoise (*Phocoenoides dalli*).



Top row (L-R): Common Murre (David Pereksta, BOEM) and harbor seal (Dave Withrow, NOAA NMFS/AFSC/NMML); bottom row (L-R): gray whale (Merrill Goshu, NOAA NMFS/AFSC/NMML) and harbor porpoise (NOAA NMFS/NEFSC).

The selected species were chosen by the Washington Department of Ecology and the Washington Department of Fish and Wildlife because they are either species of management concern or representative of specific ecological roles in the nearshore or offshore environments. The state also requested models for Short-tailed Albatross (*Phoebastria albatrus*), sei whale (*Balaenoptera borealis*), blue whale (*Balaenoptera musculus*), fin whale (*Balaenoptera physalus*), southern resident killer whale (*Orcinus orca*) and sperm whale (*Physeter macrocephalus*), but there were insufficient sightings of these species to be useful for modeling.

Table 1. List of seabird, pinniped and cetacean species chosen for modeling, conservation status, and frequency of sightings. Status is defined as: federally endangered (FE), federally threatened (FT), state endangered (SE), state threatened (ST), state sensitive (SS) and state species of special concern (SC). Definition of state status was taken from the species of concern list developed by the Washington Department of Fish and Wildlife (2013, 2015b). Segments represent standardized spatial analysis units, which are discussed more fully in the Species sightings data section.

Common name	Scientific name	Taxonomic group	Conservation status	Number of segments with sightings		
				Total	Summer	Winter
Marbled Murrelet	<i>Brachyramphus marmoratus</i>	Seabird	ST, FT	1,632	1,625	7
Rhinoceros Auklet	<i>Cerorhinca monocerata</i>	Seabird		4,830	4,593	237
Tufted Puffin	<i>Fratercula cirrhata</i>	Seabird	SE	1,744	1,738	6
Common Murre	<i>Uria aalge</i>	Seabird	SC	6,938	6,533	405
Black-footed Albatross	<i>Phoebastria nigripes</i>	Seabird		508	421	87
Northern Fulmar	<i>Fulmarus glacialis</i>	Seabird		475	463	12
Pink-footed Shearwater	<i>Puffinus creatopus</i>	Seabird		611	611	0
Sooty Shearwater	<i>Puffinus griseus</i>	Seabird		2,611	2,586	25
Steller sea lion	<i>Eumetopias jubatus</i>	Pinniped		221	221	0
harbor seal	<i>Phoca vitulina</i>	Pinniped		566	563	3
humpback whale	<i>Megaptera novaeangliae</i>	Cetacean	SE, FE	442	430	12
gray whale	<i>Eschrichtius robustus</i>	Cetacean	SS	147	118	29
harbor porpoise	<i>Phocoena phocoena</i>	Cetacean	SC	1,698	1,673	25
Dall's porpoise	<i>Phocoenoides dalli</i>	Cetacean		252	237	15

Methods

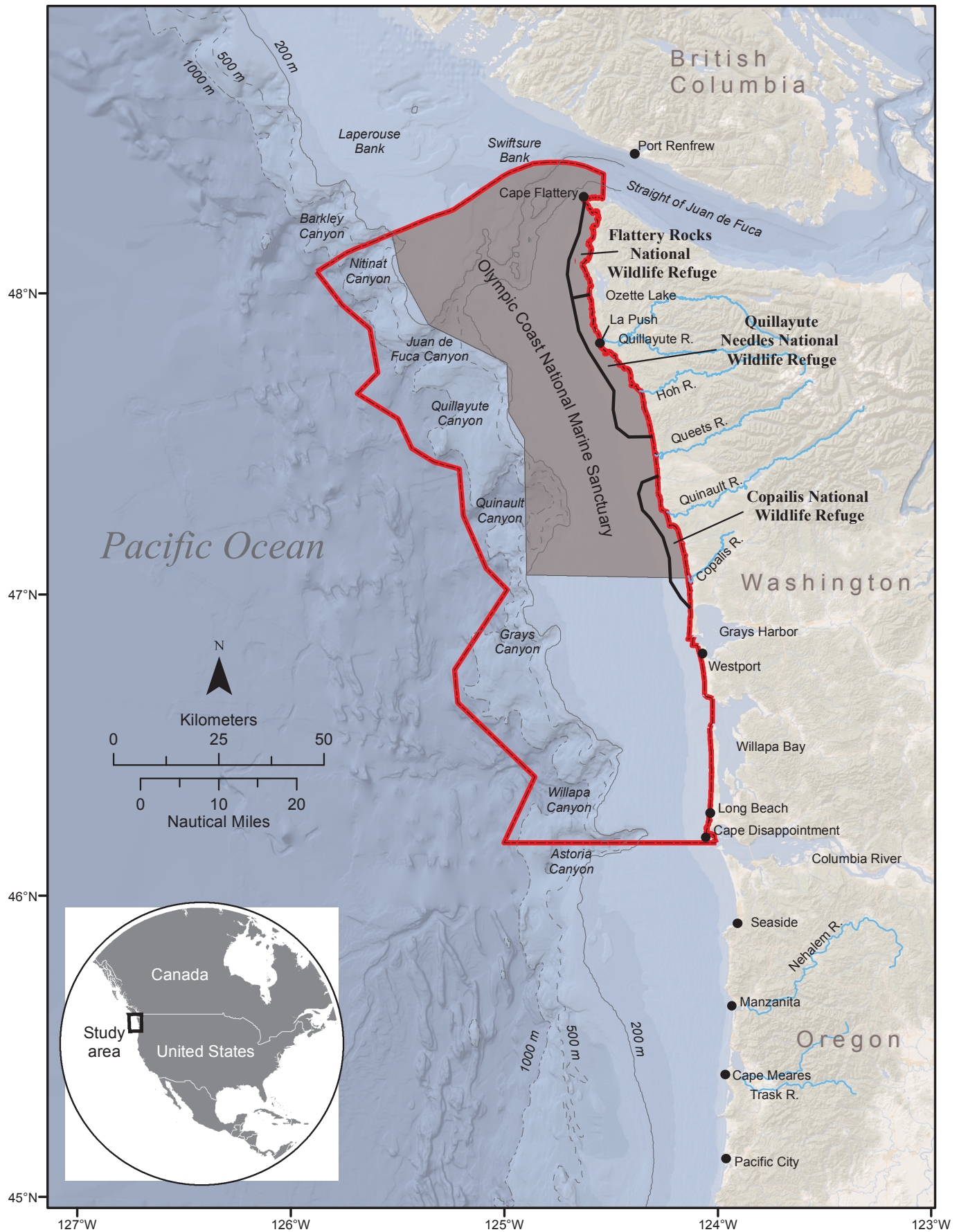


Figure 1. Map of the study area (red line) used to model seabird, pinniped and cetacean distributions. The Olympic Coast National Marine Sanctuary is designated by gray shading. This map serves to reference named places identified in this report.

Some of the selected species have state or federal protections or are listed as species of management concern. The Marbled Murrelet, Tufted Puffin and humpback whale are listed as endangered or threatened by the U.S. and/or state of Washington, and the Common Murre, gray whale, and harbor porpoise are listed as species of special concern or sensitive by the state of Washington (U.S. Fish and Wildlife Service, 2005; Washington Department of Fish and Wildlife, 2015b). To protect these and other sensitive marine populations, ongoing monitoring, mapping, and research is conducted by the state of Washington, the Bureau of Ocean Energy Management, the U.S. Geological Survey, the U.S. Fish and Wildlife Service, the National Oceanic and Atmospheric Administration (NOAA) National Marine Fisheries Service, NOAA Office of National Marine Sanctuaries, Cascadia Research Collective, Orca Network and others.



Humpback whales (Cornelia Odekoven, NOAA NOS/ONMS/OCNMS).

STUDY AREA

This study focuses on the nearshore and offshore waters of the Pacific Coast of Washington. The geographic scope extends north to south from Cape Flattery to Cape Disappointment, and east to west from the Pacific coast of Washington to approximately the 700 fathom (~1300 m) depth contour (Figure 1). The 700 fathom depth contour limit was proposed by the Washington Department of Fish and Wildlife to delimit the marine area with the most human activity (Washington Department of Ecology, 2014). The study area includes the entire Olympic Coast National Marine Sanctuary; Flattery Rocks, Quillayute Needles and Copalis National Wildlife Refuges; and the usual and accustomed fishing grounds of Hoh, Quinault, Quileute and Makah tribes. It does not extend into rivers, bays, or estuaries, such as Willapa Bay and Grays Harbor.

The study area provides important seabird and marine mammal migration routes, foraging areas and connections to nearby breeding colonies, nesting habitats and haul-out sites. More information about the communities and special places in the study area can be found in reports by NOAA (1993), U.S. Fish and Wildlife Service (2005), U.S. Department of the Navy (2006) and Office of National Marine Sanctuaries (2008, 2011).

SPECIES SIGHTINGS DATA

Species distributions were modeled using a compilation of at-sea observations chosen from multiple survey programs (Table 2). Each program collected spatially-explicit observations of seabirds, pinnipeds and/or cetaceans within a sampling domain which overlapped, and in some cases extended well beyond the study area (Figure 2). Taken together, the combined spatial distribution of survey programs represents a discontinuous patchwork of observation effort in the study area, and offers a more complete understanding of at-sea species observations than any single program. Stitching together and standardizing sightings data from multiple programs required substantial data processing and a complex modeling framework with integrated survey predictors.

The various survey programs collected sightings data along transects using small boats, large vessels and fixed-wing aircraft. In general, offshore transects were typically spaced far apart and ran perpendicular to shore or followed a saw tooth pattern across the continental shelf, and nearshore transects were more densely distributed and typically ran parallel to shore. Most programs collected data over multiple years, although not necessarily consecutively. Some survey programs collected information on seabirds, pinnipeds and cetaceans concurrently, while others focused on only one or two taxonomic groups. Figure 2 and Table 2 show the distribution of effort in the study area from each survey program used to model distributions of seabirds, pinnipeds and cetaceans. Models of seabird distributions were developed using observations collected from 2000 to 2013, and models of pinniped and cetacean distributions were developed using observations collected from 1995 to 2014. Additional information for each survey program is provided in Appendix A.

Methods

Table 2. Distribution of survey effort from each survey program used to model species distributions in the summer (April to October) and winter (November to March) seasons. Effort is represented by square kilometers surveyed and number of segments (shown in parentheses; standardized spatial analysis units). Survey programs were classified into one of four observation platform types to broadly differentiate species detection rates and observation effort.

Survey name	Platform type	Birds		Pinnipeds ¹		Cetaceans ¹	
		Apr-Oct	Nov-Mar	Apr-Oct	Nov-Mar	Apr-Oct	Nov-Mar
Harbor porpoise surveys	High-altitude fixed-wing aircraft	0.0 (0)	0.0 (0)	987.9 (1,036)	0.0 (0)	2,538.2 (1,359)	0.0 (0)
Leatherback turtle aerial survey	High-altitude fixed-wing aircraft	0.0 (0)	0.0 (0)	1,630.1 (1,708)	0.0 (0)	4,778.9 (2,549)	0.0 (0)
Pacific Continental Shelf Environmental Assessment (PaCSEA)	Low-altitude fixed-wing aircraft	297.2 (791)	89.0 (249)	198.2 (791)	59.3 (249)	212.9 (852)	59.3 (249)
California Current Ecosystem Surveys (includes ORCAWALE and CSCAPE surveys)	Large ship	561.8 (653)	0.0 (0)	2,223.7 (744)	0.0 (0)	9,526.9 (942)	0.0 (0)
Northwest Fisheries Science Center Northern California Current Seabird Surveys ²	Large ship	736.2 (869)	548.1 (679)	0.0 (0)	0.0 (0)	0.0 (0)	0.0 (0)
Olympic Coast National Marine Sanctuary Seabird and Marine Mammal Surveys	Large ship	446.3 (517)	0.0 (0)	6,524.5 (2,167)	0.0 (0)	23,944.0 (2,348)	0.0 (0)
Pacific Coast Winter Sea Duck Survey	Large ship	0.0 (0)	195.8 (287)	0.0 (0)	0.0 (0)	0.0 (0)	0.0 (0)
Pacific Orcinus Distribution Survey (PODS)	Large ship	0.0 (0)	0.0 (0)	910.1 (302)	2,254.3 (752)	4,539.0 (446)	10,225.7 (1,007)
Large whale surveys off Washington and Oregon	Small boat	0.0 (0)	0.0 (0)	459.1 (713)	89.1 (137)	1,977.7 (953)	287.7 (137)
Northwest Forest Plan Marbled Murrelet Effectiveness Monitoring Program	Small boat	5,457.3 (6,684)	0.0 (0)	3,776.9 (6,093)	0.0 (0)	8,981.7 (6,093)	0.0 (0)
Seasonal Olympic Coast National Marine Sanctuary seabird surveys	Small boat	672.4 (758)	0.0 (0)	0.0 (0)	0.0 (0)	0.0 (0)	0.0 (0)
	Totals	8,171.1 (10,272)	832.8 (1,215)	16,710.4 (13,554)	2,402.7 (1,138)	56,499.2 (15,542)	10,572.7 (1,393)

¹ Distance sampling methodologies were used during pinniped and cetacean surveys; therefore, survey effort (sq. km) was based on estimated effective strip width and varied by taxa. Values represent the mean across all modeled species within a given taxonomic group.

² Some seabird observations included in this data set were collected on PODS cruises

Survey programs were classified into one of four observation platform types: high-altitude fixed-wing aircraft, low-altitude fixed-wing aircraft, large ship and small boat. Platform types were categorized to broadly differentiate species detection rates and observation effort. High-altitude and low-altitude fixed-wing aircraft surveys were flown at altitudes of 198-213 m and 60 m, respectively. Small boat surveys were conducted on the Washington Department of Fish and Wildlife *Corliss* and *Almar* boats, and the Olympic Coast National Marine Sanctuary vessel *Tatoosh*. These were grouped together due to their size being significantly smaller and viewing height being significantly lower than large ship surveys. Large ship surveys were conducted on ocean-going vessels such as the NOAA ships *McArthur*, *McArthur II*, *Bell M. Shimada* and *David Starr Jordan*.

A series of custom-built processing routines written in R (version 3.1.3; R Core Team, 2015) were used to extract and reformat observations within survey transects. Transects were divided into a series of mutually-exclusive sections and subsequent segments according to changes in observation effort and sea state (Figure 3). Only transect sections with observers “on effort” were selected for segmentation.

We used a modified version of a processing routine written by Karin Forney and Elizabeth Becker (both in the NOAA National Marine Fisheries Service, Southwest Fisheries Science Center) to divide each transect section into discrete segments. Following the methods of Becker et al. (2010) the routine divided sections into predominantly 3 km segments, but also included a subroutine to include ‘leftover’ segments that were

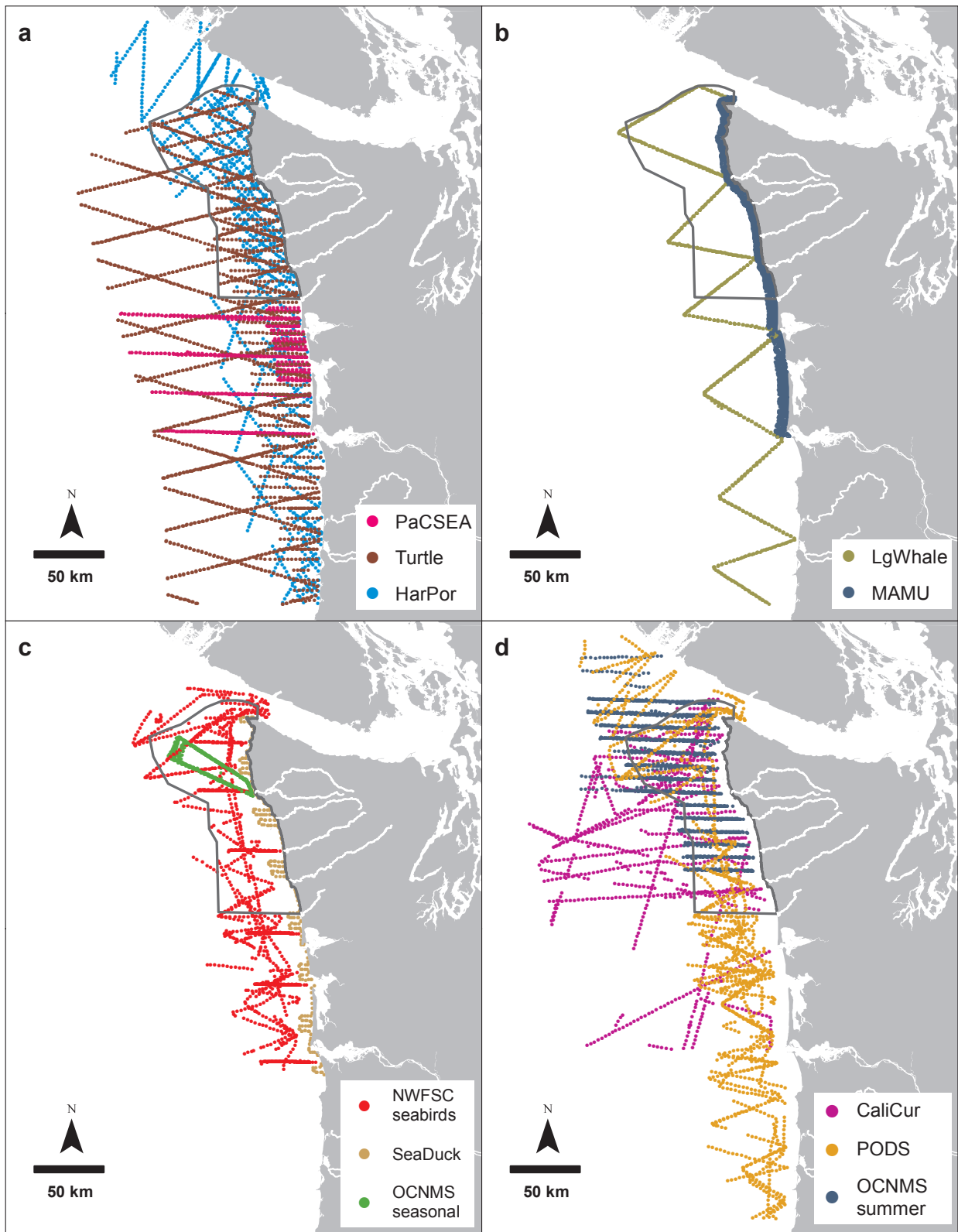


Figure 2. Spatial distribution of survey programs used to model species distributions. Survey distribution is represented by segment midpoints, analysis units described in this report. The Olympic Coast National Marine Sanctuary is designated by a thin gray line. Panel (a) shows the Pacific Continental Shelf Environmental Assessment (PaCSEA), Leatherback turtle aerial surveys (Turtle) and Harbor porpoise surveys (HarPor). Panel (b) shows Large whale surveys off Washington and Oregon (LgWhale) and surveys associated with the Northwest Forest Plan Marbled Murrelet Effectiveness Monitoring Program (MAMU). Panel (c) shows Northwest Fisheries Science Center Northern California Current seabird surveys (NWFSC seabirds), Pacific Coast winter sea duck survey (SeaDuck) and Seasonal Olympic Coast National Marine Sanctuary seabird surveys (OCNMS seasonal). Panel (d) shows Southwest Fisheries Science Center California Current ecosystem surveys (CaliCur), Pacific Orcinus distribution surveys (PODS) and Olympic Coast National Marine Sanctuary seabird and marine mammal surveys (OCNMS summer).

Methods

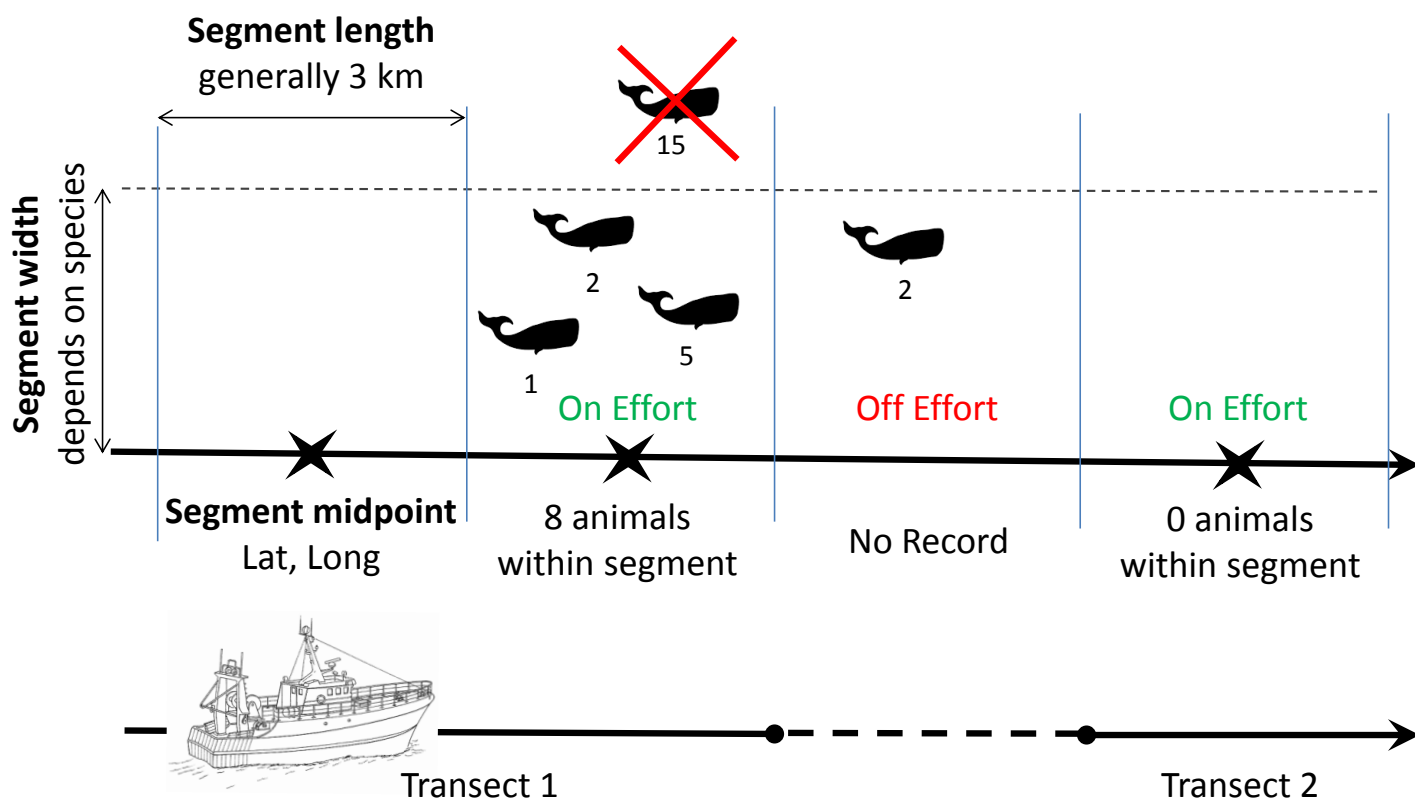


Figure 3: Schematic of the segmentation process used to partition animal observations along transects.

less than 3 km. The routine first determined the number of 3 km segments which fit within each “on effort” section and the length leftover after segmentation. If the remainder was greater than or equal to 1.5 km long, the corresponding shorter segment was assigned randomly to a location along the full effort section. If the remainder was less than 1.5 km long, the subsegment was added randomly to one of the 3 km segments. The routine randomizes the location of transect breakpoints, but does not change the location of observations. The randomization was necessary to ensure smaller subsegments did not always occur at the end of a transect, which can bias results because after a sighting, observers often go “off effort” (e.g., to obtain better group size estimates or confirm species identification).

To accurately divide transects into standardized segments, continuous geographic positions of the observation platform were needed. Some survey programs used in the modeling process provided continuous platform tracking data along with species observations, and these tracks were used to determine segment breakpoints along a transect. When continuous geographic positions were unavailable, but species observations included geographic positions, the positions were used to linearly interpolate platform track lines between observations. The estimated platform track lines consisted of regularly spaced coordinates at spatial resolutions of approximately 10 m. The platform tracks were also used to calculate the midpoint of each segment from the average of x- and y-coordinates within each segment. Segments and track lines were not needed for Pacific Continental Shelf Environmental Assessment (PaCSEA) and Northwest Fisheries Science Center Northern California Current Seabird Surveys, because the data provided were already processed into 3 km segments with midpoint coordinates.

All individuals of the same species within a segment regardless of size or life history stage were summed to produce species counts per segment. The resulting metric, counts per segment, was entered into relative density models with an effort offset, corresponding to area surveyed and calculated as the product of segment strip width and segment length (see *Effort offset* for more information on the use of survey area in the modeling

process). Consequently, model output is a measure of relative density defined as counts of individuals per sq. km. Datasets came from survey programs which used either standard strip transect or distance sampling methodologies (Buckland et al., 2001). Seabird observations were generally made using strip transect methods with a strip width of 150, 200 or 300 m. When strip width was not defined, only observations within 300 m of the vessel were analyzed. All surveys used in pinniped and cetacean analyses employed distance sampling, except the PaCSEA and pre-2008 Northwest Forest Plan Marbled Murrelet Effectiveness Monitoring Program, which used strip transect methods. Effective strip width was used to calculate survey area for surveys that used distance sampling methods. Prior to analyses, effective strip width was estimated separately for each species and platform-type combination by performing a conventional distance analysis. Specifically, we used an intercept-only detection function, half-normal key function and cosine adjustment terms of order 1-5 in the “Distance” package for R (Miller, 2015; R Core Team, 2015). For the two pinniped and cetacean surveys which did not apply distance sampling, segment strip width (150 or 200 m) was used in the survey area calculation. Strip widths and estimated effective strip widths used to calculate survey area are summarized by platform type in Table 3.

Table 3. Segment strip widths and estimated effective strip widths in meters by platform type.

Platform type	Birds	Pinnipeds	Humpback whale	Gray whale	Harbor porpoise	Dall's porpoise
High-altitude fixed-wing aircraft	-	318	942	942	313	299
Low-altitude fixed-wing aircraft	150	150	150	150	150	150
Large ship ¹	300 ³	1,006	4,347	5,949	1,903	1,399
Small boat ²		214	1,355	435	221	754

¹ Pacific Coast Winter Sea Duck Survey occasionally used strip widths of 200 m for seabirds
² Prior to 2008, Northwest Forest Plan Marbled Murrelet Effectiveness Monitoring Program surveys used a strip width of 200 m for pinnipeds and cetaceans
³ Large ships and small boats were grouped into a single platform type for seabird models

Predicted densities are considered relative, not absolute, measures of abundance per unit area. Estimates are relative because species counts were not corrected for track line detection probability, thus are likely biased low. Our models assume that detection probability varies by species, but the effect of detection on predicted relative density for a given species is consistent across the study area (see below for explanation of survey-specific sightability). Therefore, as relative measures, density estimates from our models can be compared across the study area within a given species, but cannot be compared across species or used to ascertain absolute population numbers. Relative density is sufficient to achieve our objective of identifying species-specific areas of higher density within the study region.

A subset of segments within each survey program was used for analysis. For modeling seabird and pinniped distributions, the subset included segments extending 10 km outside the outer perimeter of the study area. For modeling cetacean distributions, the subset included segments extending approximately 50 km farther north and west, and 100 km farther south of the study area. The greater number of segments used in the cetacean analyses was helpful to increase the number of cetacean sightings.

Segments were grouped into two non-overlapping time periods based on month of observation: April to October (summer season) and November to March (winter season). These two seasons generally correspond to the major upwelling and downwelling oceanographic seasons off the coast of Washington, respectively (Mann and Lazier, 2005). The spatial distribution of animals is expected to differ between these two time periods, due to changes in physical water properties, weather, life history patterns, prey or forage availability, and primary productivity.

Methods

PREDICTIVE MODELING FRAMEWORK

A boosted generalized additive modeling framework (Bühlmann and Hothorn, 2007; Hofner et al., 2012) assuming zero-inflated count distributions was used to estimate relationships between the numbers of individuals counted per segment and a suite of environmental predictor variables, after accounting for area surveyed. Those relationships were then used to predict the relative density of each species throughout the study area. Separate models were developed for each combination of species and season for which there were sufficient data. Our main objective was to provide accurate predictions, so we chose a modeling framework that allowed for flexible relationships and multi-way interactions between predictor variables while accounting for sampling heterogeneity between and within datasets. This modeling framework was successfully applied to seabirds along the U.S. Atlantic coast (Kinlan et al., 2014).

PREDICTOR VARIABLES

A wide range of predictor variables were used to model variation in the number of animals sighted per transect segment and to predict the relative density of animals throughout the study area (Table 4). Predictor variables fell into one of six categories: survey, temporal, geographic, topographic, physical oceanographic or biological oceanographic. Descriptions of the predictors follow, and Appendix B provides detailed processing steps.

Survey predictor variables were selected to account for variation in counts arising from heterogeneity in the type of survey platform, characteristics of the survey platform (e.g., observation height), observer identity and expertise, species focus, and sighting conditions. These factors influence the probability that individual animals will be detected and correctly identified to the species level. Of these factors, only the type of survey platform was consistently recorded in all datasets, and thus was directly usable as a predictor variable. Large ship and small boat survey platform types (Tables 2-3) were grouped into a single platform type for seabird analyses; therefore, the predictor variable for platform type had two levels in seabird analyses (ship/boat versus aircraft). All four levels of platform type were used in pinniped and cetacean analyses. In addition to survey platform, Beaufort Sea State was recorded in all datasets used in pinniped and cetacean analyses. Beaufort Sea State was not included in seabird models because not all surveys recorded sea state data. The distance-weighted average Beaufort Sea State along each segment was calculated and used as a predictor for all surveys, except for the PaCSEA survey, which was provided with the maximum Beaufort Sea State along each segment. We attempted to account for the effects of the remaining factors through two random-effect predictor variables representing survey identity (ID) and transect ID, respectively. The exact definition of transect ID differed somewhat between datasets, but unique transect IDs generally represented pre-defined survey transects or individual days of effort.

Temporal predictor variables were selected to account for variation in the numbers of animals within the study area over time. Julian day was used to account for changes within a season (e.g., arising from migratory movements in and out of the study area), and year was used to account for changes across years (e.g., arising from changes in population abundance or distributional shifts). Effects of Julian day and year were modeled as smooth continuous changes over time. Four climate indices (Table 4) were also included as temporal predictor variables to account for variation arising from linkages between periodical climate variability and animal density.

Geographic predictor variables were selected to account for variation in counts arising from spatial location per se. Isotropic x- and y-coordinates (based on projected longitude and latitude values) were included as predictor variables and their effects were modeled two ways. The first (x, y)-coordinate term allowed for smooth changes in numbers across the study area arising from spatial factors not captured by the other predictor variables. For example, none of the predictor variables capture terrestrial colony history or association with fishing vessels. The second term was formulated using radial basis functions to capture residual spatial autocorrelation in the data, after accounting for the effects of other predictor variables. Absolute distance to shelf break (200 m isobath), distance to colony (for Tufted Puffin and Common Murre), distance to nesting habitat (for Marbled Murrelet) and abundance weighted distance to haul-outs (for Steller sea lion and harbor seal) were also included as geographic predictor variables.

Table 4. Predictor variables used in the models. Additional information is provided in Appendix B for predictors with an asterisk.

Predictor variable	Code	Native resolution	Source
Survey variables			
Survey platform	platform	n/a	Survey datasets
Beaufort Sea State (pinniped and cetacean models)	seastate	n/a	Survey datasets
Survey ID	survey	n/a	Survey datasets
Transect ID	transect	n/a	Survey datasets
Temporal variables			
Julian day	jday	1 day	Survey datasets
Year	year	1 year	Survey datasets
Multivariate El Niño-Southern Oscillation Index (current and 12 month lag)	mei, mei.lag12	Monthly	NOAA ESRL
North Pacific Gyre Oscillation Index (current and 12 month lag)	npgo, npgo.lag12	Monthly	Georgia Tech
Pacific Decadal Oscillation Index (current and 12 month lag)	pdo, pdo.lag12	Monthly	NOAA ESRL
Upwelling index (current and 12 month lag)	upi, upi.lag12	Monthly	Pacific Fisheries Environmental Laboratory
Geographic variables			
X-coordinate	coords.x	n/a	Survey datasets
Y-coordinate	coords.y	n/a	Survey datasets
Distance to 200 m isobath*	dist2isobath	50 km	Derived from depth layer
Distance to Tufted Puffin colony*	dist2tupu	3 km	Derived from Washington Seabird Colony Catalog (source: WDFW)
Distance to Common Murre colony*	dist2comu	3 km	Derived from Washington Seabird Colony Catalog (source: WDFW)
Distance to Marbled Murrelet nesting habitat*	dist2mamu	3 km	Derived from Marbled Murrelet critical habitat (source: USFWS site)
Abundance weighted distance to Steller sea lion haul-out*	wdist2slst	3 km	Derived from Washington Seal and Sea Lion Haul-out Database (source: WDFW)
Abundance weighted distance to harbor seal haul-out*	wdist2shar	3 km	Derived from Washington Seal and Sea Lion Haul-out Database (source: WDFW)
Topographic variables			
Depth*	depth	30 seconds (~0.7 km)	MARSPEC
Bathymetric position index (3 km)*	bpi.3km	30 seconds (~0.7 km)	Derived from depth layer
Bathymetric position index (20 km)*	bpi.20km	30 seconds (~0.7 km)	Derived from depth layer
Planform curvature*	plcurv	30 seconds (~0.7 km)	MARSPEC
Profile curvature*	prcurv	30 seconds (~0.7 km)	MARSPEC
Slope*	slope	30 seconds (~0.7 km)	MARSPEC
Physical oceanographic variables (seasonal climatologies)			
Probability of anticyclonic eddy ring*	anticyc	0.25 degrees (~25 km)	AVISO
Probability of cyclonic eddy ring*	cyc	0.25 degrees (~25 km)	AVISO
Sea surface salinity*	salinity	30 seconds (~0.7 km)	MARSPEC
Sea surface temperature*	sst	0.05 degrees (~5.5 km)	Aqua MODIS
Probability of sea surface temperature front*	front	0.05 degrees (~5.5 km)	GOES Imager
Biological oceanographic variables (seasonal and non-seasonal climatologies)			
Surface chlorophyll <i>a</i> *	chl _a	0.05 degrees (~5.5 km)	Aqua MODIS
Frequency of chlorophyll peaks index*	fcpi	9 km	Provided by Rob Suryan

Methods

Topographic variables were selected to account for variation in counts arising from the direct and indirect effects of depth and seafloor features on animal distributions. Six different bathymetric datasets were used as topographic variables (Table 4). Depth, planform curvature, profile curvature and slope were available through MARSPEC (Ocean Climate Layers for Marine Spatial Ecology), a high-resolution GIS database of ocean climate and topographic layers (<http://www.marspec.org>; Sbrocco and Barber, 2013). Two bathymetric position indices were derived from the MARSPEC depth layer at different spatial scales.

Physical oceanographic predictor variables were designed to account for variation in counts arising from the direct and indirect effects of the physical state and dynamics of the ocean. Five physical oceanographic predictor variables were developed from a range of data sources, including one from MARSPEC (Table 4). Remote sensing data were used to characterize sea surface salinity (PSU) and temperature (°C). Probabilities of cyclonic and anticyclonic eddy rings and probability of sea surface temperature fronts were derived from the remotely sensed variables.

Two biological oceanographic predictor variables, chlorophyll *a* concentration (mg/m³) and the frequency of chlorophyll peaks index (FCPI) developed by Suryan et al. (2012), were included to account for variation in counts arising from the direct and indirect effects of ocean productivity (Table 4). Although both predictors comprise measures of chlorophyll *a* concentration, they were not highly correlated (Tables 5-6). This was expected since the FCPI is an indicator of anomalous conditions that differ from the chlorophyll *a* concentration average.

To associate dynamic physical and biological oceanographic variables with long-term static representations of animal density, we developed long-term seasonal climatologies for all dynamic variables, except FCPI. This process transforms dynamic variables into static variables. Data time series ranging from 11 to 22 years were used to estimate monthly mean climatologies. Monthly climatologies from April to October and November to March were averaged to generate seasonal climatologies, corresponding to the major upwelling and downwelling oceanographic seasons off the coast of Washington, respectively (Mann and Lazier, 2005). The same seasons were also used to partition animal observations. FCPI was provided to us as a non-seasonal climatology. However, FCPI has a strong seasonal signal given that FCPI is related to peak seasonal chlorophyll *a* concentration values during June and July (Suryan et al., 2012).

Geographic, topographic, physical oceanographic and biological oceanographic predictor variables were spatially explicit. Each variable was calculated on a standard study grid projected onto zone 10N of the Universal Transverse Mercator coordinate system and with a spatial resolution of 3 km. When the native spatial resolution of a predictor variable was finer than that of the study grid, predictor values were averaged within study grid cells. When the native spatial resolution of a predictor variable was similar to or coarser than that of the study grid, bilinear interpolation was used to derive predictor values at the center of study grid cells. For many data sets the native spatial extent did not perfectly align with our land mask. To fill in missing values close to shore, we extrapolated values to the coastline using the “Springs” algorithm in the “inpaint_nans” MATLAB function (<http://www.mathworks.com/matlabcentral/fileexchange/4551-inpaint-nans>). Each survey transect segment was matched to the predictor variable values from the study grid cell that contained the midpoint of that segment.

A small number of the spatially explicit predictor variables were correlated with each other (Tables 5-6). Since some correlations remain relatively high (i.e., greater than 0.7), inferences regarding the association between relative variable importance and a functional ecological relationship with animal density should be made with caution. The accuracy of predictions is less affected by collinearity among predictor variables.

Methods

Table 5. Pairwise Spearman's rank correlation coefficients (ρ) for spatial predictor variables (excluding x - and y -coordinates) used in seabird models for the months of April to October (above diagonal) and November to March (below diagonal). High correlations are highlighted ($0.7 \leq |\rho| < 0.8$ in yellow, $0.8 \leq |\rho| < 0.9$ in orange).

	dist2isobath	dist2tupu	dist2comu	dist2mamu	depth	bpi.3km	bpi.20km	plcurv	prcurv	slope	anticyc	cyc	salinity	sst	front	chla	fcpi
dist2isobath		-0.15	-0.14	-0.65	0.66	-0.10	-0.31	-0.24	0.17	-0.59	-0.08	0.17	-0.63	0.31	-0.34	0.59	-0.17
dist2tupu	-0.11				-0.32	-0.42	-0.37	0.11	-0.08	-0.06	0.27	0.63	-0.26	0.65	-0.03	-0.62	0.00
dist2comu	-0.10				-0.30	-0.40	-0.35	0.07	-0.03	-0.08	0.28	0.61	-0.25	0.64	-0.02	-0.57	-0.01
dist2mamu	-0.59				-0.76	-0.11	0.05	0.25	-0.14	0.55	-0.07	0.21	0.54	-0.10	0.48	-0.80	0.25
depth	0.78	-0.26	-0.25	-0.80		0.26	0.12	-0.18	0.08	-0.51	-0.28	-0.01	-0.59	0.01	-0.39	0.72	-0.29
bpi.3km	0.01	-0.08	-0.08	-0.02	0.15		0.64	0.09	-0.21	0.34	-0.12	-0.36	0.17	-0.38	0.00	0.20	-0.17
bpi.20km	-0.02	0.00	0.01	-0.01	0.21	0.50		0.03	-0.13	0.28	-0.04	-0.38	0.30	-0.42	0.16	0.09	-0.07
plcurv	-0.06	0.00	-0.01	-0.02	-0.09	0.17	-0.19		-0.45	0.13	-0.03	0.03	0.09	-0.05	-0.09	-0.26	0.06
prcurv	0.21	-0.12	-0.11	-0.11	0.12	-0.33	-0.16	-0.32		-0.11	-0.03	-0.09	0.02	0.02	0.08	0.20	-0.11
slope	-0.77	0.17	0.17	0.53	-0.75	0.10	-0.01	0.07	-0.19		0.07	-0.28	0.62	-0.36	0.38	-0.41	0.12
anticyc	0.49	-0.04	-0.04	-0.30	0.34	-0.03	0.05	-0.11	0.15	-0.45		-0.22	0.18	0.32	0.14	-0.18	0.27
cyc	-0.13	0.49	0.49	0.47	-0.46	-0.07	0.09	-0.12	-0.03	0.13	0.30		-0.55	0.55	-0.13	-0.30	-0.07
salinity	-0.68	-0.14	-0.14	0.74	-0.72	0.06	0.09	0.01	-0.11	0.63	-0.41	0.13		-0.63	0.53	-0.33	0.35
sst	-0.21	0.60	0.60	0.46	-0.48	-0.02	0.12	-0.11	-0.07	0.24	0.28	0.85	0.17		-0.15	-0.16	-0.14
front	0.09	-0.09	-0.09	-0.09	0.10	0.19	0.26	-0.16	0.08	0.09	0.05	0.01	-0.02	0.07		-0.27	0.29
chla	0.68	-0.24	-0.23	-0.84	0.83	-0.04	-0.10	0.02	0.14	-0.66	0.32	-0.45	-0.87	-0.53	0.02		-0.23
fcpi	-0.21	-0.11	-0.11	0.43	-0.24	0.03	0.17	-0.16	0.02	0.08	0.03	0.32	0.51	0.30	0.06	-0.49	

Table 6. Pairwise Spearman's rank correlation coefficients (ρ) for spatial predictor variables (excluding x - and y -coordinates) used in pinniped (above diagonal) and cetacean (below diagonal) models for the months of April to October. High correlations are highlighted ($0.7 \leq |\rho| < 0.8$ in yellow, $0.8 \leq |\rho| < 0.9$ in orange).

	dist2isobath	wdist2slst	wdist2shar	depth	bpi.3km	bpi.20km	plcurv	prcurv	slope	anticyc	cyc	salinity	sst	front	chla	fcpi
dist2isobath		-0.03	0.63	0.65	-0.07	-0.22	-0.16	0.22	-0.62	-0.18	0.07	-0.59	0.21	-0.47	0.62	-0.35
wdist2slst			0.27	0.48	0.28	0.27	0.03	0.02	-0.15	-0.32	-0.51	0.06	-0.60	-0.22	0.57	-0.15
wdist2shar				0.76	0.07	0.00	-0.07	0.07	-0.58	-0.36	-0.05	-0.70	0.04	-0.58	0.74	-0.25
depth	0.46				0.23	0.16	-0.14	0.07	-0.67	-0.44	-0.03	-0.65	-0.15	-0.57	0.87	-0.35
bpi.3km	-0.06			0.22		0.60	0.11	-0.29	0.18	-0.04	-0.29	0.06	-0.21	0.02	0.14	-0.11
bpi.20km	-0.19			0.16	0.58		-0.03	-0.17	0.11	0.07	-0.28	0.14	-0.20	0.15	0.06	0.01
plcurv	-0.11			-0.18	0.13	-0.02		-0.41	0.09	-0.04	0.04	0.04	0.00	-0.08	-0.17	-0.01
prcurv	0.22			0.04	-0.31	-0.18	-0.38		-0.11	-0.01	-0.08	0.01	0.03	0.01	0.14	-0.10
slope	-0.47			-0.71	0.14	0.09	0.13	-0.09		0.25	-0.20	0.62	-0.10	0.51	-0.62	0.16
anticyc	-0.10			-0.55	-0.06	0.04	0.03	0.00	0.34		-0.24	0.32	0.37	0.34	-0.43	0.34
cyc	0.06			-0.01	-0.27	-0.26	0.02	-0.08	-0.20	-0.22		-0.42	0.38	-0.12	-0.18	0.00
salinity	-0.43			-0.63	0.06	0.12	0.06	0.01	0.62	0.35	-0.38		-0.48	0.57	-0.52	0.43
sst	0.25			-0.30	-0.19	-0.18	0.06	0.05	0.03	0.45	0.27	-0.37		-0.03	-0.25	-0.18
front	-0.45			-0.54	0.02	0.14	-0.06	-0.01	0.48	0.34	-0.13	0.54	0.01		-0.52	0.41
chla	0.44			0.90	0.13	0.06	-0.20	0.11	-0.67	-0.55	-0.11	-0.55	-0.36	-0.51		-0.34
fcpi	-0.42			-0.25	-0.10	0.00	-0.03	-0.11	0.08	0.27	0.05	0.31	-0.18	0.39	-0.25	

Methods

PREDICTIVE MODELING PROCESS

Likelihoods and model components

The number of individuals of a given species counted per transect segment was modeled using zero-inflated Poisson (1) and zero-inflated negative binomial likelihoods (2) to account for the overdispersed nature of the count data. Each component/parameter of the likelihood was modeled as a separate function of the predictor variables (Schmid et al., 2008; Mayr et al., 2012). For the zero-inflated Poisson likelihood,

$$L(p, \mu; \mathbf{y}) = \prod_{i=1}^n [p + (1-p)e^{-\mu}]^{I_{y_i=0}} \left[(1-p) \frac{\mu^{y_i} e^{-\mu}}{y_i!} \right]^{I_{y_i>0}}, \quad (1)$$

the two model components were the probability of an “extra” zero (p ; also referred to as the “zero-inflation component”) and the mean of the Poisson distribution (μ ; also referred to as the “count component”). The same components were modeled for the zero-inflated negative binomial likelihood,

$$L(p, \mu, \theta; \mathbf{y}) = \prod_{i=1}^n \left[p + (1-p) \left(\frac{\theta}{\theta + \mu} \right)^\theta \right]^{I_{y_i=0}} \left[(1-p) \frac{\Gamma(y_i + \theta)}{y_i! \Gamma(\theta)} \left(\frac{\theta}{\theta + \mu} \right)^\theta \left(\frac{\mu}{\theta + \mu} \right)^{y_i} \right]^{I_{y_i>0}}, \quad (2)$$

(with μ being the mean of the negative binomial distribution) in addition to the dispersion parameter of the negative binomial distribution (θ). The probability of an extra zero was modeled on the logit scale, while the mean of the Poisson/negative binomial distribution and the dispersion parameter of the negative binomial distribution were modeled on the log scale.

In the above equations, y_i represents the total count for segment i and \mathbf{y} the vector of counts for all segments. n represents the total number of segments, $I_{y_i=0}$ is an indicator for whether or not $y_i = 0$ (i.e., $I_{y_i=0}$ equals 1 when $y_i = 0$, zero otherwise), $I_{y_i>0}$ is an indicator for whether or not $y_i > 0$, and $\Gamma()$ is the usual gamma function: $\Gamma(\alpha) = \int_0^\infty t^{\alpha-1} e^{-t} dt$.

Base-learners

Within the boosting framework, each model component was constructed as a function of an ensemble of “base-learners.” Each base-learner represented a specific functional relationship between a model component and one or more predictor variables. We utilized a suite of base-learners each representing different predictor variables, and different sets of base-learners were employed for different model components (Table 7).

Table 7. Base-learners employed in the boosted generalized additive modeling framework. Base-learner names are from the “mboost” package for R (Hothorn et al., 2015; R Core Team, 2015), and predictor variable names are defined in Table 4.

Name	Description	Predictor variables	Model component
bols	linear	intercept	p, μ, θ
bols	linear (fixed effect)	platform	p, μ, θ
brandom	random effect	survey	θ
brandom	random effect	transect	p, μ
bbs	penalized regression spline ¹	seastate	p, μ
bbs	penalized regression spline ¹	jday	p, μ
bbs	penalized regression spline ¹	year	p, μ
bspacial	penalized tensor product ¹	coords.x, coords.y	p, μ
brad	penalized radial basis ²	coords.x, coords.y	p, μ
btree	tree ³	all climate indices (current and lagged)	p, μ
btree	tree ⁴	all geographic (except coords.x and coords.y), topographic, physical and biological oceanographic variables	p, μ

¹ P-spline basis

³ Maximum depth = 1

² Matern correlation function

⁴ Maximum depth = 4 or 5

All spatially explicit predictor variables, except geographic coordinates, were included together in a single tree base-learner. The trees for that learner had a maximum depth of four or five, which allowed for interacting effects among the spatially explicit predictor variables. Geographic coordinates appeared in two base-learners, and those variables always entered the model as a pair. The remaining survey and temporal predictor variables entered the model individually, either through their own base-learners or, in the case of climate indices, one at a time through a tree base-learner with a maximum depth of one. Thus, our model structure did not allow for interactions between temporal and spatial predictor variables.

Effort offset

The mean of the Poisson/negative binomial distribution model component (μ) was additionally modeled with an effort offset, corresponding to segment survey area in sq. km, that was log transformed prior to entering the model (see *Species sightings data* for more information on calculating survey area). Therefore, resulting model predictions correspond directly to relative density values (individuals per sq. km) rather than relative count values (individuals per segment).

Stochastic gradient boosting

Stochastic gradient boosting was used to fit models whereby a sub-sample of the data was fitted in each boosting iteration (Friedman, 2002). Rather than resampling the data for each boosting iteration, a set of 25 or 50 random samples was created before boosting, and one sample was randomly drawn from this set for each boosting iteration. Root mean square error was used to select the base-learner that gave the best fit to the gradient (all data) in each boosting iteration.

Boosting “offsets”

Model component estimates were initialized (“offset” in boosting terminology; Hofner et al., 2012) by conducting a preliminary generalized linear model analysis. For that analysis, predictor variables were first reduced through principal component and cluster analyses to a smaller set of derived predictors. Those new predictors were then discretized into different numbers of classes. For each number of classes a generalized linear model with a zero-inflated Poisson or zero-inflated negative binomial likelihood was fit, and the mean estimates for each model component were calculated. Model component estimates were then averaged across the fitted models with the different numbers of predictor classes, weighted by the Akaike Information Criterion for those models.

Tuning of shrinkage rate and number of boosting iterations

A stratified (by transect ID) k-fold cross-validation approach was used to determine values for the shrinkage rate (nu) and number of boosting iterations ($mstop$) that resulted in the best predictive performance. The shrinkage rate was tuned first by fixing the number of boosting iterations and evaluating out-of-bag model performance in terms of the thresholded continuous rank probability score (Gneiting and Raftery, 2007) for different shrinkage rates. The number of boosting iterations was tuned second by fixing the shrinkage rate and evaluating out-of-bag model performance in terms of the negative log-likelihood. The number of boosting iterations at which performance was maximized was averaged across cross-validation samples (excluding the top and bottom 5%) and used as the number of boosting iterations for the final model fitting. If the number of boosting iterations was less than or greater than specified values, the shrinkage rate was decreased or increased, respectively, and the number of boosting iterations was tuned again. We allowed for a maximum of 20,000 boosting iterations, so models with boosting iterations above ~19,990 should be interpreted with caution as their performance may have improved with additional boosting iterations.

Methods

Model performance and selection

Four candidate models were fit to each species-season combination: 1) zero-inflated Poisson with a maximum tree depth of four specified for all spatially explicit predictor variables except the geographic coordinates (Table 4); 2) zero-inflated Poisson with a maximum tree depth of five; 3) zero-inflated negative binomial with a maximum tree depth of four; and 4) zero-inflated negative binomial with a maximum tree depth of five. The performance of each of the four candidate models was evaluated from a suite of performance metrics (Table 8) and a final best model was selected for each species and season. The range of performance metrics were chosen to assess model fit to observations, quantify model uncertainty, identify caveats, and describe the relationships between observations and predictors.

Table 8. Model performance metrics and corresponding quality levels. Quality levels are presented as numeric values from 5 (highest quality) to 1 (lowest quality).

Name	Description	Data	Stage	Quality categories
PDE	percent deviance explained ¹	all	final fit	5: ≥60%
				4: 40-60%
				3: 20-40%
				2: 10-20%
				1: <10%
AUC	area under the receiver operating characteristic curve	all, converted to presence/absence"	final fit	5: >0.9
				4: 0.8-0.9
				3: 0.7-0.8
				2: 0.6-0.7
				1: <0.6
<i>r</i>	Gaussian rank correlation coefficient ²	non-zero	final fit	5: >0.6
				4: 0.4-0.6
				3: 0.2-0.4
				2: 0.1-0.2
				1: <0.1
% error	median absolute residual error as percentage of mean number of individuals per segment with sightings	non-zero, out-of-bag"	cross-validation during tuning of mstop ³	5: <25%
				4: 25-50%
				3: 50-100%
				2: 100-200%
				1: >200%

¹ To calculate percent deviance explained, the saturated likelihood was assumed to be the maximum possible likelihood value, and the null likelihood was calculated from an intercepts-only zero-inflated model fit to the data (unpublished)

² Bodenhofer et al. (2013) and Boudt et al. (2012)

³ Median value across cross-validation replicates

Bootstrapping

We applied non-parametric bootstrapping to obtain a measure of central tendency for predicted relative density less prone to overfitting and to characterize uncertainty in the predictions. Two hundred bootstrap iterations were conducted producing a sample of predictions from which we calculated quantiles, confidence intervals and the coefficient of variation (CV). For each bootstrap iteration, the set of unique transect IDs was resampled with replacement, and the data for each transect ID were assigned weights proportional to the frequency of that ID in the sample. These data weights were then applied when fitting the model during that bootstrap iteration. Predictor variables that were not included in the final model were excluded from the bootstrapping procedure.

Spatial prediction

The final fitted model for each species and season was used to predict relative density, defined as the relative expected number of individuals per sq. km, throughout the study area. Relative density integrated both the zero-inflated and Poisson/negative binomial components of the likelihood. We chose the median value (50% quantile) of bootstrap iterations to represent the single best prediction of relative density. The median was chosen over the average among bootstrap results because of the inherent skewness associated with zero-inflated distributions.

It is important to recognize that the model predictions do not represent actual absolute density. During visual surveys, individual birds, pinnipeds and cetaceans may be missed either because they are below the surface of the water (availability bias), or simply because observers failed to notice them (perception bias; Barlow, 2015). The failure to count some individuals biases estimates of density downward relative to actual density. Animal movement can also bias estimates of density. Cetaceans may be attracted or repelled by ships, small boats and planes biasing estimates upward or downward, respectively. Flying birds or fast moving cetaceans can also bias estimates, with the direction of the bias depending on the speed and direction of the animals' movement relative to those of the survey platform (Spear et al., 1999). Our model predictions should only be interpreted as indices of density, assuming that any species-specific bias that may be present is constant across space and time.

Spatially explicit predicted values were calculated for each cell of the study grid from the values of the spatially explicit predictor variables for that cell. Thus, the predicted relative density in a given grid cell corresponds to predictions for a transect segment whose mid-point falls within that grid cell. All other predictor variables were set to their mean values.

Implementation

The analysis was coded in R (version 3.1.3; R Core Team, 2015) and relied on multiple existing contributed packages (e.g., mboost; Hothorn et al., 2015).

Review

Reviewers participated in several rounds of model output evaluations. This collaborative process led to significant improvements in model quality and predictive mapping products. Over the course of model review, the following recommended changes were made: excluding observations outside the study area and a narrow encircling buffer; improving the transect segmentation process using a routine developed by the SWFSC; incorporating oceanographic climate indices as predictor variables; adding diagnostic plots to address the impact of heterogeneous survey effort through space and time; determining an effective strip width for pinniped and cetacean observations; creating improved pinniped haul-out predictors; and assessing different methods to categorize relative density in model outputs.

PREDICTIVE MODELING PRODUCTS

Maps

To facilitate the use of model outputs by researchers and environmental planners, we distilled model outputs into five maps. The maps enable concurrent viewing of sighting data, relative density predictions and model uncertainty. The first map presented for each species shows the gradient of predicted relative densities along with sighting data and a layer showing areas of greater model uncertainty, where $CV \geq 0.5$ (Figures 6-38 [even numbers]). The CV threshold does not suggest any meaningful ecological cutoff or indicator for management action, but is a useful single threshold to identify areas of higher uncertainty in model predictions and generally matched areas where predictions visually deviated from observation data or where reviewers had less confidence in predictions. The color gradient classes in these maps are based on the cumulative distribution of predicted relative densities and represent 5% quantile intervals of the sum of predictions, calculated separately for each species-season combination.

Methods

Long-term predicted relative density and CV for each species were also mapped individually, along with 5% and 95% quantiles based on the non-parametric bootstrapping procedure (Figures 7-39 [odd numbers]). The two quantile maps are representative of the lower and upper bounds of a 90% confidence interval for predicted relative density. These maps are helpful for understanding uncertainty in predictions and can be useful in a situation when one wants to be more or less conservative with designation of an ecologically important area.

Variable importance

While our primary objective was not to determine the ecological drivers and mechanisms behind the spatial distributions of marine species in the study area, our model results do provide some indication of which variables were most useful for predicting those distributions. Those variables may provide useful starting points for future studies seeking ecological inference. It is important to understand that predictors serve as proxies for unmeasured underlying ecological processes linking species to their environment, and information on variable importance does not convey importance of specific ecological processes.

We calculated the relative importance of a given predictor variable in the final fitted models by summing the decrease in the negative log-likelihood in each boosting iteration attributable to that predictor variable. Thus, variable importance reflects the frequency with which a given predictor variable occurred in the selected base-learners across boosting iterations and that variable's ability to explain variation in the data when it was selected. When multiple predictor variables occurred in the selected base-learner for a given boosting iteration, the decrease in the negative log-likelihood was divided evenly among those predictor variables. Relative variable importance was re-scaled so that it summed to one across predictor variables.

DISTRIBUTION OF SURVEY EFFORT

The distribution of survey effort was assessed using the number of transect segments available for modeling and the total surveyed area. These two effort metrics provide similar data for seabirds, but provide complementary information for pinniped and cetaceans since the detection area varied significantly by marine mammal species and platform.

The distribution of survey effort was heterogeneously distributed in the study area across time (Figure 4). Most survey effort was concentrated in May to July for seabirds, and May to September for pinnipeds and cetaceans. These high-effort months occur in the summer season of our models, and correspond to the oceanographic upwelling season. The difference in total number of segments between seabird and marine mammal surveys is due to the different surveys used to develop corresponding models (Table 2). Differences in total survey area between all three taxonomic groupings result from the use of different surveys and different effective strip widths. Less survey effort was allocated to the study area from October to April. These low-effort months are mostly in the winter season of our models. Of all effort in the winter season, the vast majority occur in March.



Harbor seal
(Dave Withrow, NOAA NMFS/AFSC/NMML)

The distribution of summer and winter season effort varied across years. Across all taxa the number of summer season segments increased over time, but the total survey area in the summer season did not have a clear temporal trend. This difference was related to changes in survey composition. Total area surveyed during the summer season was greatest in 2007 and 2008, and least in 1999. Winter season effort was available between 2008 and 2012 for seabirds, and between 2004 and 2012 for pinnipeds and cetaceans, both ranges representing far fewer years of effort than available in the summer season.



Harbor porpoise
(Ari Friedlaender, Oregon State University)

The distribution of survey effort varied in space reflecting the different objectives and spatial targets of survey programs (Figure 5). Regardless of season, the majority of the study area deeper than 500 m did not receive any survey effort. Survey effort for seabirds in the summer season was heavily concentrated in the nearshore waters located in the northern half of the study area. In general this area received 10 times more effort than other portions of the study area and was associated with the Northwest Forest Plan Marbled Murrelet Effectiveness Monitoring Program. Seabird effort in the winter season was more evenly spread across the span of the continental shelf, with slightly more effort in the southern half of the study area. The survey effort for pinniped and cetacean observations in the summer season was highest in the northern half of the study area within Olympic Coast National Marine Sanctuary, and effort was distributed relatively evenly across the span of the continental shelf.



Marbled Murrelet
(David Pereksta, BOEM)

Results and Discussion

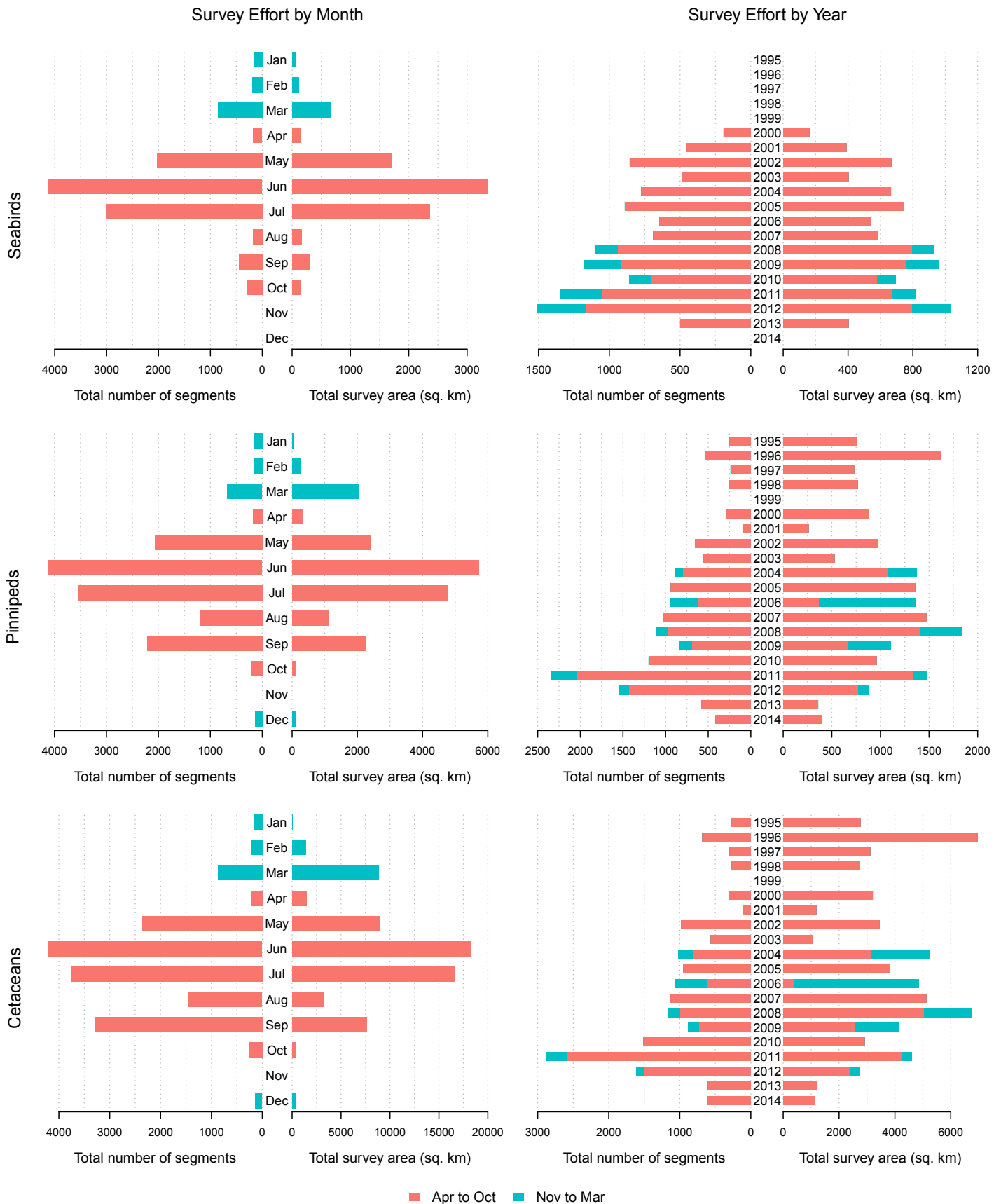


Figure 4. Distribution of survey effort by month and year in the data set used to model seabird, pinniped and cetacean distributions. Effort is represented by square kilometers surveyed and total number of segments (standardized spatial analysis units) used for modeling. Effort associated with the summer (April to October) and winter (November to March) seasons are stacked as red and cyan colored bars, respectively.

Survey Effort

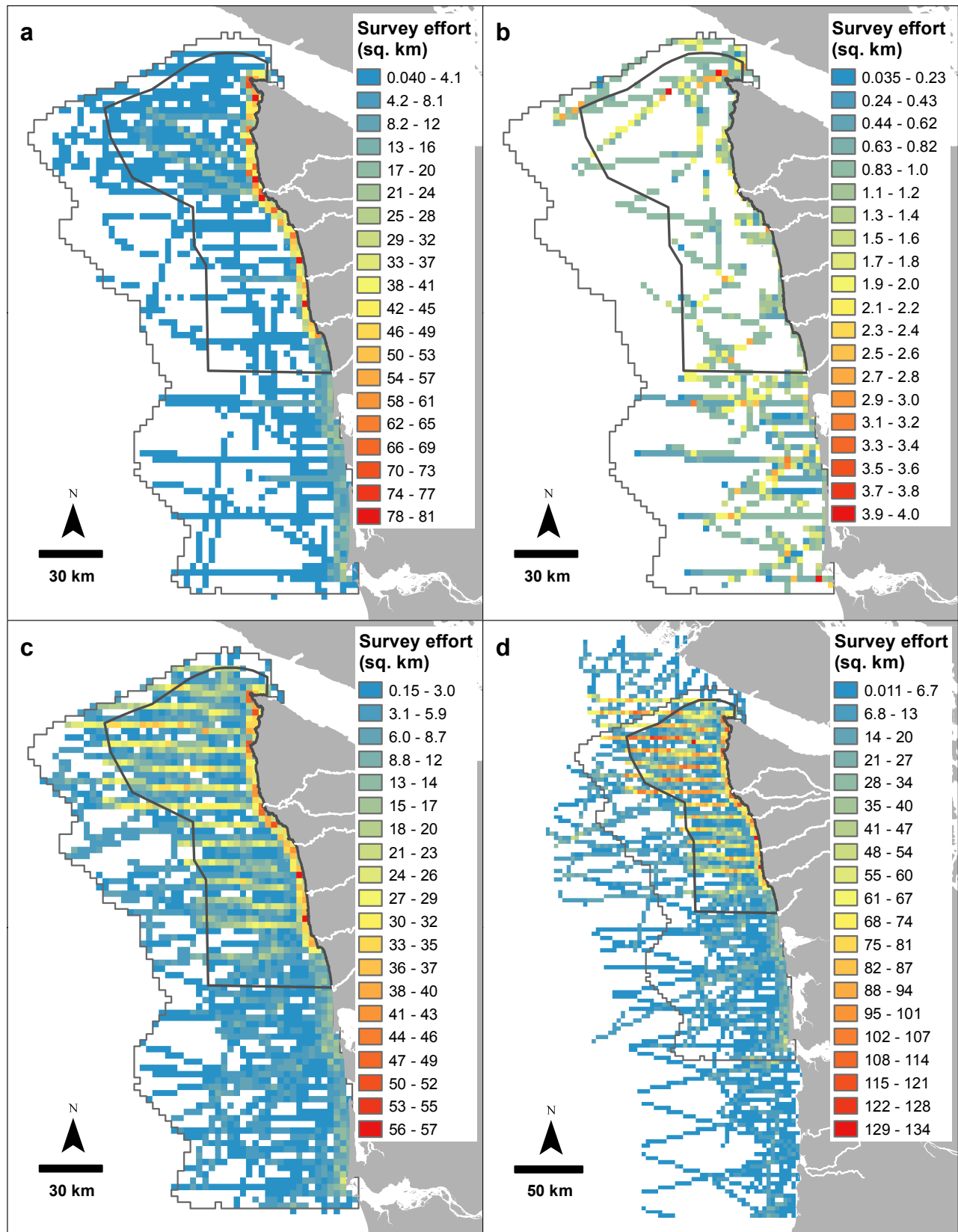


Figure 5. Spatial distribution of survey effort (square kilometers) for summer (April to October) seabird (a), winter (November to March) seabird (b), and summer pinniped (c) and cetacean (d) models within the study area. The Olympic Coast National Marine Sanctuary is designated by a heavy gray line and the prediction area by a light gray line. Distance sampling methodologies were used during pinniped and cetacean surveys; therefore, survey effort was based on estimated effective strip width and varied by taxa. Values shown represent the mean across all modeled species within a given taxonomic group.

Results and Discussion

PREDICTED SPATIAL DISTRIBUTIONS

Predicted spatial distributions varied by species and by season (Figures 6-38). Across all species and season combinations relative density patterns exhibited patchiness, and across-shelf and along-shelf gradients. For three species of seabirds with sufficient data to model both summer and winter season distributions, we found significant differences between seasonal patterns of relative density.

Many of the species selected for modeling utilized shallow nearshore habitats in the summer season: Marbled Murrelet, Rhinoceros Auklet, Tufted Puffin, Common Murre, Sooty Shearwater, Steller sea lion, harbor seal, gray whale and harbor porpoise. Predicted relative density for these species was greatest within 10 to 15 km from shore. Relative density predictions for Sooty Shearwater were more evenly spread out across the shelf than other nearshore species; however, greatest relative densities generally were within 30 km from shore. For nearshore species, relative density predictions were not uniform across the swath of nearshore water. Predicted relative density for gray whale was greatest in the northern half of the study area (this pattern is discussed relative to timing of migration below). Predicted relative density for Sooty Shearwater was greatest between Willapa Bay and the Columbia River, where consistently strong salinity gradients enhance local marine productivity (Morgan et al., 2005). The relative density of breeding seabird species and pinnipeds were generally greatest near breeding colonies and populated haul-outs, respectively. Areas of high predicted relative density for all nearshore species included the area around Tatoosh Island, sites in Flattery Rocks, Quillayute Needles and Copalis National Wildlife Refuges, as well as the coastal area between refuges.



Steller sea lion
(Sally Mizroch, NOAA NMFS/AFSC/NMML)



Tufted Puffin
(David Pereksta, BOEM)

Of the selected pelagic species (Black-footed Albatross, Northern Fulmar, Pink-footed Shearwater, humpback whale, Dall's porpoise), all exhibited high predicted relative density in the northern part of the study area within a region delimited by Laperouse Bank, Swiftsure Bank, Nitinat Canyon and Barkley Canyon. The Juan de Fuca Eddy creates a seasonal upwelling comprised of nutrient-rich water (Hickey and Banas, 2003) in this region and makes it one of the most productive habitats in the Northeastern Pacific (Ware and Thomson, 2005). Predicted relative density for pelagic species was also generally higher along the shelf-edge than in deeper or shallower areas. For three species (Black-footed Albatross, Pink-footed Shearwater, humpback whale), predicted relative density was locally higher on the shelf edge when adjacent to a submarine canyon.



Humpback whale
(Amy Kennedy, NOAA NMFS/AFSC/NMML)

There were sufficient data during winter to model three seabird species (Rhinoceros Auklet, Common Murre, Black-footed Albatross). Winter season distributions of relative density for all three species are very different than summer season predictions. In each case, areas with the highest relative densities shifted farther offshore into deeper water during the winter season compared with summer season patterns.

Results and Discussion

Spatial patterns of predicted relative density typically aligned with sighting data. However, for some species (Marbled Murrelet, Rhinoceros Auklet, Common Murre, gray whale, harbor porpoise, Dall's porpoise), predictions of high relative density were off the coast of British Columbia where sightings were limited or absent. These predictions are not unexpected given known biogeographical distributions of these species (Perrin et al., 2002; USFWS, 2005), and the environmental similarities and proximity between areas off British Columbia and Washington.



Dall's porpoise (Kate Stafford (NOAA/NMFS/AFSC/NMML)).

Predictions of relative density are accompanied by estimates of uncertainty, specifically the CV, in modeled predictions (Figures 7-39). CVs were highly variable among different species and across the study area for individual species. In many cases, the CV of predictions was higher in areas with limited sighting data, and where predicted relative density was highest or lowest for a given species. Some relative density predictions were associated with very high CVs (>1) indicating substantial uncertainty and signal that these predictions should be interpreted cautiously.



Rhinoceros Auklet (David Pereksta, BOEM)

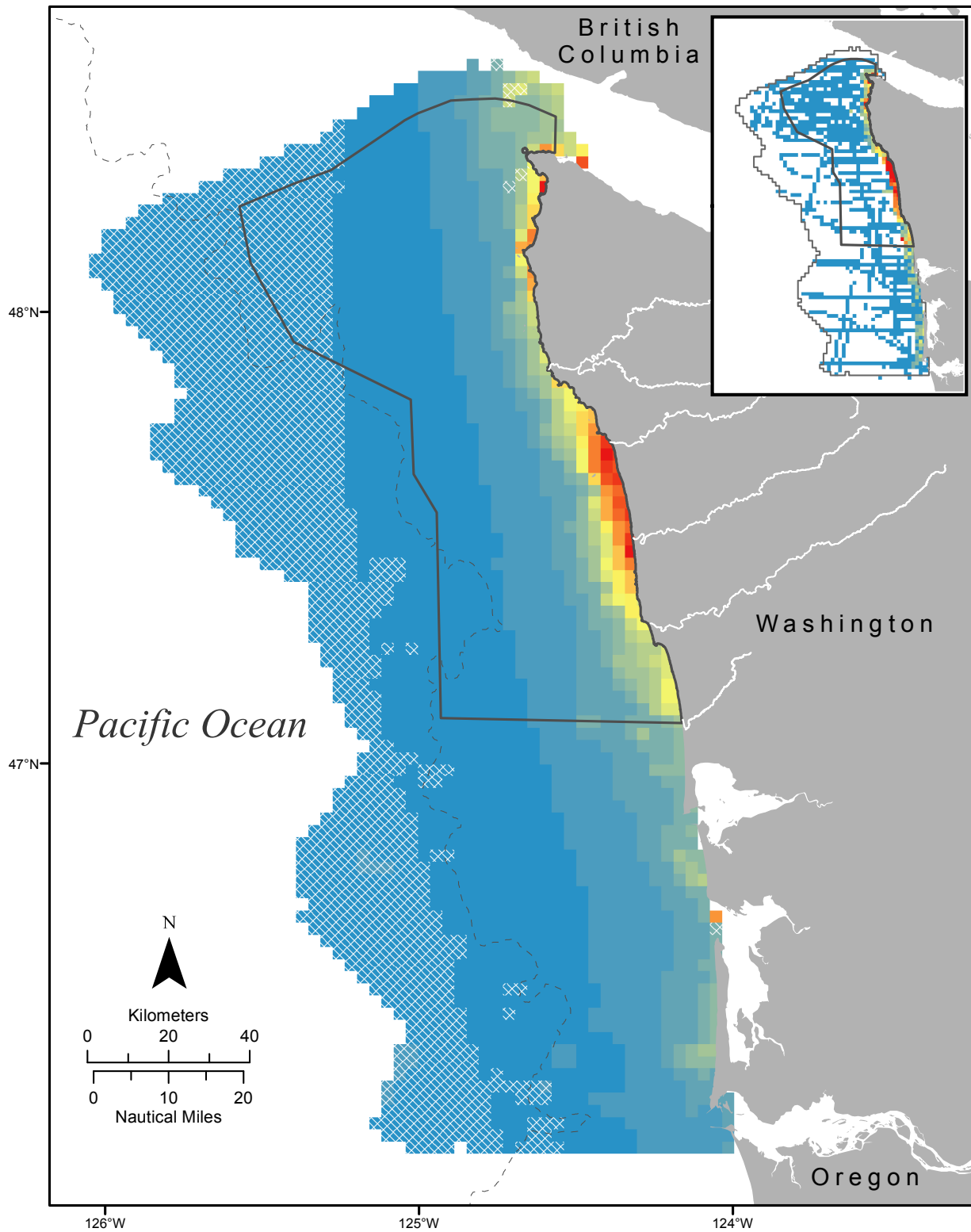
Certain model predictions of high relative density are particularly questionable, because they either were noted as anomalous by reviewers or they did not align well with observations. The gray whale model predicted high relative density south of the Columbia River off the coast of Oregon and moderately high density offshore of Astoria Canyon; however, these predictions are not corroborated by observations (Fig. 34 inset). In addition, gray whale densities were predicted to be higher in the northern half of the study area, even though gray whales migrate through the entire latitudinal range of the study area. The lower predicted relative densities in the southern half of the study area are likely associated with the timing of survey effort relative to annual migrations between southern breeding grounds and northern feeding grounds. The Northern Fulmar and Pink-footed Shearwater models predicted low relative densities offshore of Willapa Bay, but there are noticeable observations of high relative density in the same area. Although these noted areas deserve greater scrutiny, their presence does not invalidate the whole corresponding model or model predictions in other areas.



Gray whale (John Calambokidis, Cascadia Research Collective)

Results and Discussion

Marbled Murrelet (*Brachyramphus marmoratus*): April to October



Relative density Min Max

Figure 6. Long-term relative density (individuals per sq. km) prediction map for Marbled Murrelet (*Brachyramphus marmoratus*) during the months of April to October. White cross-hatching represents areas of greater prediction uncertainty, where the coefficient of variation was greater than or equal to 0.5. The Olympic Coast National Marine Sanctuary is designated by a solid gray line and the 500 m isobath contour is shown as a dashed gray line. Observed density (individuals per sq. km) is shown on the inset map. Prediction and observed density color gradient classes are based on the cumulative distribution of predicted relative densities and represent 5% quantile intervals of the sum of predictions. Refer to Figure D1 for the relationship between relative density and color gradient classes.

Results and Discussion

Marbled Murrelet (*Brachyramphus marmoratus*): April to October

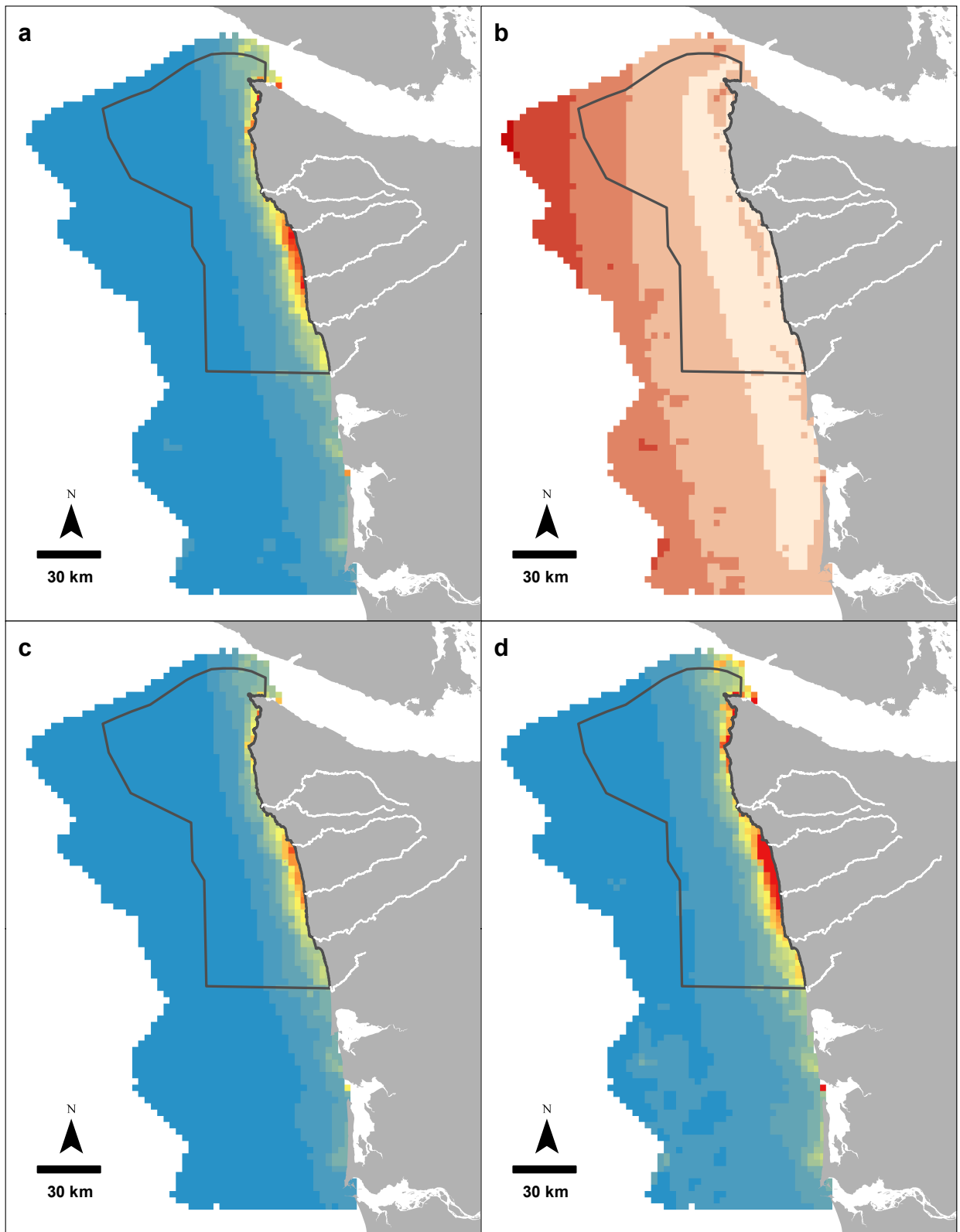
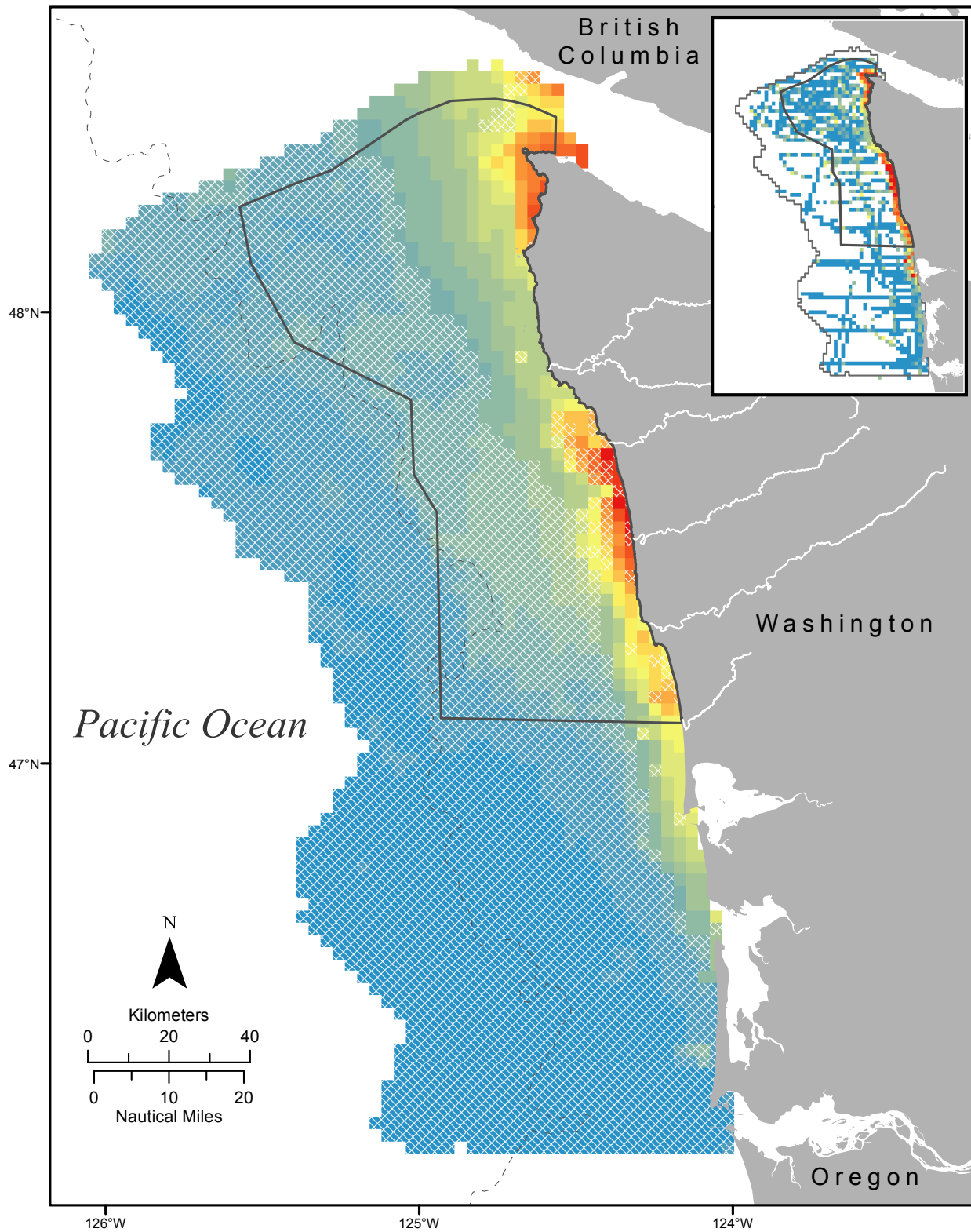


Figure 7. Long-term relative density (individuals per sq. km) prediction maps for Marbled Murrelet (*Brachyramphus marmoratus*) during the months of April to October: a) 50% quantile of bootstrap (median), b) coefficient of variation, c) 5% quantile of bootstrap, d) 95% quantile of bootstrap. The color gradient classes for panels c and d are the same as for panel a.

Results and Discussion

Rhinoceros Auklet (*Cerorhinca monocerata*): April to October



Relative density Min Max

Figure 8. Long-term relative density (individuals per sq. km) prediction map for Rhinoceros Auklet (*Cerorhinca monocerata*) during the months of April to October. White cross-hatching represents areas of greater prediction uncertainty, where the coefficient of variation was greater than or equal to 0.5. The Olympic Coast National Marine Sanctuary is designated by a solid gray line and the 500 m isobath contour is shown as a dashed gray line. Observed density (individuals per sq. km) is shown on the inset map. Prediction and observed density color gradient classes are based on the cumulative distribution of predicted relative densities and represent 5% quantile intervals of the sum of predictions. Refer to Figure D2 for the relationship between relative density and color gradient classes.

Results and Discussion

Rhinoceros Auklet (*Cerorhinca monocerata*): April to October

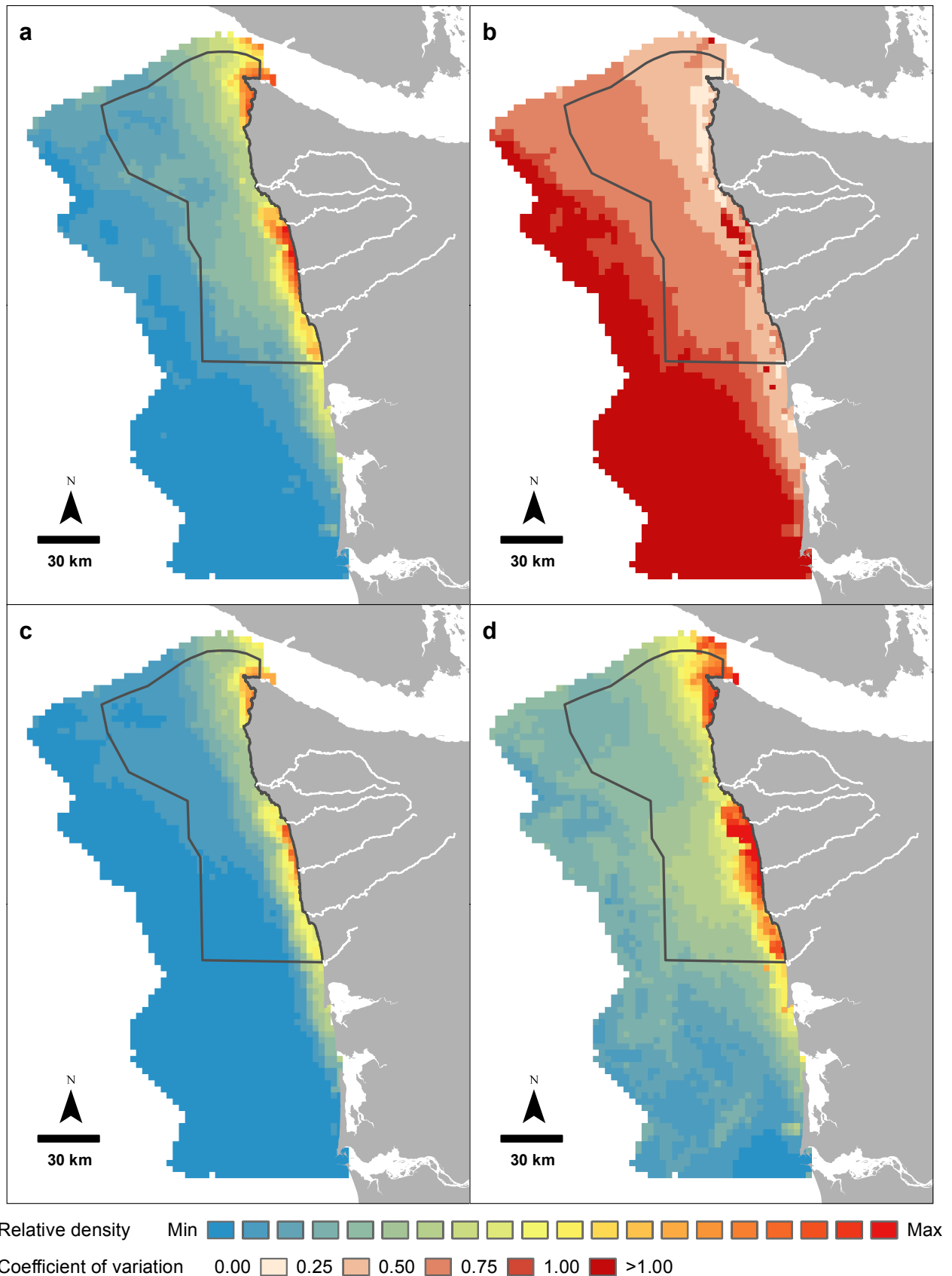


Figure 9. Long-term relative density (individuals per sq. km) prediction maps for Rhinoceros Auklet (*Cerorhinca monocerata*) during the months of April to October: a) 50% quantile of bootstrap (median), b) coefficient of variation, c) 5% quantile of bootstrap, d) 95% quantile of bootstrap. The color gradient classes for panels c and d are the same as for panel a.

Results and Discussion

Rhinoceros Auklet (*Cerorhinca monocerata*): November to March

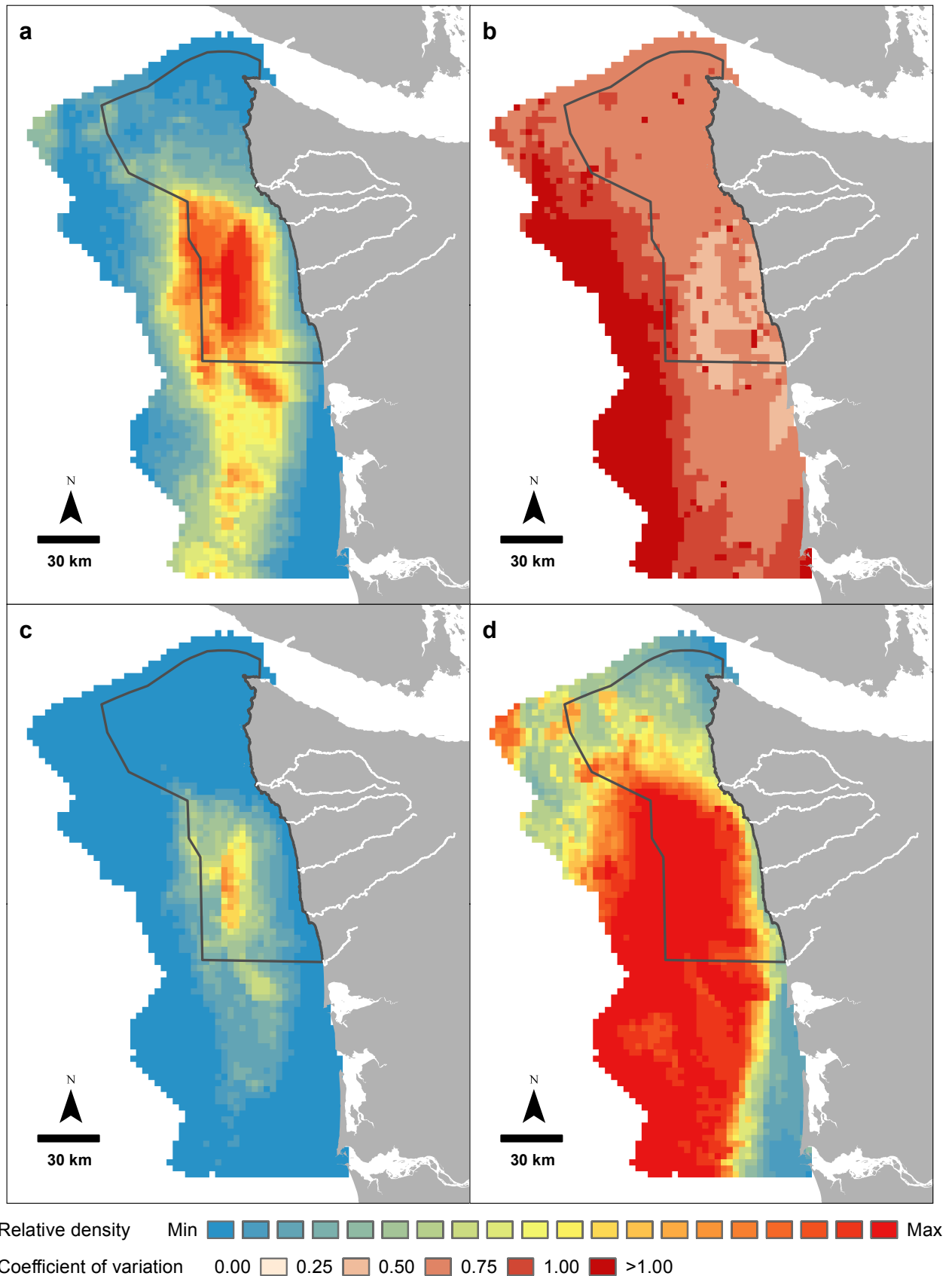
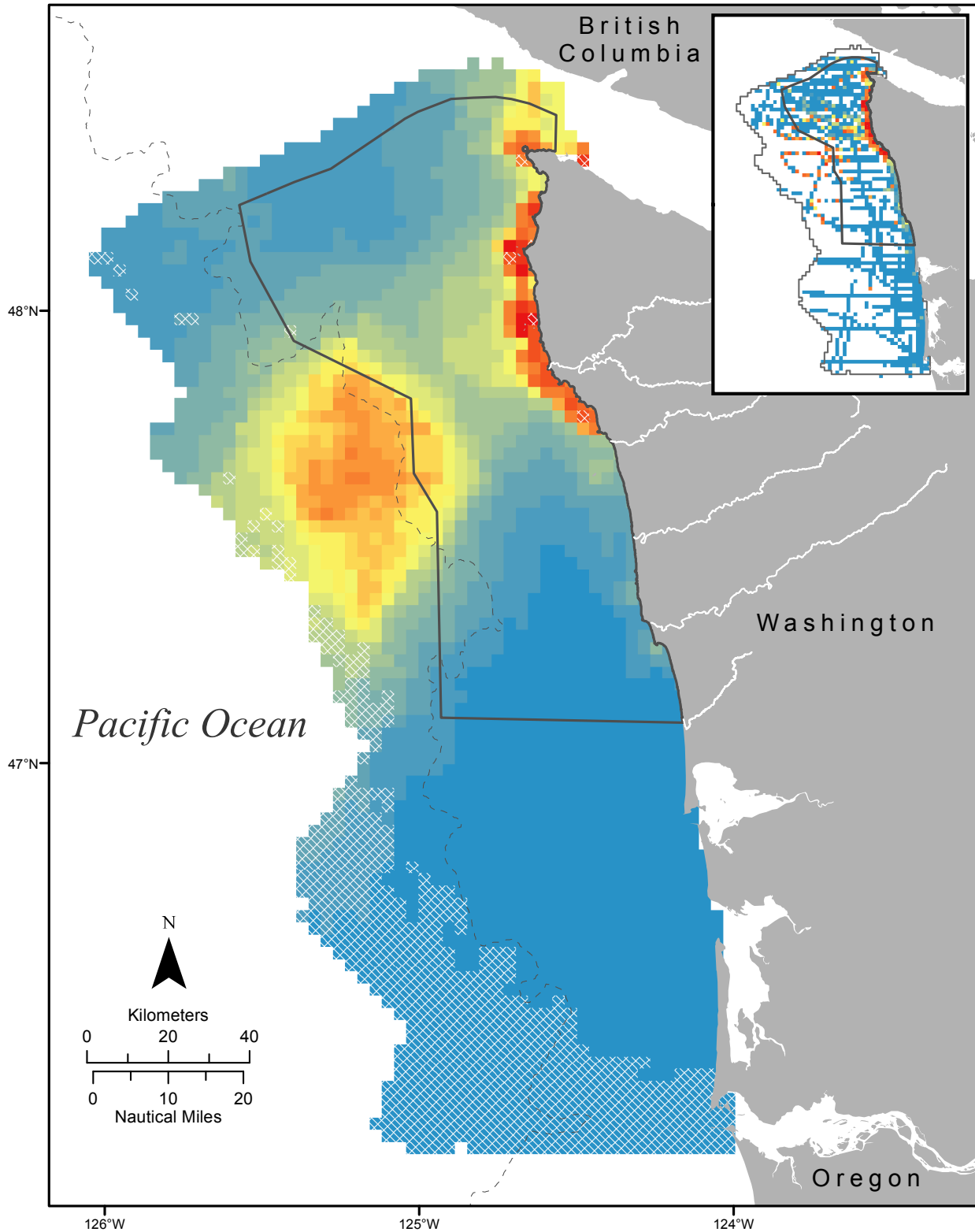


Figure 11. Long-term relative density (individuals per sq. km) prediction maps for Rhinoceros Auklet (*Cerorhinca monocerata*) during the months of November to March: a) 50% quantile of bootstrap (median), b) coefficient of variation, c) 5% quantile of bootstrap, d) 95% quantile of bootstrap. The color gradient classes for panels c and d are the same as for panel a.

Results and Discussion

Tufted Puffin (*Fratercula cirrhata*): April to October



Relative density Min Max

Figure 12. Long-term relative density (individuals per sq. km) prediction map for Tufted Puffin (*Fratercula cirrhata*) during the months of April to October. White cross-hatching represents areas of greater prediction uncertainty, where the coefficient of variation was greater than or equal to 0.5. The Olympic Coast National Marine Sanctuary is designated by a solid gray line and the 500 m isobath contour is shown as a dashed gray line. Observed density (individuals per sq. km) is shown on the inset map. Prediction and observed density color gradient classes are based on the cumulative distribution of predicted relative densities and represent 5% quantile intervals of the sum of predictions. Refer to Figure D4 for the relationship between relative density and color gradient classes.

Results and Discussion

Tufted Puffin (*Fratercula cirrhata*): April to October

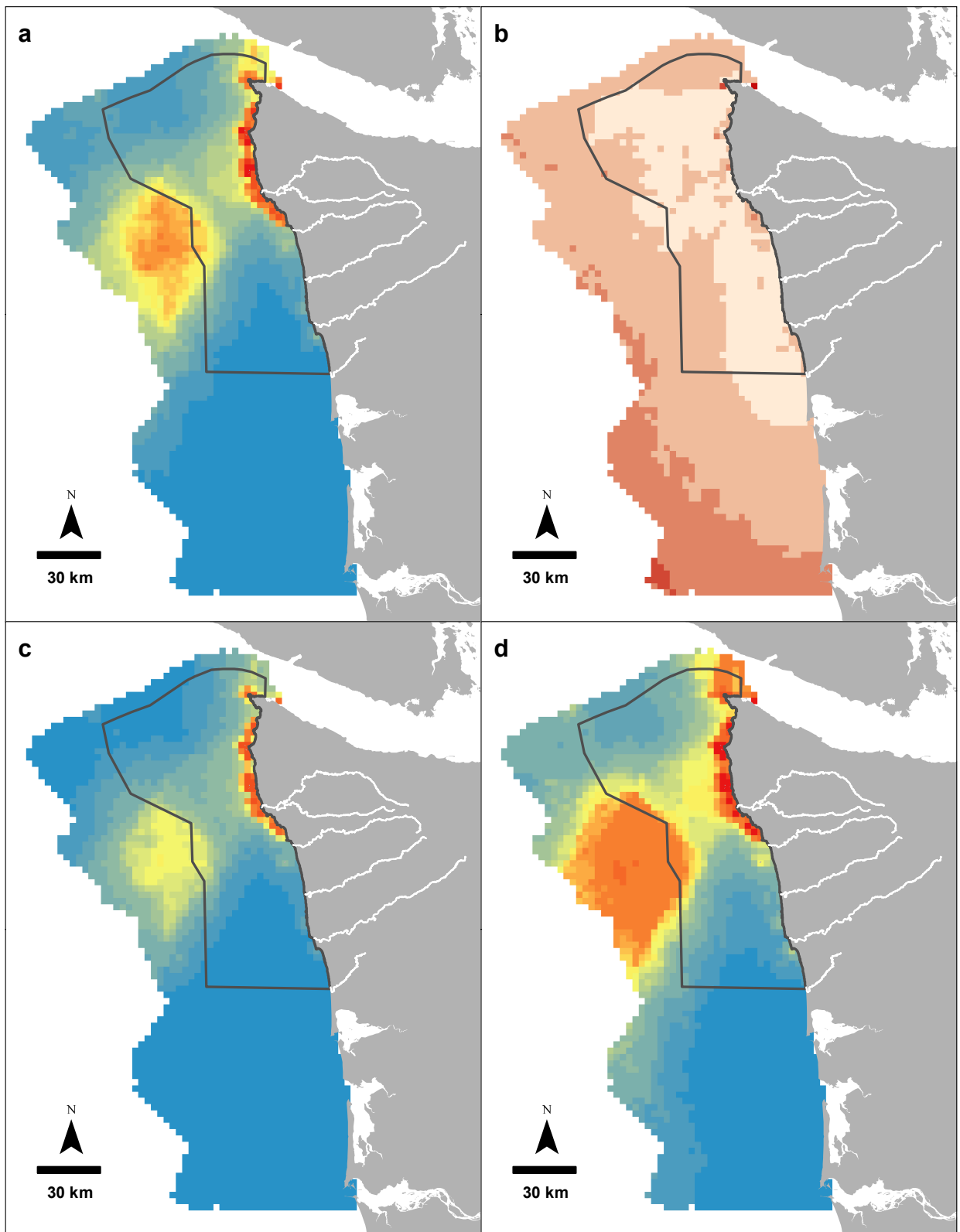


Figure 13. Long-term relative density (individuals per sq. km) prediction maps for Tufted Puffin (*Fratercula cirrhata*) during the months of April to October: a) 50% quantile of bootstrap (median), b) coefficient of variation, c) 5% quantile of bootstrap, d) 95% quantile of bootstrap. The color gradient classes for panels c and d are the same as for panel a.

Results and Discussion

Common Murre (*Uria aalge*): April to October

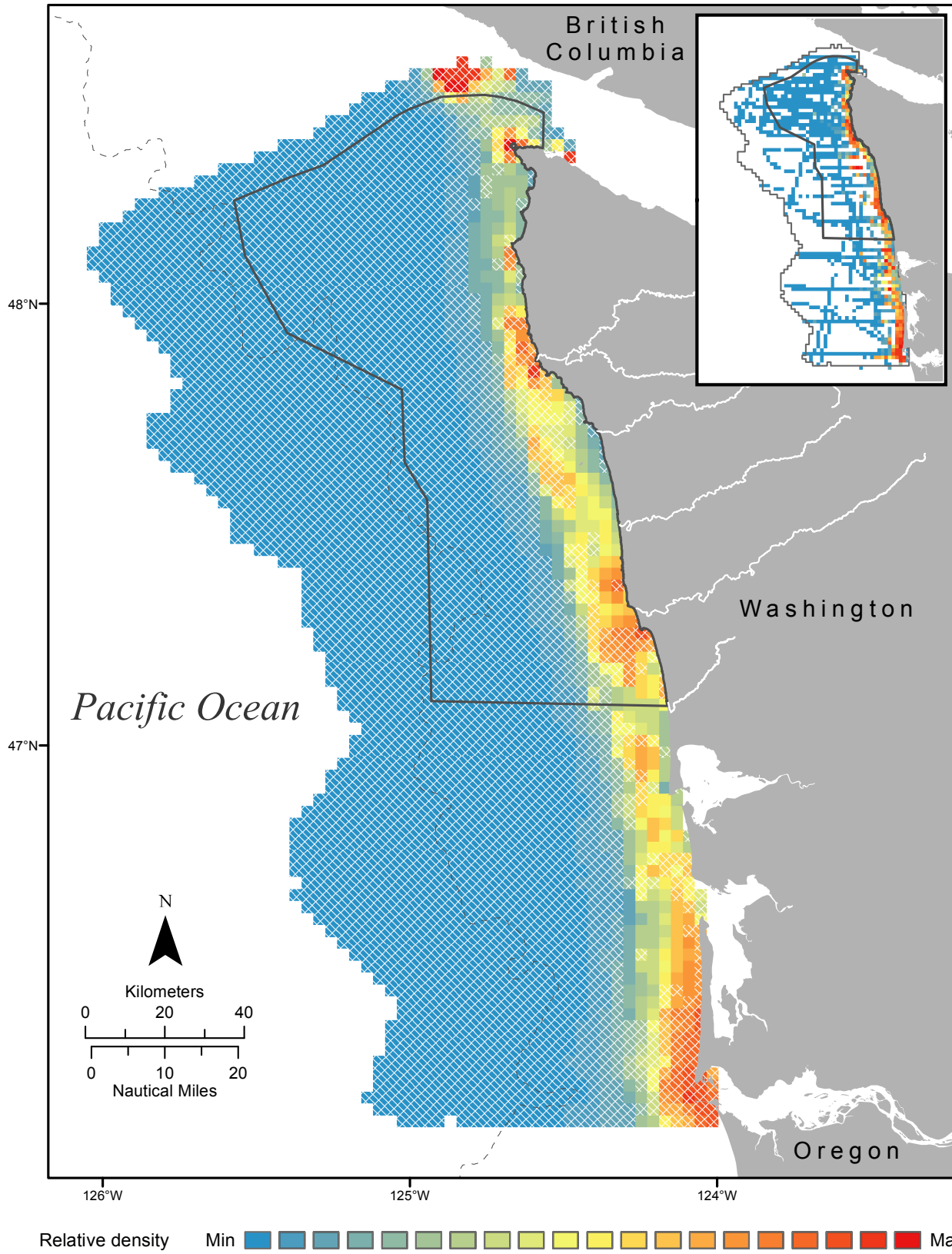


Figure 14. Long-term relative density (individuals per sq. km) prediction map for Common Murre (*Uria aalge*) during the months of April to October. White cross-hatching represents areas of greater prediction uncertainty, where the coefficient of variation was greater than or equal to 0.5. The Olympic Coast National Marine Sanctuary is designated by a solid gray line and the 500 m isobath contour is shown as a dashed gray line. Observed density (individuals per sq. km) is shown on the inset map. Prediction and observed density color gradient classes are based on the cumulative distribution of predicted relative densities and represent 5% quantile intervals of the sum of predictions. Refer to Figure D5 for the relationship between relative density and color gradient classes.

Results and Discussion

Common Murre (*Uria aalge*): April to October

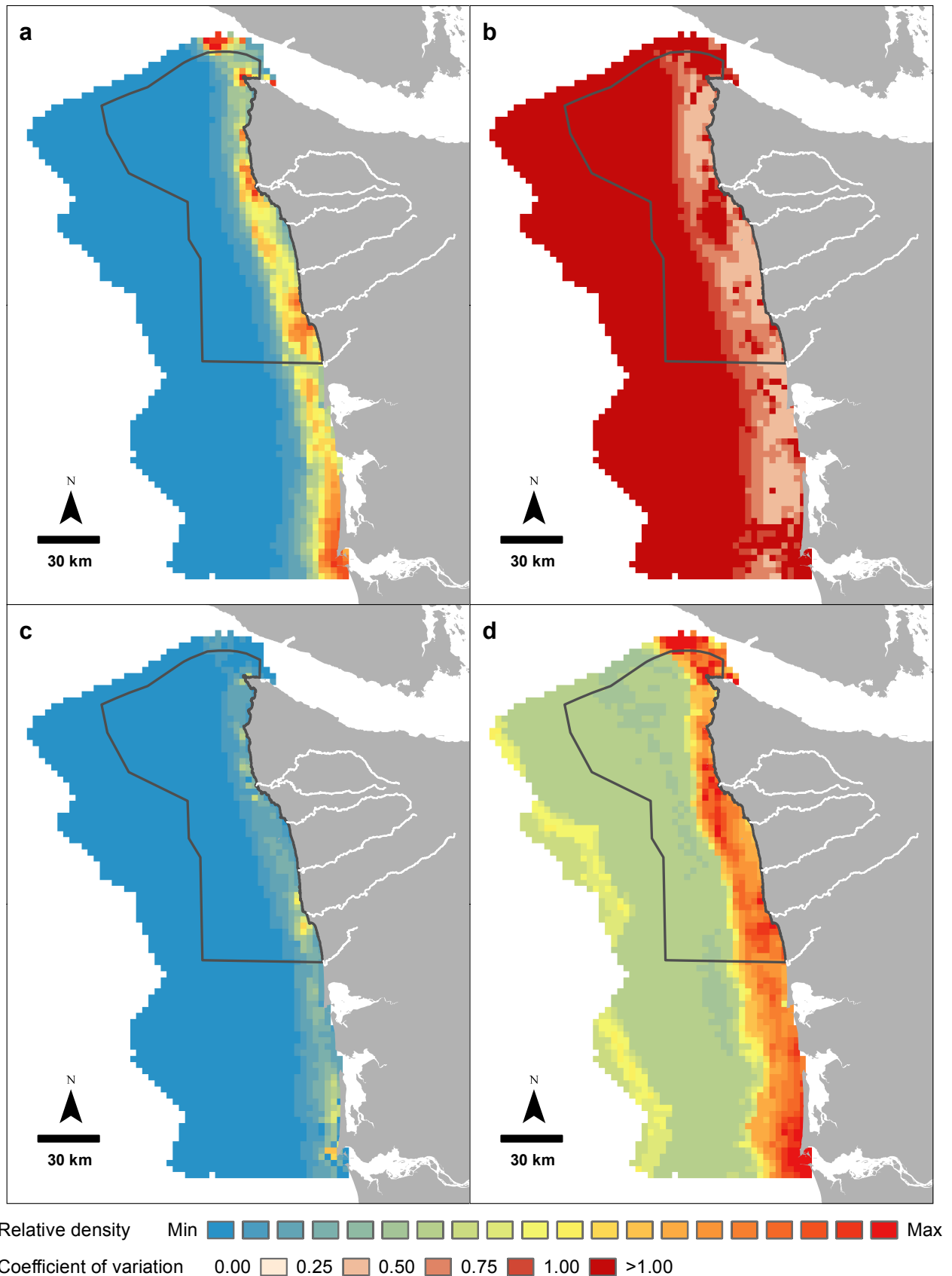
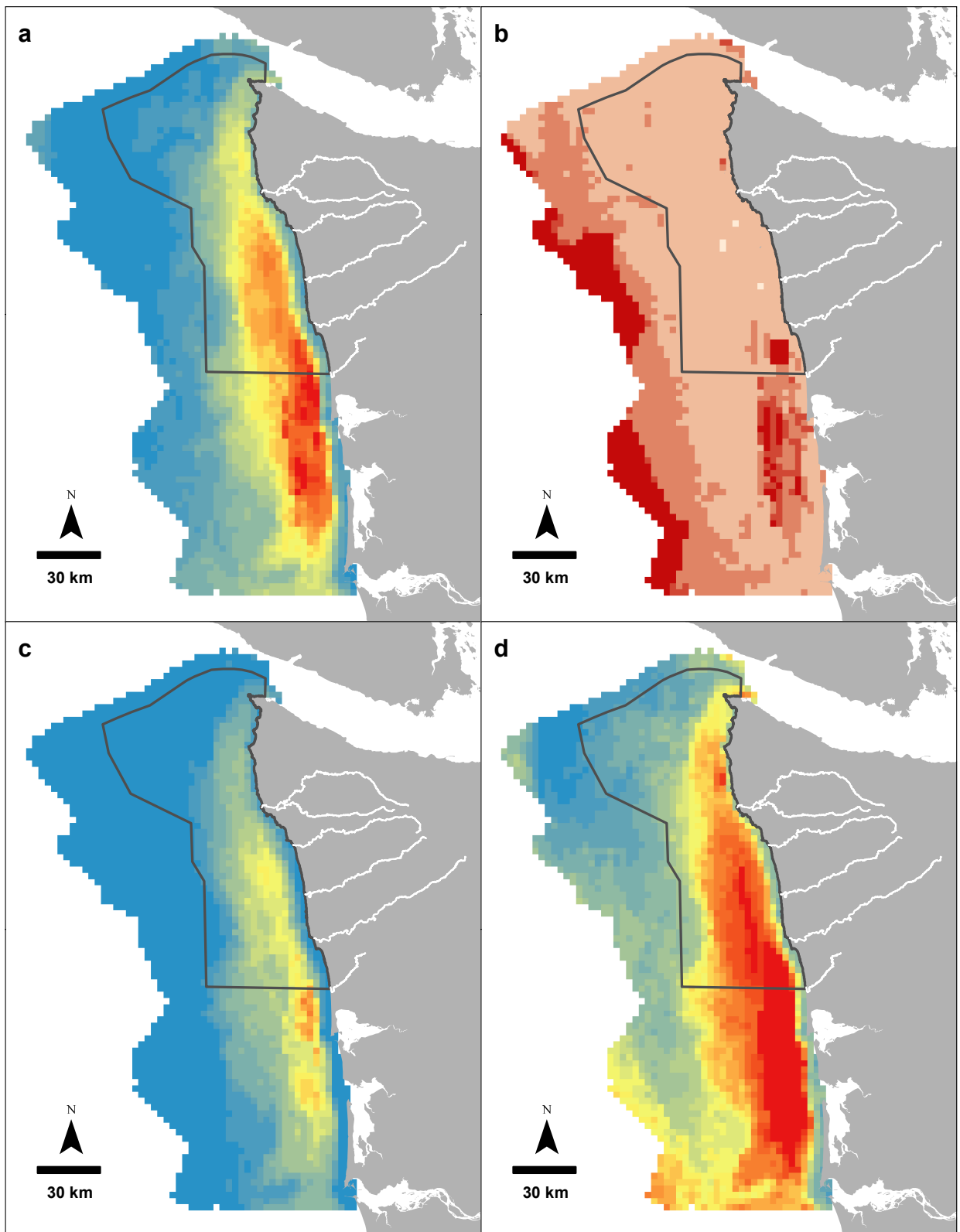


Figure 15. Long-term relative density (individuals per sq. km) prediction maps for Common Murre (*Uria aalge*) during the months of April to October: a) 50% quantile of bootstrap (median), b) coefficient of variation, c) 5% quantile of bootstrap, d) 95% quantile of bootstrap. The color gradient classes for panels c and d are the same as for panel a.

Results and Discussion

Common Murre (*Uria aalge*): November to March

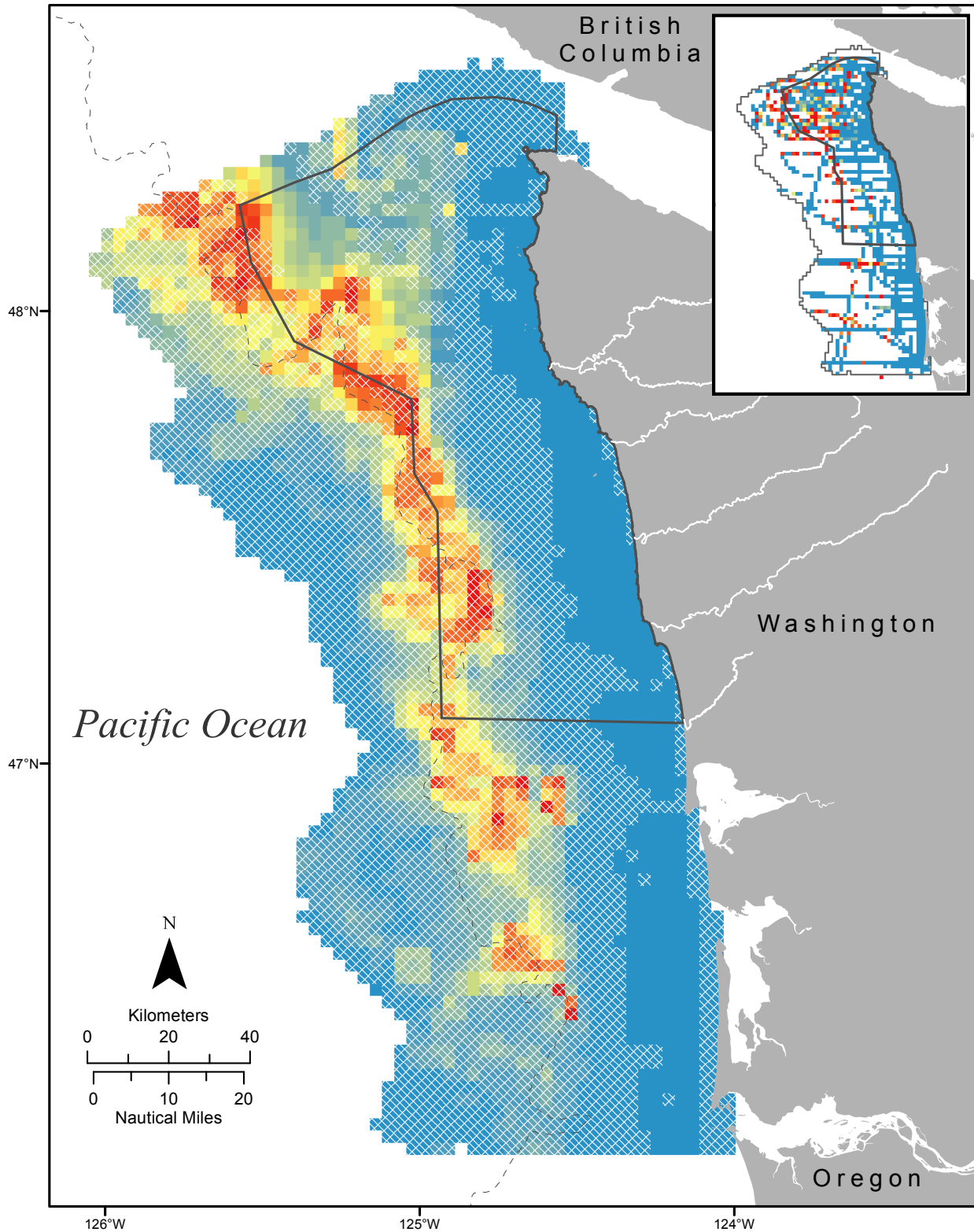


Relative density Min Max
 Coefficient of variation 0.00 0.25 0.50 0.75 1.00 >1.00

Figure 17. Long-term relative density (individuals per sq. km) prediction maps for Common Murre (*Uria aalge*) during the months of November to March: a) 50% quantile of bootstrap (median), b) coefficient of variation, c) 5% quantile of bootstrap, d) 95% quantile of bootstrap. The color gradient classes for panels c and d are the same as for panel a.

Results and Discussion

Black-footed Albatross (*Phoebastria nigripes*): April to October



Relative density Min Max

Figure 18. Long-term relative density (individuals per sq. km) prediction map for Black-footed Albatross (*Phoebastria nigripes*) during the months of April to October. White cross-hatching represents areas of greater prediction uncertainty, where the coefficient of variation was greater than or equal to 0.5. The Olympic Coast National Marine Sanctuary is designated by a solid gray line and the 500 m isobath contour is shown as a dashed gray line. Observed density (individuals per sq. km) is shown on the inset map. Prediction and observed density color gradient classes are based on the cumulative distribution of predicted relative densities and represent 5% quantile intervals of the sum of predictions. Refer to Figure D7 for the relationship between relative density and color gradient classes.

Results and Discussion

Black-footed Albatross (*Phoebastria nigripes*): April to October

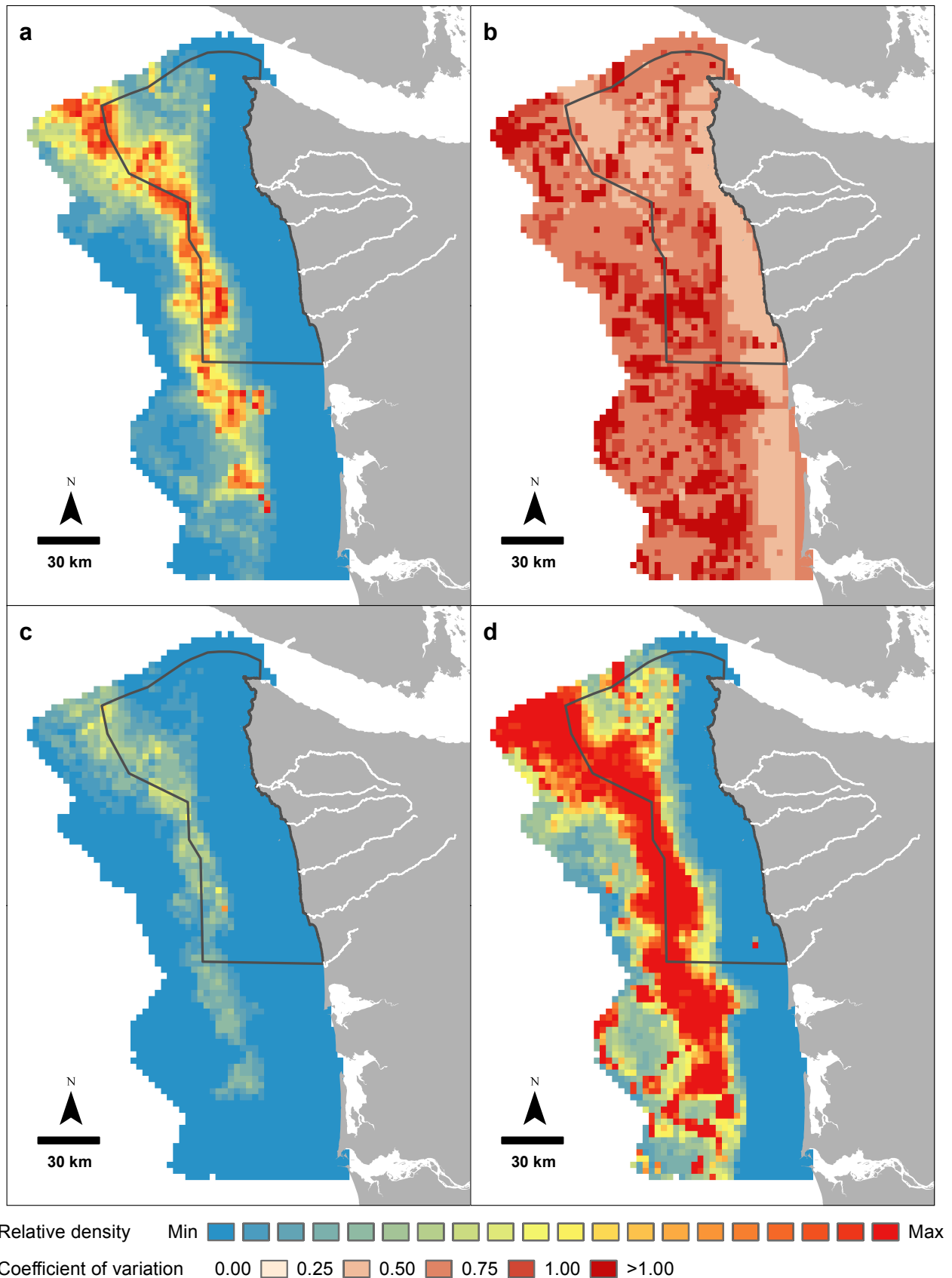
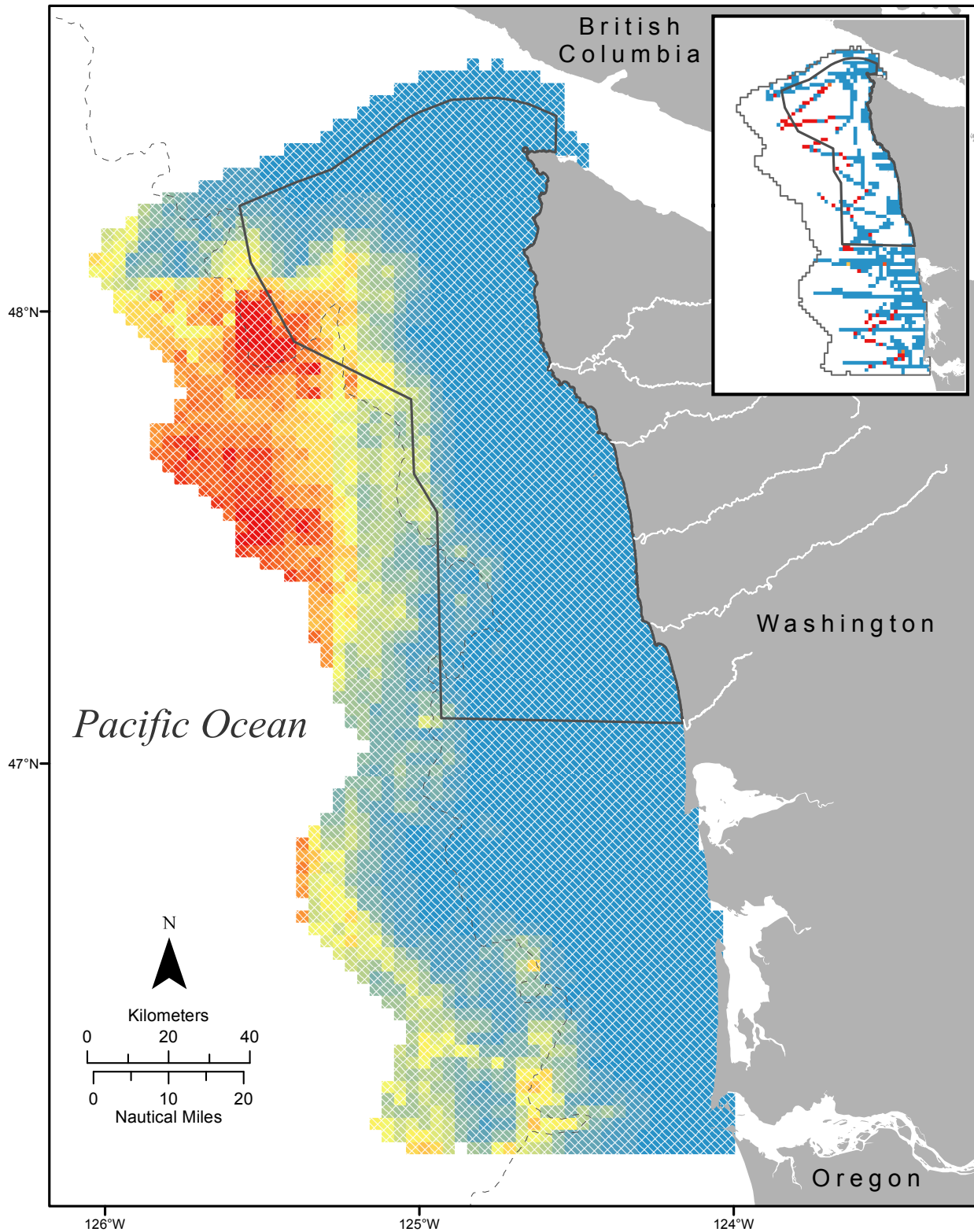


Figure 19. Long-term relative density (individuals per sq. km) prediction maps for Black-footed Albatross (*Phoebastria nigripes*) during the months of April to October: a) 50% quantile of bootstrap (median), b) coefficient of variation, c) 5% quantile of bootstrap, d) 95% quantile of bootstrap. The color gradient classes for panels c and d are the same as for panel a.

Results and Discussion

Black-footed Albatross (*Phoebastria nigripes*): November to March



Relative density Min Max

Figure 20. Long-term relative density (individuals per sq. km) prediction map for Black-footed Albatross (*Phoebastria nigripes*) during the months of November to March. White cross-hatching represents areas of greater prediction uncertainty, where the coefficient of variation was greater than or equal to 0.5. The Olympic Coast National Marine Sanctuary is designated by a solid gray line and the 500 m isobath contour is shown as a dashed gray line. Observed density (individuals per sq. km) is shown on the inset map. Prediction and observed density color gradient classes are based on the cumulative distribution of predicted relative densities and represent 5% quantile intervals of the sum of predictions. Refer to Figure D8 for the relationship between relative density and color gradient classes.

Results and Discussion

Black-footed Albatross (*Phoebastria nigripes*): November to March

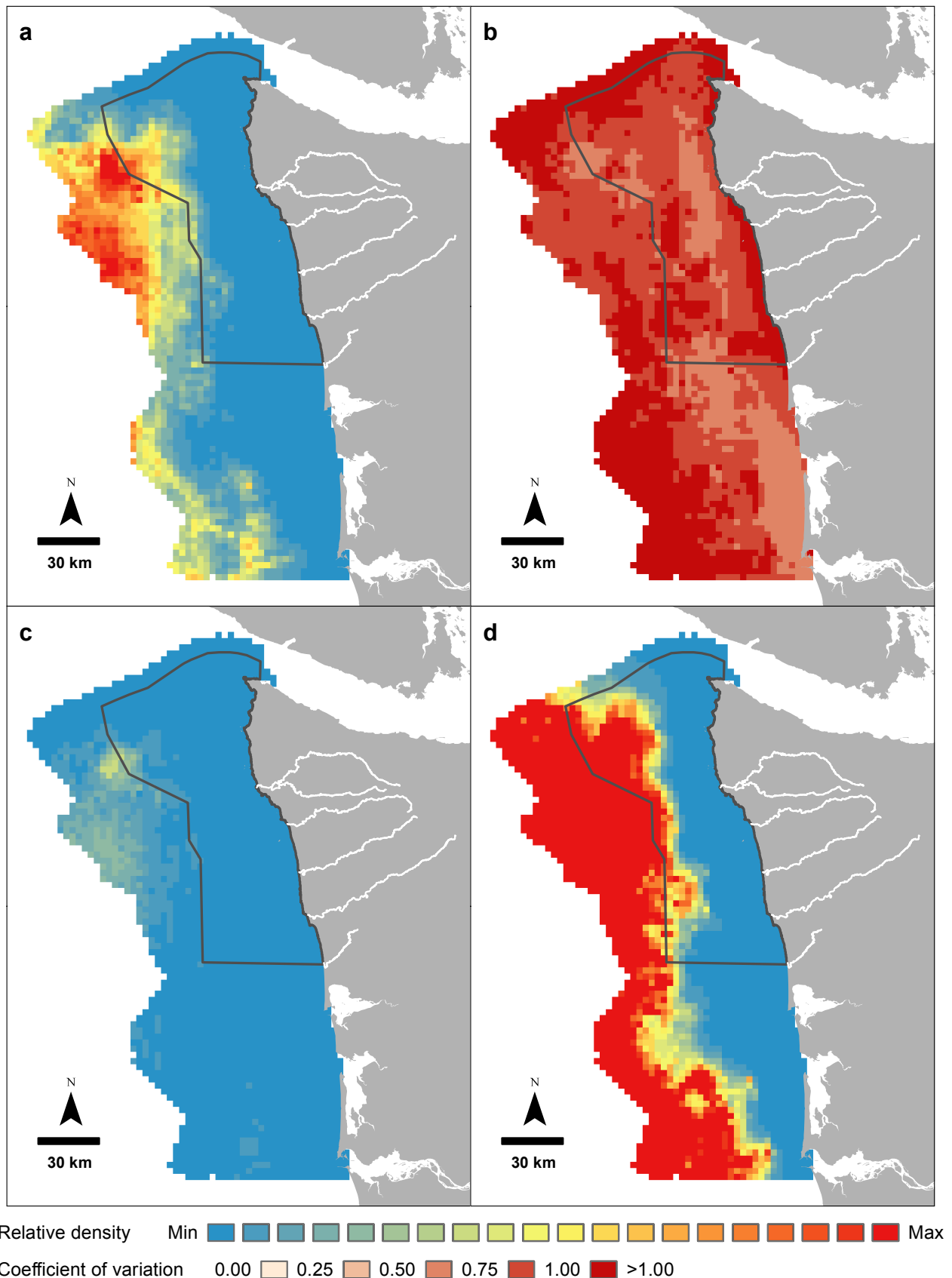
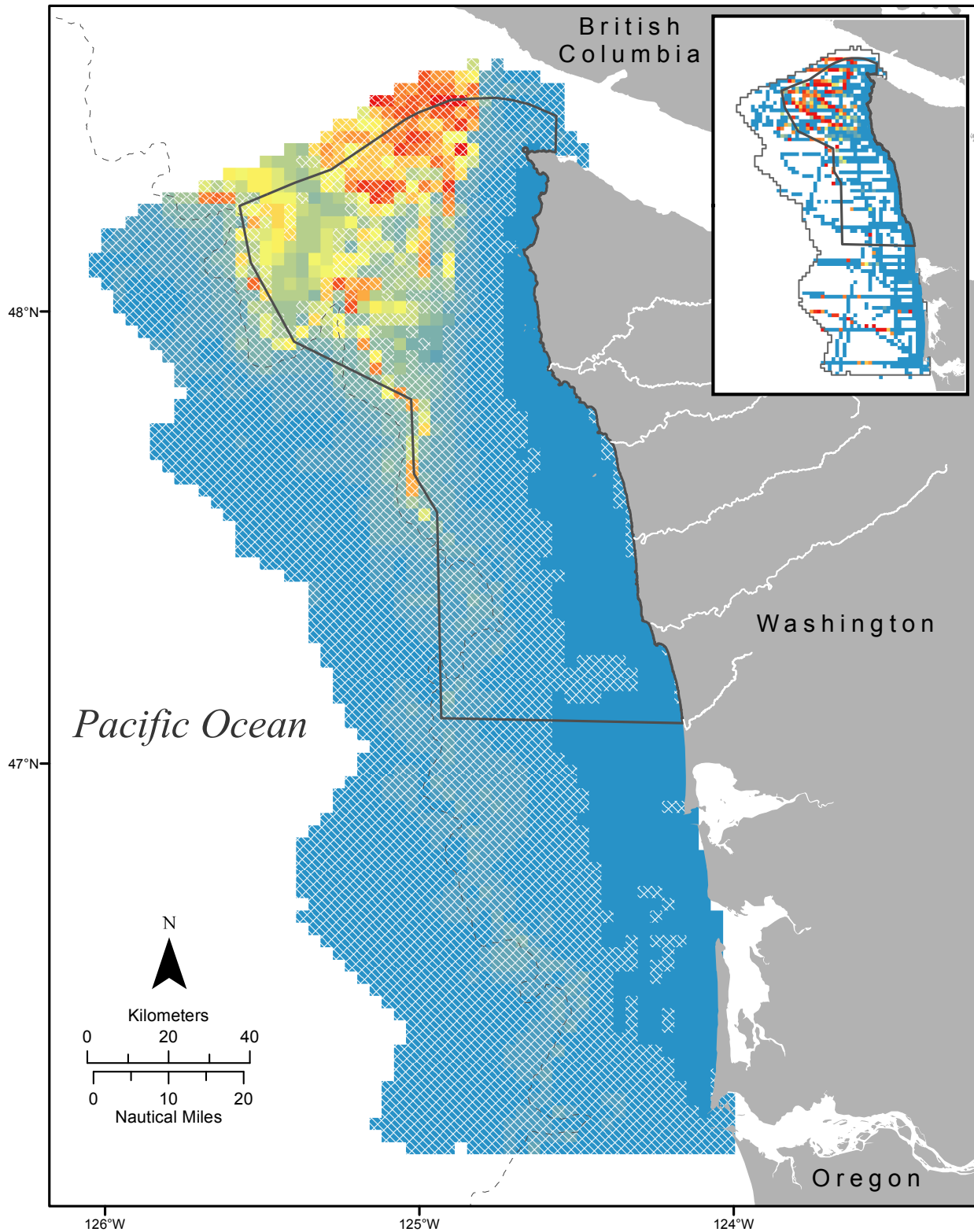


Figure 21. Long-term relative density (individuals per sq. km) prediction maps for Black-footed Albatross (*Phoebastria nigripes*) during the months of November to March: a) 50% quantile of bootstrap (median), b) coefficient of variation, c) 5% quantile of bootstrap, d) 95% quantile of bootstrap. The color gradient classes for panels c and d are the same as for panel a.

Results and Discussion

Northern Fulmar (*Fulmarus glacialis*): April to October



Relative density Min Max

Figure 22. Long-term relative density (individuals per sq. km) prediction map for Northern Fulmar (*Fulmarus glacialis*) during the months of April to October. White cross-hatching represents areas of greater prediction uncertainty, where the coefficient of variation was greater than or equal to 0.5. The Olympic Coast National Marine Sanctuary is designated by a solid gray line and the 500 m isobath contour is shown as a dashed gray line. Observed density (individuals per sq. km) is shown on the inset map. Prediction and observed density color gradient classes are based on the cumulative distribution of predicted relative densities and represent 5% quantile intervals of the sum of predictions. Refer to Figure D9 for the relationship between relative density and color gradient classes.

Results and Discussion

Northern Fulmar (*Fulmarus glacialis*): April to October

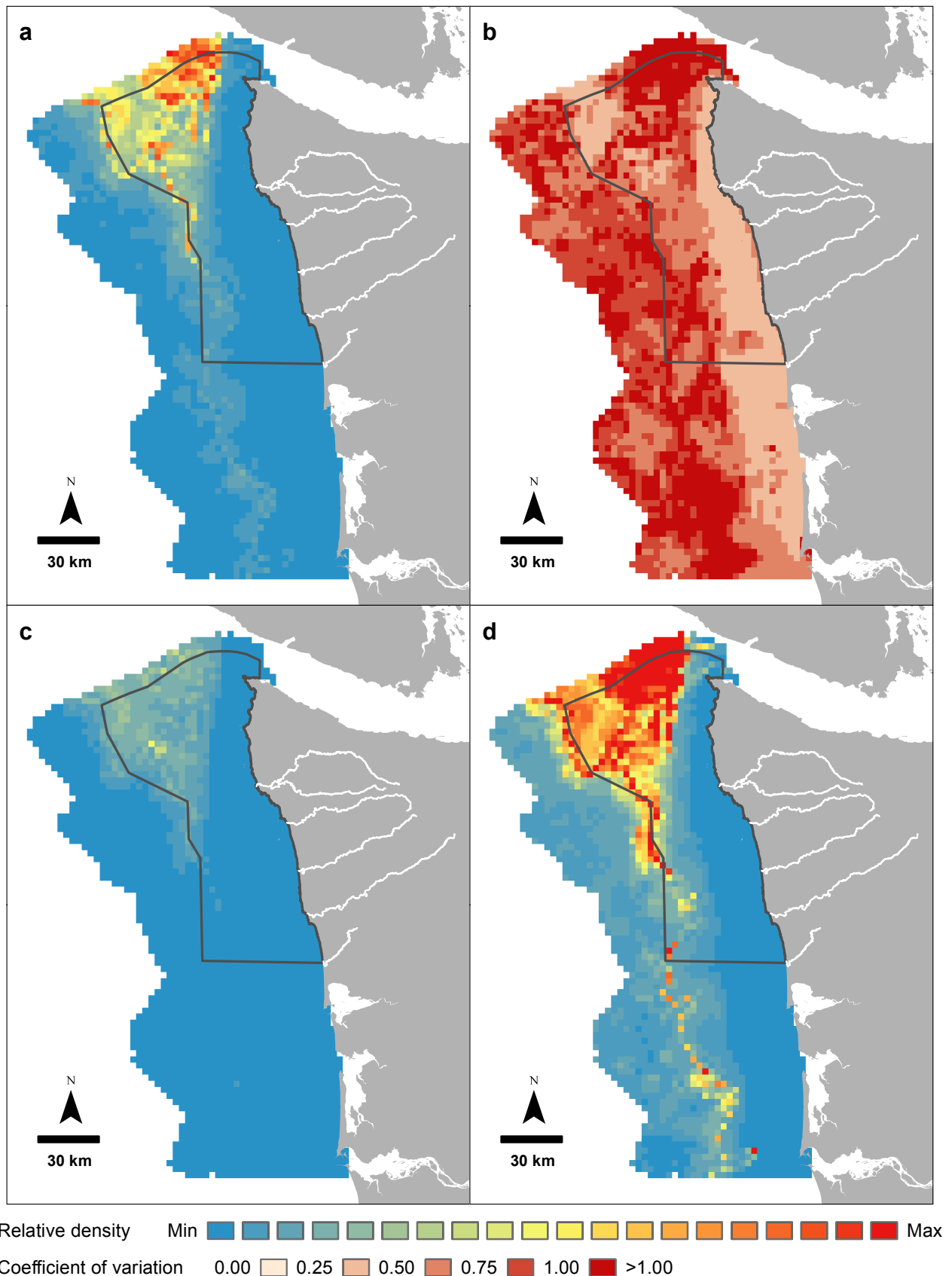
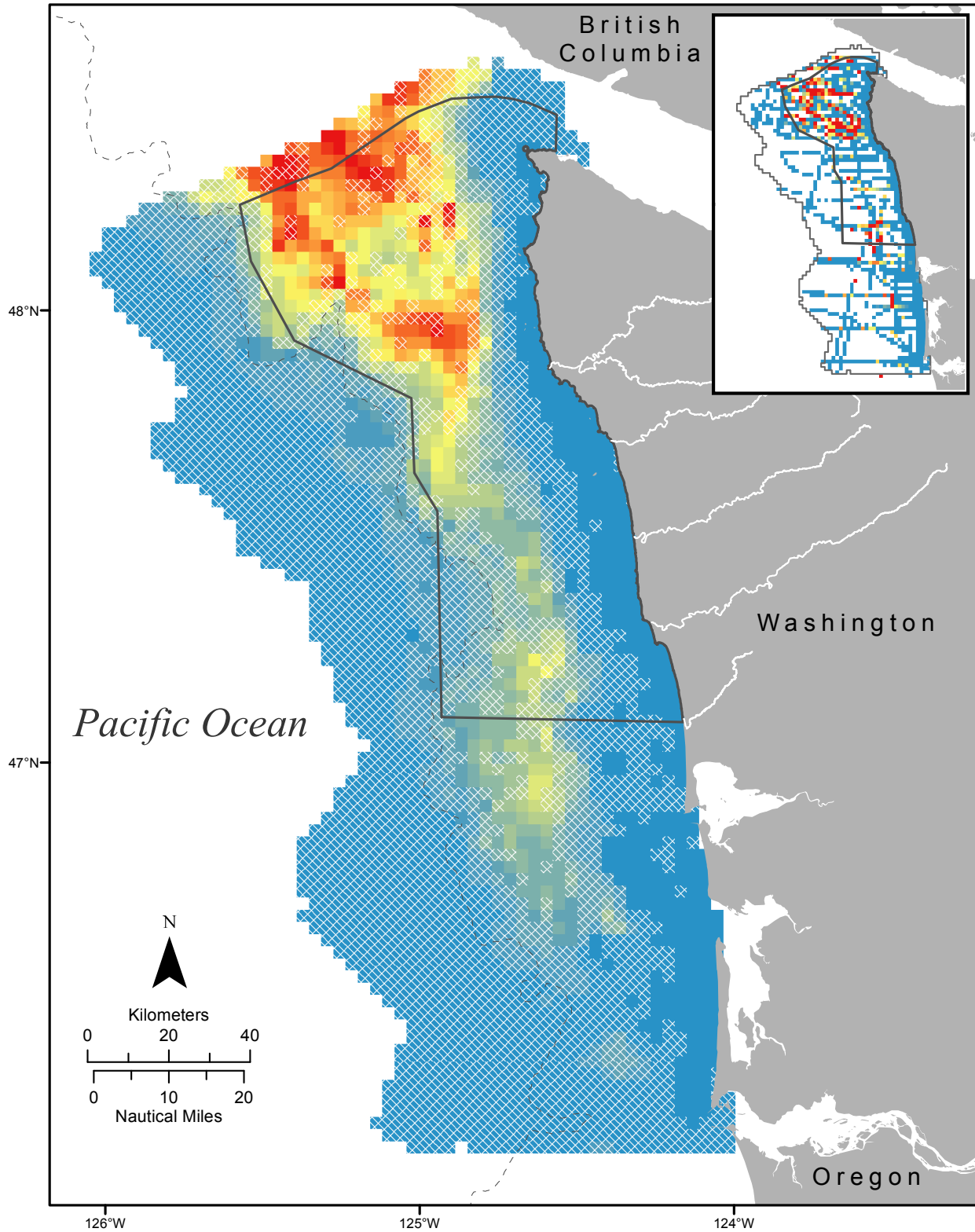


Figure 23. Long-term relative density (individuals per sq. km) prediction maps for Northern Fulmar (*Fulmarus glacialis*) during the months of April to October: a) 50% quantile of bootstrap (median), b) coefficient of variation, c) 5% quantile of bootstrap, d) 95% quantile of bootstrap. The color gradient classes for panels c and d are the same as for panel a.

Results and Discussion

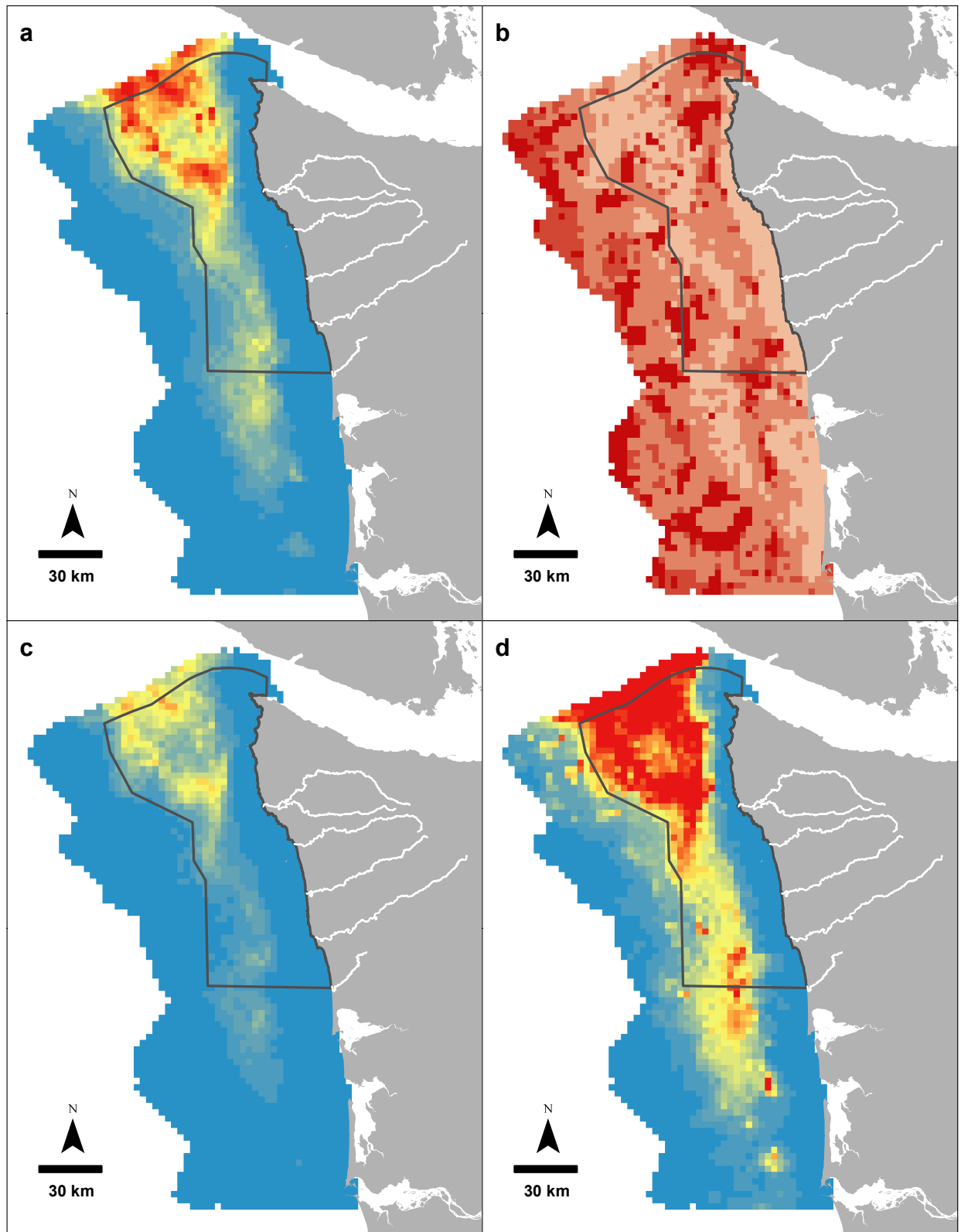
Pink-footed Shearwater (*Puffinus creatopus*): April to October



Relative density Min

Results and Discussion

Pink-footed Shearwater (*Puffinus creatopus*): April to October

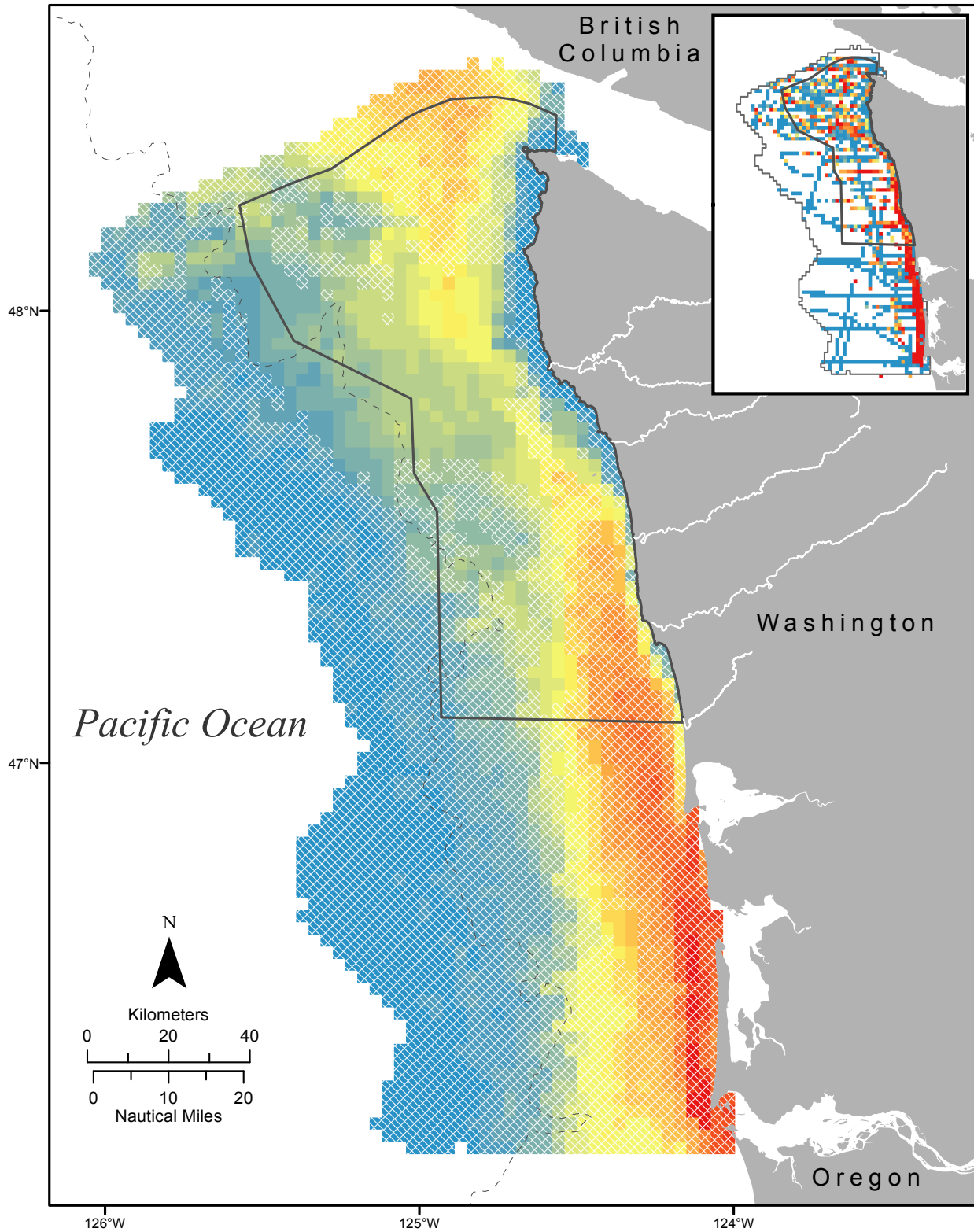


Relative density Min Max
Coefficient of variation 0.00 >1.00

Figure 25. Long-term relative density (individuals per sq. km) prediction maps for Pink-footed Shearwater (*Puffinus creatopus*) during the months of April to October: a) 50% quantile of bootstrap (median), b) coefficient of variation, c) 5% quantile of bootstrap, d) 95% quantile of bootstrap. The color gradient classes for panels c and d are the same as for panel a.

Results and Discussion

Sooty Shearwater (*Puffinus griseus*): April to October



Relative density Min Max

Figure 26. Long-term relative density (individuals per sq. km) prediction map for Sooty Shearwater (*Puffinus griseus*) during the months of April to October. White cross-hatching represents areas of greater prediction uncertainty, where the coefficient of variation was greater than or equal to 0.5. The Olympic Coast National Marine Sanctuary is designated by a solid gray line and the 500 m isobath contour is shown as a dashed gray line. Observed density (individuals per sq. km) is shown on the inset map. Prediction and observed density color gradient classes are based on the cumulative distribution of predicted relative densities and represent 5% quantile intervals of the sum of predictions. Refer to Figure D11 for the relationship between relative density and color gradient classes.

Results and Discussion

Sooty Shearwater (*Puffinus griseus*): April to October

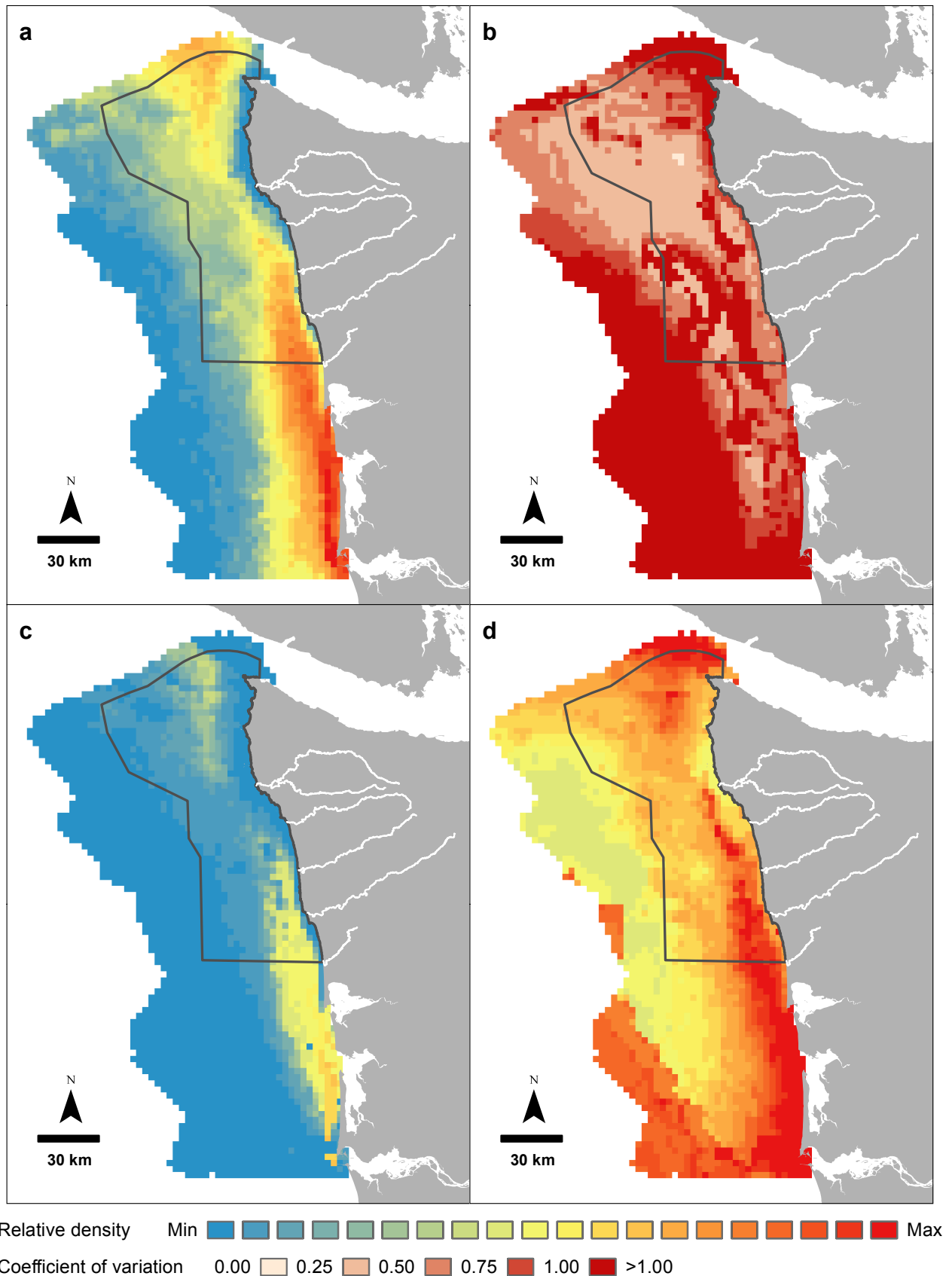


Figure 27. Long-term relative density (individuals per sq. km) prediction maps for Sooty Shearwater (*Puffinus griseus*) during the months of April to October: a) 50% quantile of bootstrap (median), b) coefficient of variation, c) 5% quantile of bootstrap, d) 95% quantile of bootstrap. The color gradient classes for panels c and d are the same as for panel a.

Results and Discussion

Steller sea lion (*Eumetopias jubatus*): April to October

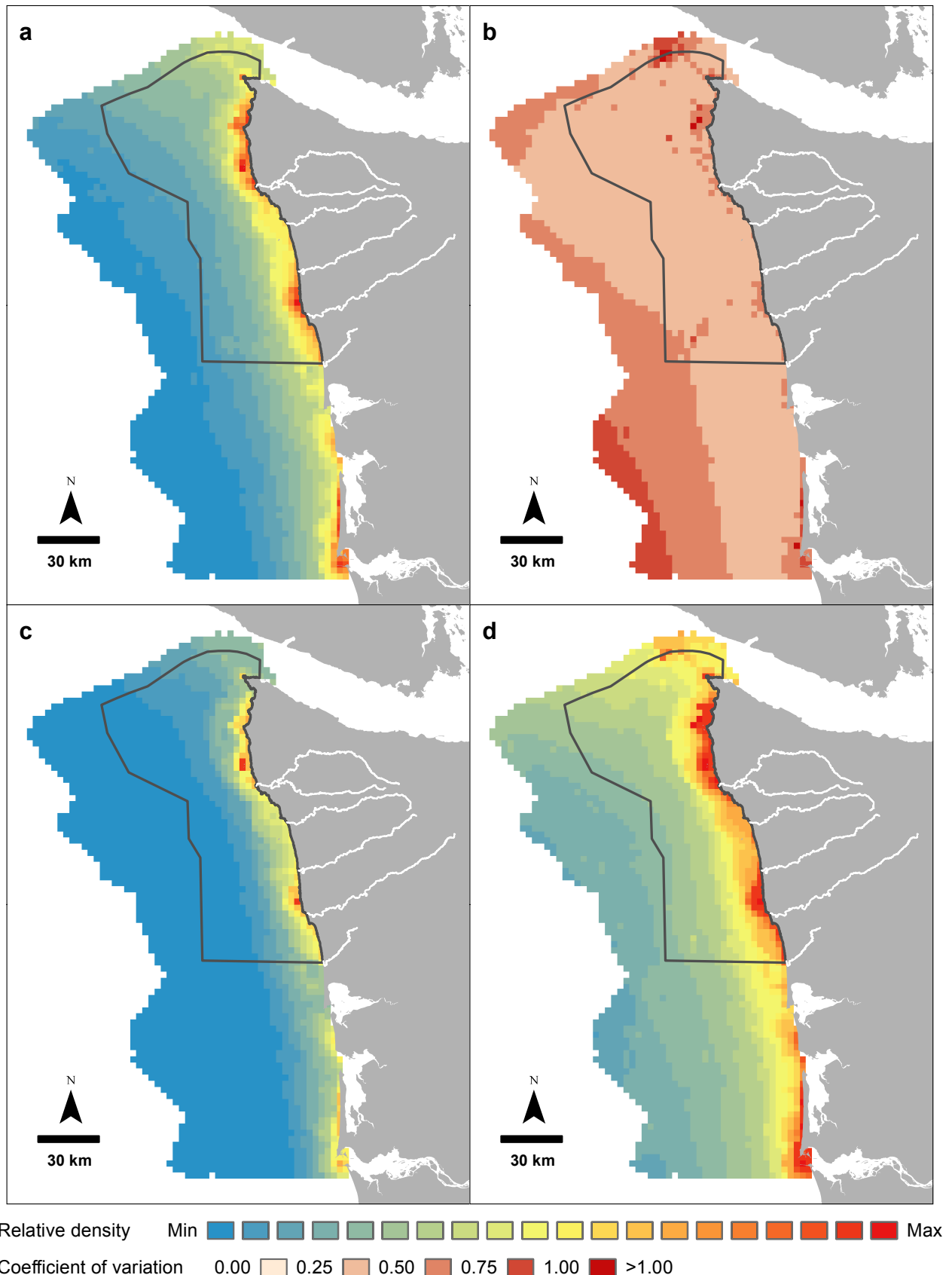


Figure 29. Long-term relative density (individuals per sq. km) prediction maps for Steller sea lion (*Eumetopias jubatus*) during the months of April to October: a) 50% quantile of bootstrap (median), b) coefficient of variation, c) 5% quantile of bootstrap, d) 95% quantile of bootstrap. The color gradient classes for panels c and d are the same as for panel a.

Results and Discussion

harbor seal (*Phoca vitulina*): April to October

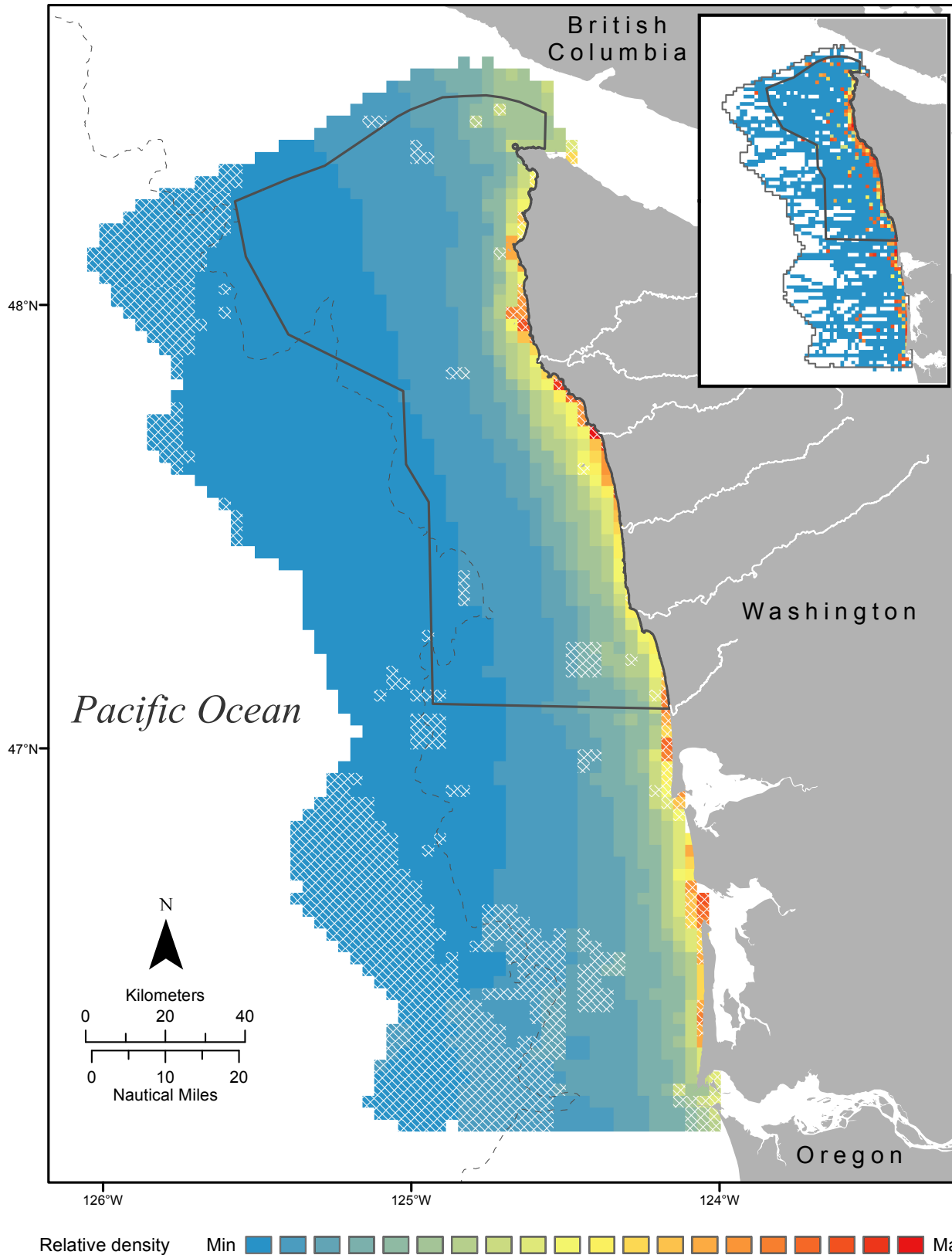


Figure 30. Long-term relative density (individuals per sq. km) prediction map for harbor seal (*Phoca vitulina*) during the months of April to October. White cross-hatching represents areas of greater prediction uncertainty, where the coefficient of variation was greater than or equal to 0.5. The Olympic Coast National Marine Sanctuary is designated by a solid gray line and the 500 m isobath contour is shown as a dashed gray line. Observed density (individuals per sq. km) is shown on the inset map. Prediction and observed density color gradient classes are based on the cumulative distribution of predicted relative densities and represent 5% quantile intervals of the sum of predictions. Refer to Figure D13 for the relationship between relative density and color gradient classes.

Results and Discussion

harbor seal (*Phoca vitulina*): April to October

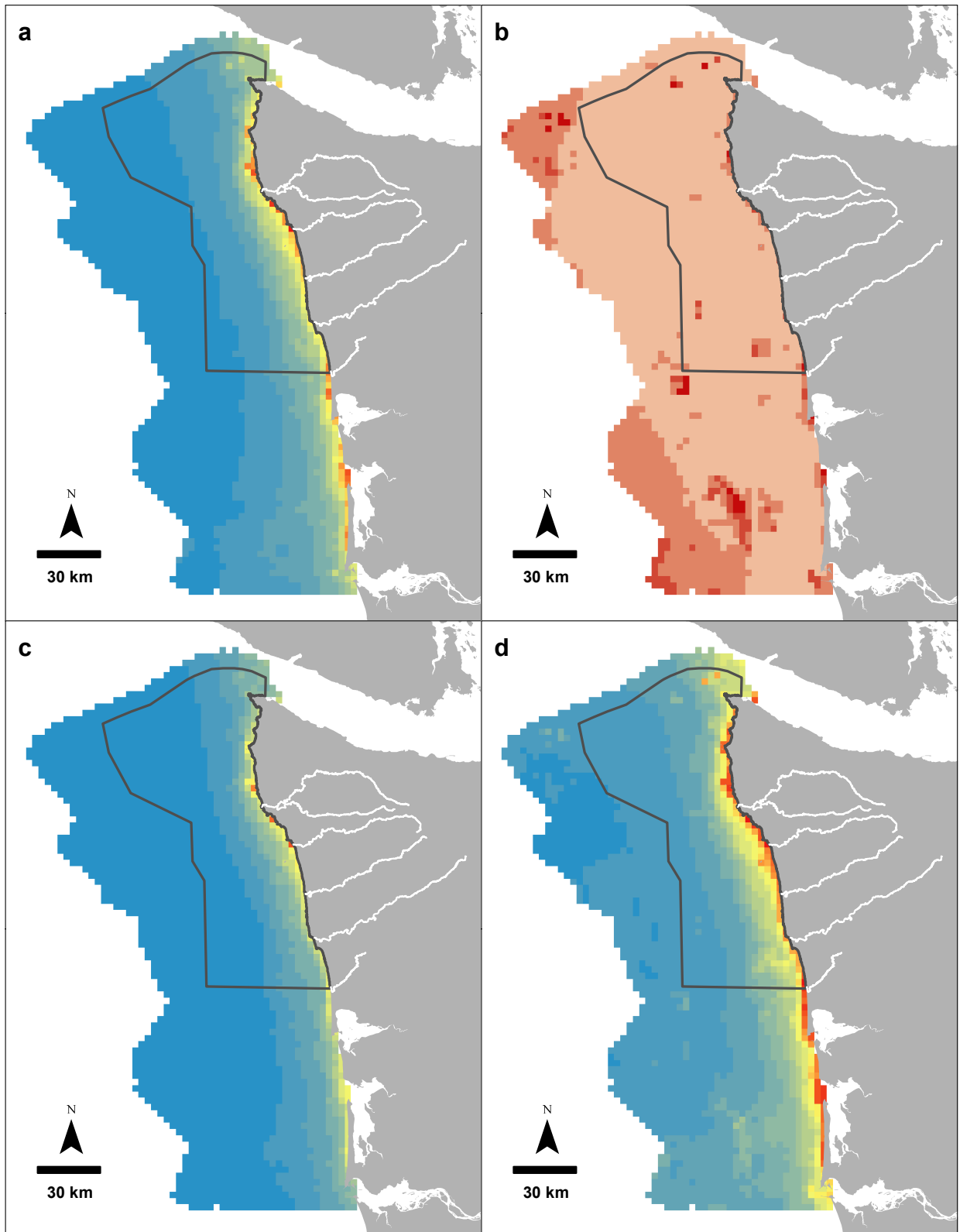


Figure 31. Long-term relative density (individuals per sq. km) prediction maps for harbor seal (*Phoca vitulina*) during the months of April to October: a) 50% quantile of bootstrap (median), b) coefficient of variation, c) 5% quantile of bootstrap, d) 95% quantile of bootstrap. The color gradient classes for panels c and d are the same as for panel a.

Results and Discussion

humpback whale (*Megaptera novaeangliae*): April to October

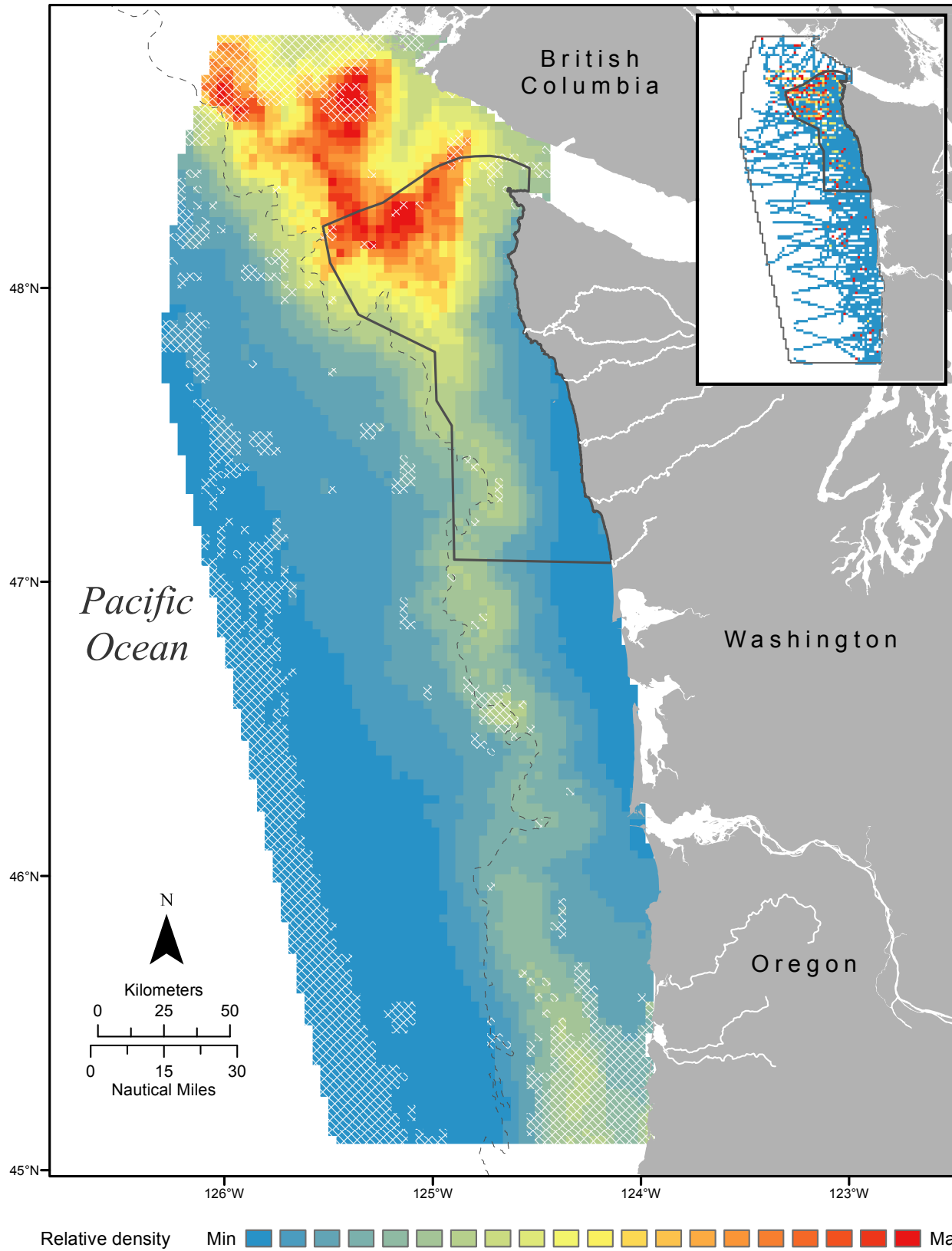


Figure 32. Long-term relative density (individuals per sq. km) prediction map for humpback whale (*Megaptera novaeangliae*) during the months of April to October. White cross-hatching represents areas of greater prediction uncertainty, where the coefficient of variation was greater than or equal to 0.5. The Olympic Coast National Marine Sanctuary is designated by a solid gray line and the 500 m isobath contour is shown as a dashed gray line. Observed density (individuals per sq. km) is shown on the inset map. Prediction and observed density color gradient classes are based on the cumulative distribution of predicted relative densities and represent 5% quantile intervals of the sum of predictions. Refer to Figure D14 for the relationship between relative density and color gradient classes.

Results and Discussion

humpback whale (*Megaptera novaeangliae*): April to October

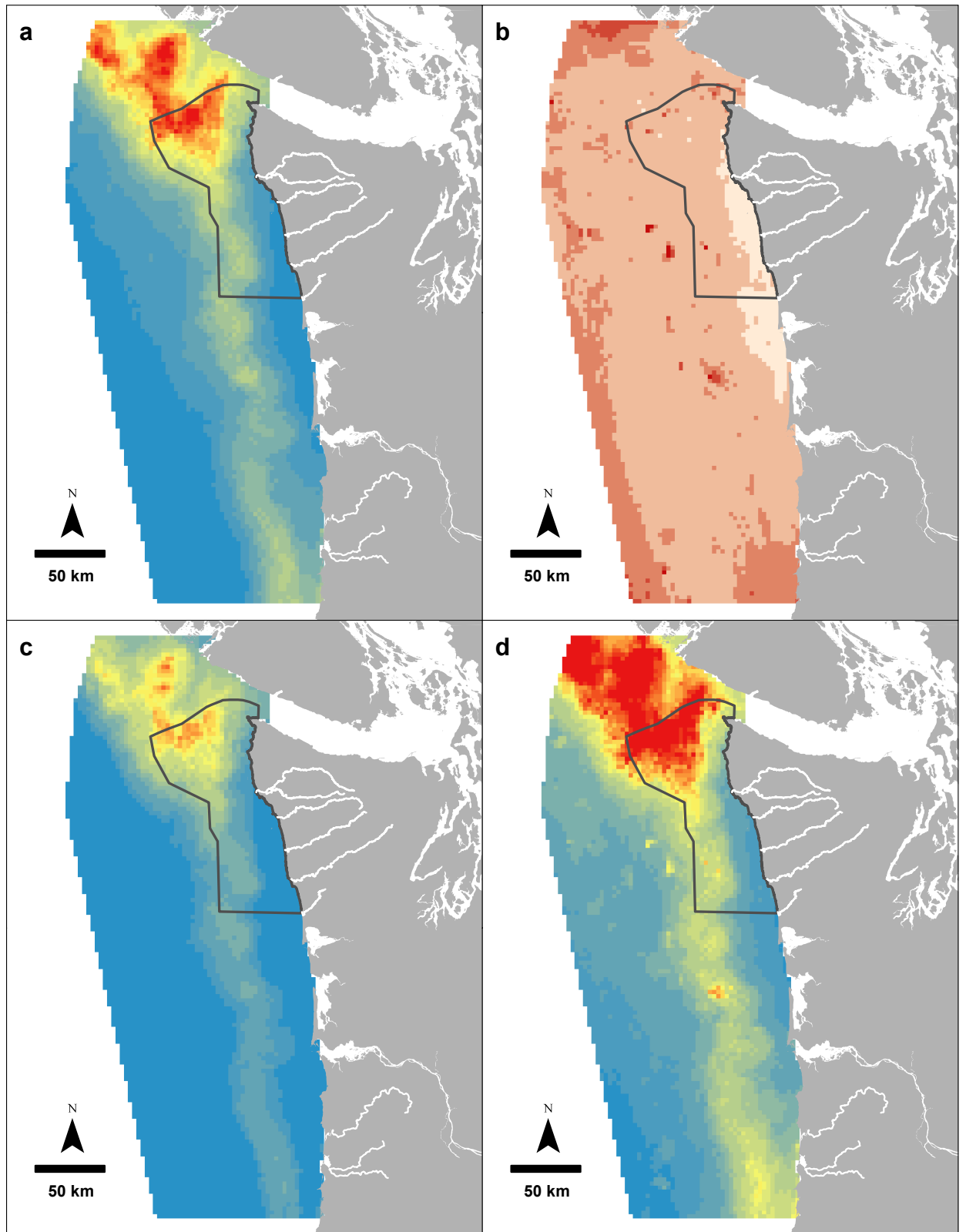


Figure 33. Long-term relative density (individuals per sq. km) prediction maps for humpback whale (*Megaptera novaeangliae*) during the months of April to October: a) 50% quantile of bootstrap (median), b) coefficient of variation, c) 5% quantile of bootstrap, d) 95% quantile of bootstrap. The color gradient classes for panels c and d are the same as for panel a.

Results and Discussion

gray whale (*Eschrichtius robustus*): April to October

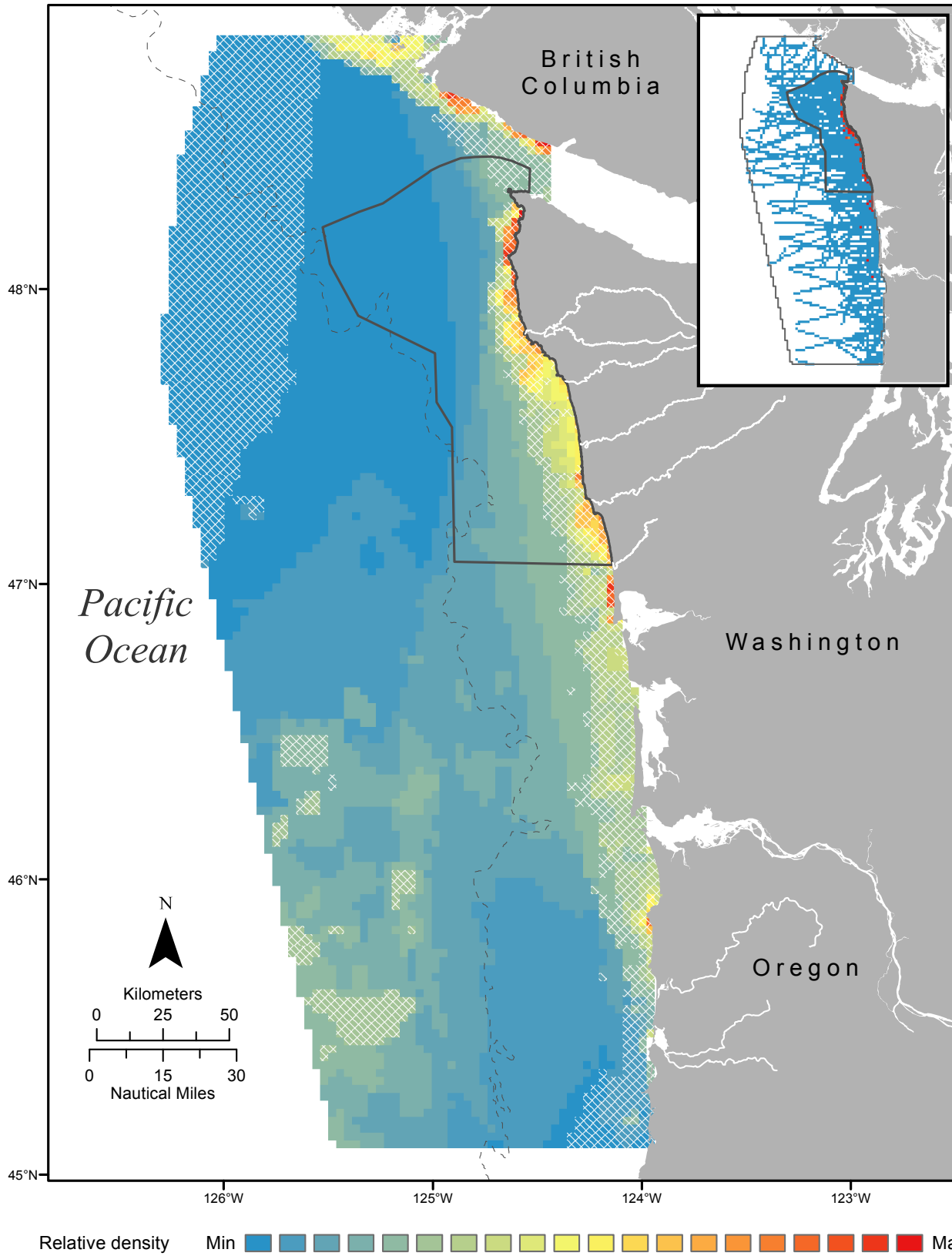


Figure 34. Long-term relative density (individuals per sq. km) prediction map for gray whale (*Eschrichtius robustus*) during the months of April to October. White cross-hatching represents areas of greater prediction uncertainty, where the coefficient of variation was greater than or equal to 0.5. The Olympic Coast National Marine Sanctuary is designated by a solid gray line and the 500 m isobath contour is shown as a dashed gray line. Observed density (individuals per sq. km) is shown on the inset map. Prediction and observed density color gradient classes are based on the cumulative distribution of predicted relative densities and represent 5% quantile intervals of the sum of predictions. Refer to Figure D15 for the relationship between relative density and color gradient classes.

Results and Discussion

gray whale (*Eschrichtius robustus*): April to October

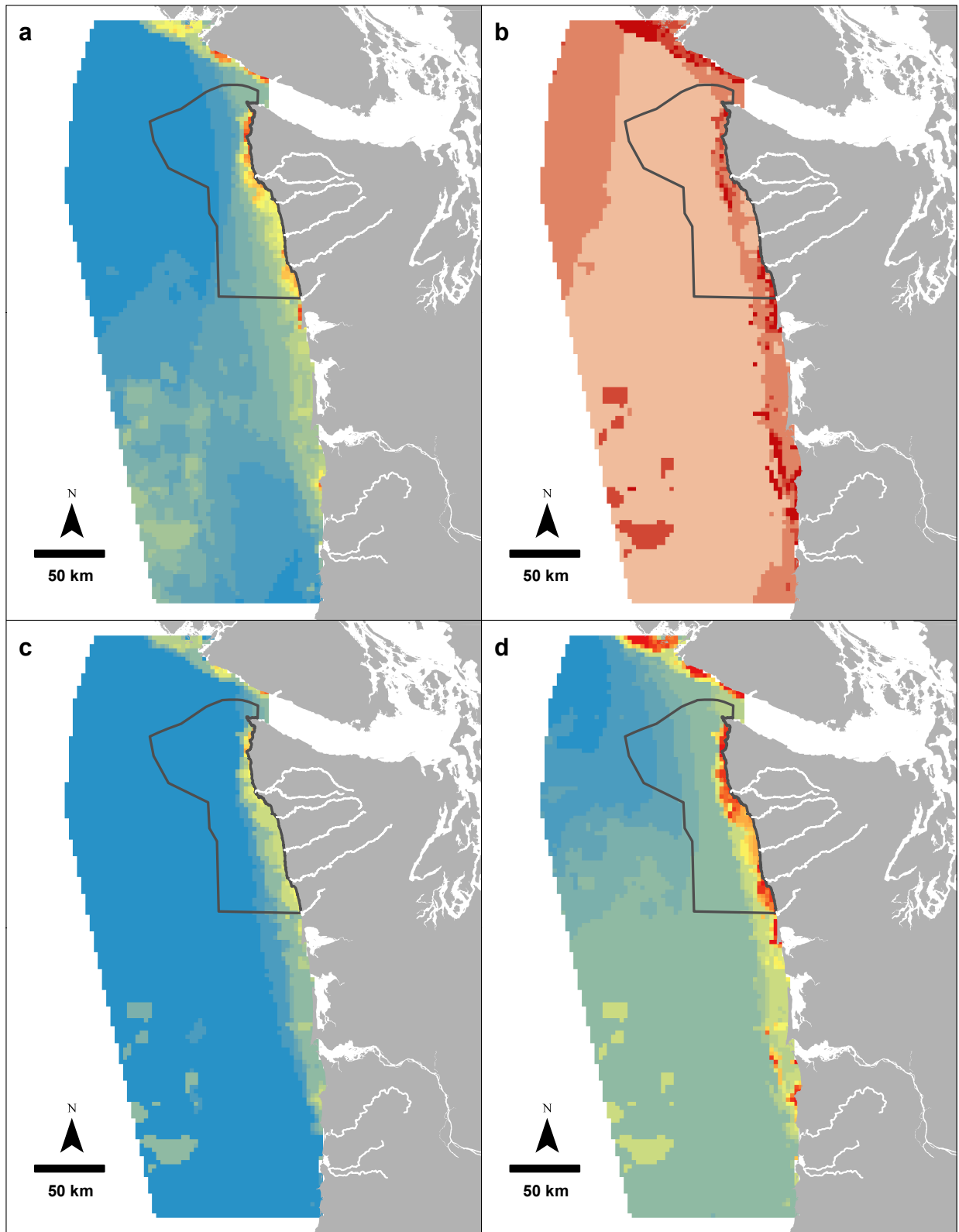


Figure 35. Long-term relative density (individuals per sq. km) prediction maps for gray whale (*Eschrichtius robustus*) during the months of April to October: a) 50% quantile of bootstrap (median), b) coefficient of variation, c) 5% quantile of bootstrap, d) 95% quantile of bootstrap. The color gradient classes for panels c and d are the same as for panel a.

Results and Discussion

harbor porpoise (*Phocoena phocoena*): April to October

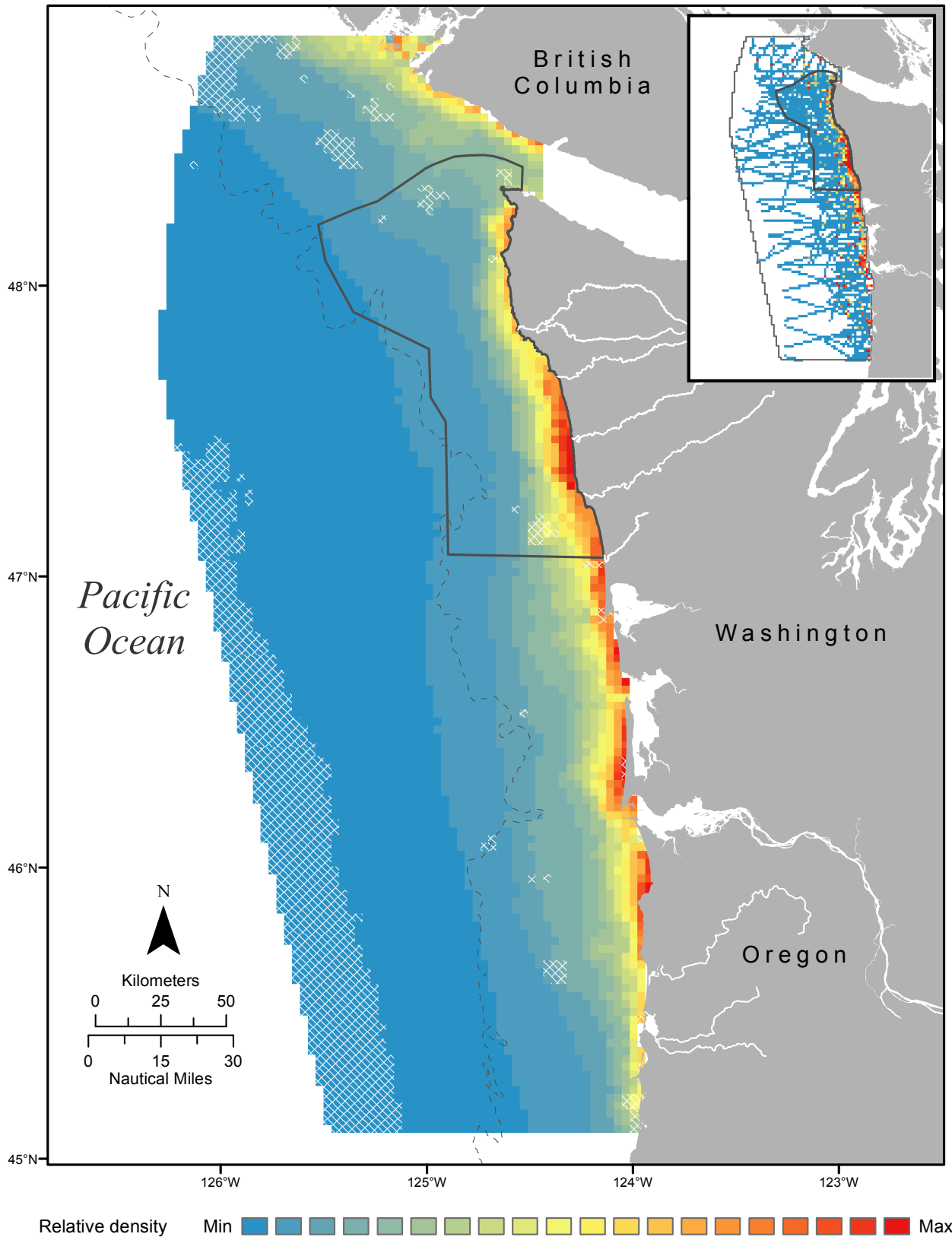


Figure 36. Long-term relative density (individuals per sq. km) prediction map for harbor porpoise (*Phocoena phocoena*) during the months of April to October. White cross-hatching represents areas of greater prediction uncertainty, where the coefficient of variation was greater than or equal to 0.5. The Olympic Coast National Marine Sanctuary is designated by a solid gray line and the 500 m isobath contour is shown as a dashed gray line. Observed density (individuals per sq. km) is shown on the inset map. Prediction and observed density color gradient classes are based on the cumulative distribution of predicted relative densities and represent 5% quantile intervals of the sum of predictions. Refer to Figure D16 for the relationship between relative density and color gradient classes.

Results and Discussion

harbor porpoise (*Phocoena phocoena*): April to October

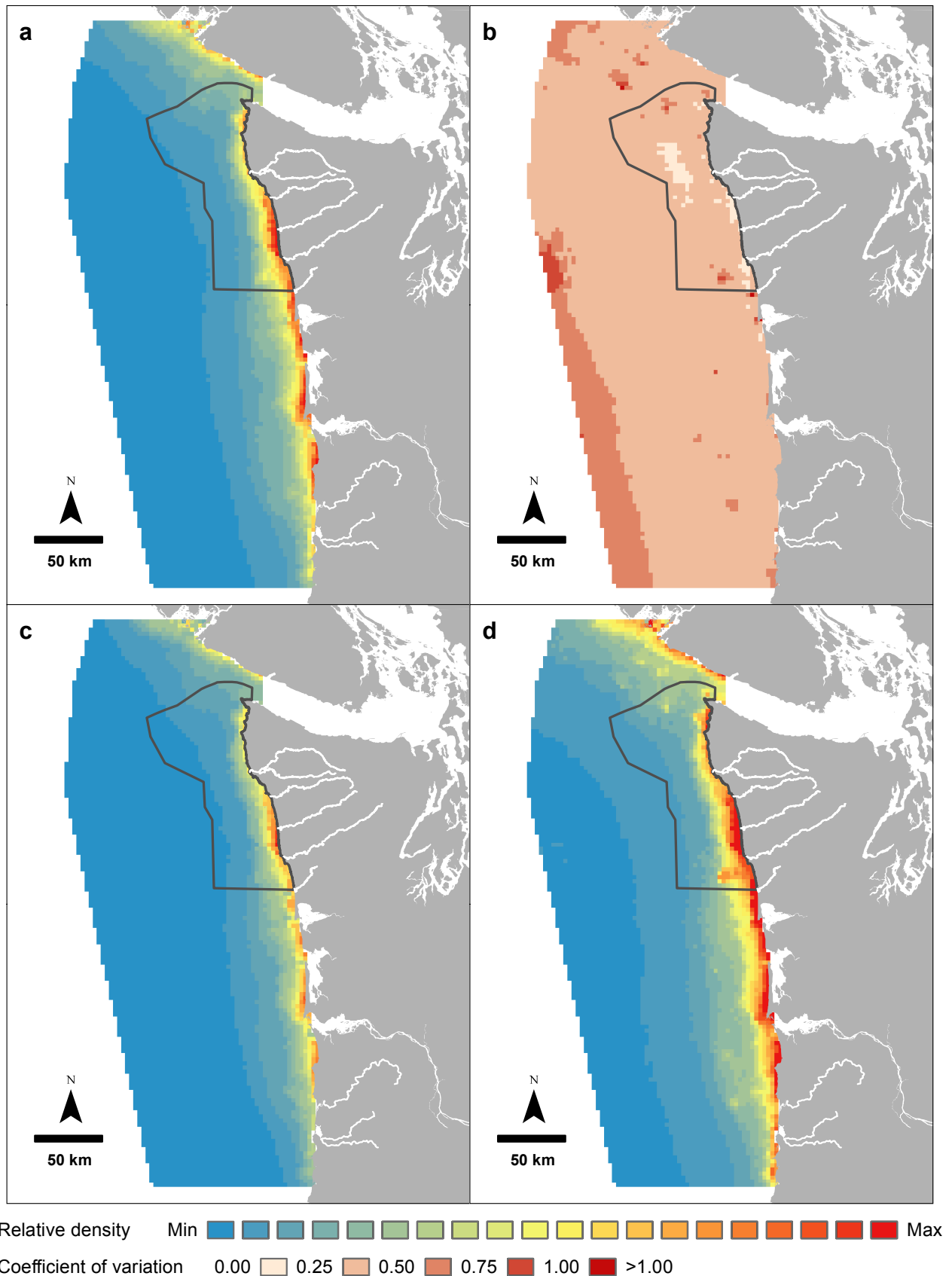


Figure 37. Long-term relative density (individuals per sq. km) prediction maps for harbor porpoise (*Phocoena phocoena*) during the months of April to October: a) 50% quantile of bootstrap (median), b) coefficient of variation, c) 5% quantile of bootstrap, d) 95% quantile of bootstrap. The color gradient classes for panels c and d are the same as for panel a.

Results and Discussion

Dall's porpoise (*Phocoenoides dalli*): April to October

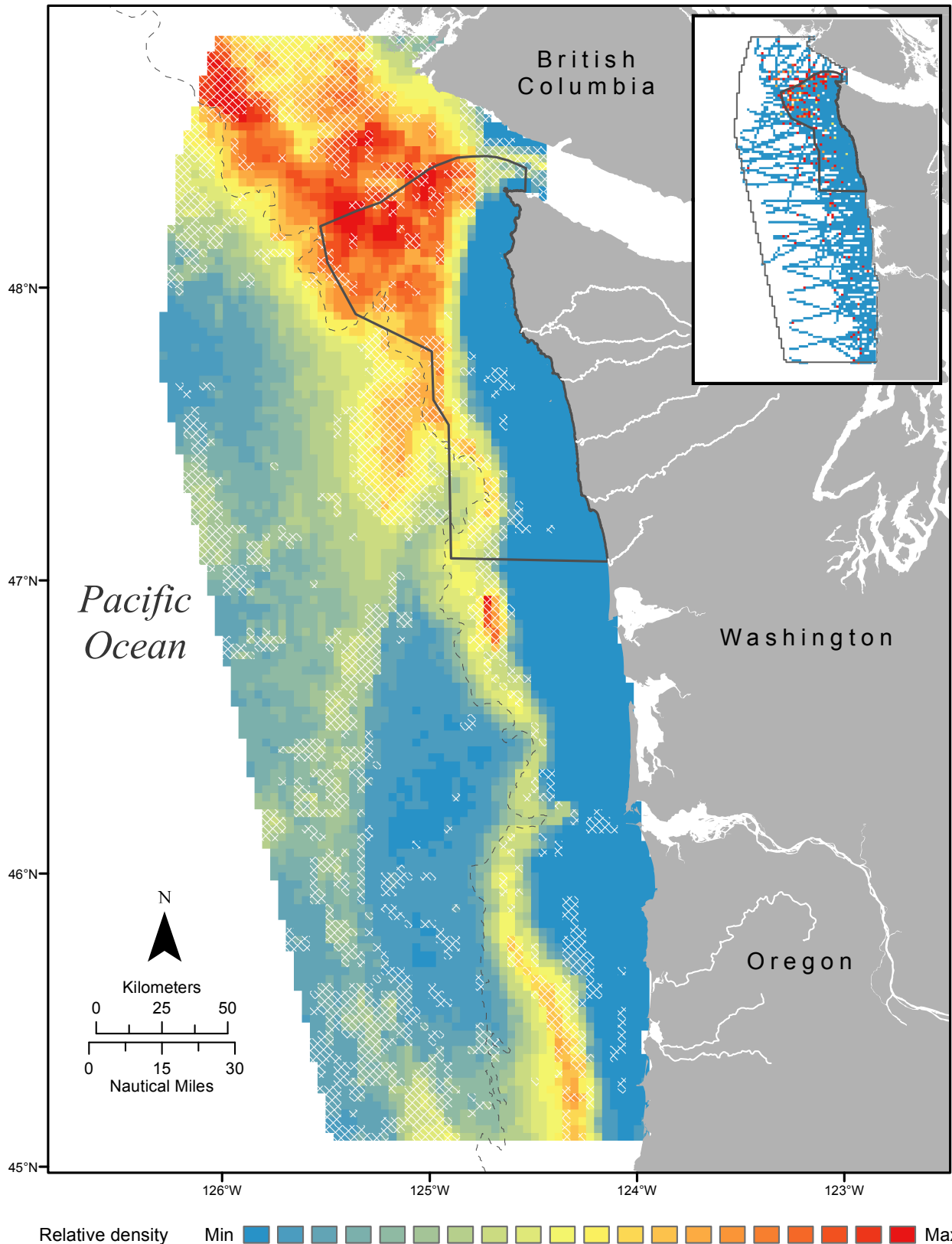


Figure 38. Long-term relative density (individuals per sq. km) prediction map for Dall's porpoise (*Phocoenoides dalli*) during the months of April to October. White cross-hatching represents areas of greater prediction uncertainty, where the coefficient of variation was greater than or equal to 0.5. The Olympic Coast National Marine Sanctuary is designated by a solid gray line and the 500 m isobath contour is shown as a dashed gray line. Observed density (individuals per sq. km) is shown on the inset map. Prediction and observed density color gradient classes are based on the cumulative distribution of predicted relative densities and represent 5% quantile intervals of the sum of predictions. Refer to Figure D17 for the relationship between relative density and color gradient classes.

Results and Discussion

Dall's porpoise (*Phocoenoides dalli*): April to October

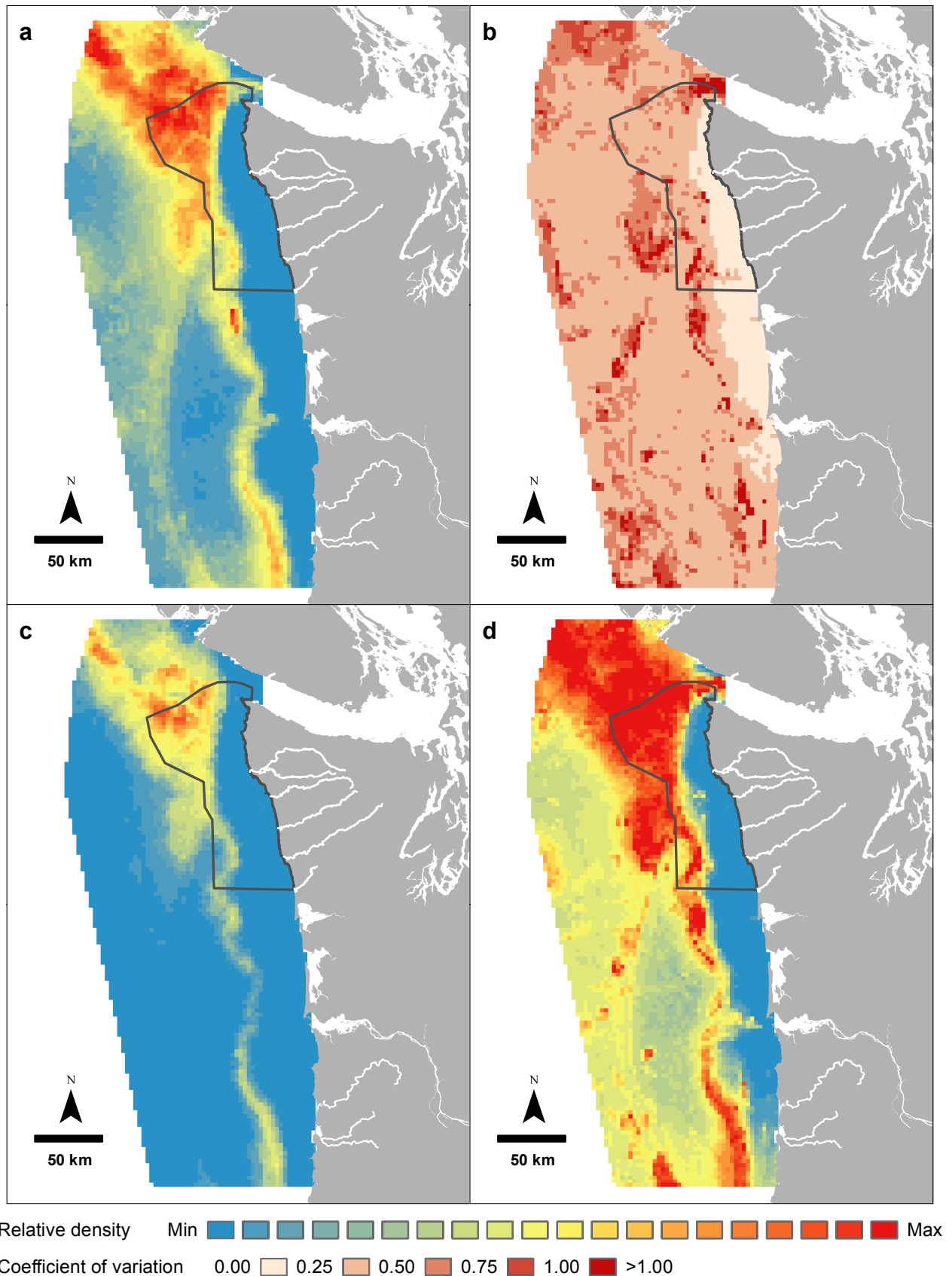


Figure 39. Long-term relative density (individuals per sq. km) prediction maps for Dall's porpoise (*Phocoenoides dalli*) during the months of April to October: a) 50% quantile of bootstrap (median), b) coefficient of variation, c) 5% quantile of bootstrap, d) 95% quantile of bootstrap. The color gradient classes for panels c and d are the same as for panel a.

Results and Discussion

PREDICTIVE MODEL PERFORMANCE

Of the seventeen final predictive models, seven were zero-inflated Poisson and ten were zero-inflated negative binomial models. All but one of the models selected for marine mammal species were zero-inflated negative binomial models, whereas seabird models were more equally split among model types. The final models more frequently had a maximum tree depth of four (eleven models) versus five (six models). Most of the final models converged well before the allowed maximum number of boosting iterations, but three of the final models (Marbled Murrelet, Steller sea lion, harbor seal) reached the maximum number of iterations before converging.



Steller sea lion
Vladimir Burkanov, NOAA NMFS/AFSC/NMML

Final model performance was variable across species and seasons. In addition, performance metrics were not necessarily in agreement within a single model, meaning all metrics were helpful to assess model performance. In general, summer season seabird models performed better than pinniped, cetacean, or winter season seabird models. Table 9 and Appendix C show model performance metrics for final selected models and all fitted models, respectively (see Model performance and selection for more information on model selection). The area under the receiver operating characteristic curve (AUC), one of the most widely used of the model performance metrics presented, ranged from 86% to 97% across all species. Summer season Northern Fulmar and winter season Black-footed Albatross models had the highest AUC scores. Percent deviance explained scores ranged from 24% to 83% across all models, and summer season Sooty Shearwater and Common Murre models had the highest percent deviance explained (PDE) scores. The Gaussian rank correlation coefficient ranged from 0.26 to 0.75, with the highest values for summer season Common Murre and Rhinoceros Auklet models. The median absolute residual error as percentage of individuals per segment with sightings ranged from 6% to 92%, and summer season Sooty Shearwater had the best (lowest) value.



Black-footed Albatross
(David Pereksta, BOEM)

In six models (Marbled Murrelet, Rhinoceros Auklet [summer], Rhinoceros Auklet [winter], Tufted Puffin, Black-footed Albatross [winter], Steller sea lion) transect ID was selected more times than any other predictor for both the zero-inflation and count components. When transect ID, which was modeled as a random effect term, is chosen most often, it suggests that the environmental predictors are doing a poor job of explaining variability in density. Consequently, these models could probably be improved with additional predictors.

Considering all model performance metrics, the final models for Marbled Murrelet, Rhinoceros Auklet (winter), Tufted Puffin, Common Murre (summer), Black-footed Albatross (summer and winter), Northern Fulmar, Pink-footed Shearwater and Sooty Shearwater had the best overall performance (level 5), while the model for Dall's porpoise had the worst performance (level 3). The performances of all other models were classified as level 4. It is important to recognize that the model performance metrics only reflect the statistical fit of the models to the data; they do not reflect model errors associated with biases in the observation data, or the quality of model predictions away from the data.

Table 9. Performance metrics for the final selected model of each species-season combination. Also shown are number of transect segments with sightings, number of individuals sighted, proportion of transect segments with sightings (prevalence), and mean number of individuals per transect segment with sightings. All performance metrics were equally considered, according to their respective quality levels (Table 8), to determine overall model fit.

Species	Season	No. seg. with sightings	No. indiv.	Preval.	Mean no. indiv. per seg. with sightings	Model type	Max. tree depth	No. boosting iterations	PDE	AUC	r	% error	Quality level of overall model fit
Marbled Murrelet	summer	1,625	5,604	0.16	3.4	ZINB	4	20,000	52%	0.92	0.64	32%	5
Rhinoceros Auklet	summer	4,593	116,224	0.45	25.3	ZIP	4	12,769	74%	0.86	0.69	20%	5
Rhinoceros Auklet	winter	237	1,022	0.20	4.3	ZIP	4	12,393	52%	0.89	0.49	26%	4
Tufted Puffin	summer	1,738	11,777	0.18	6.8	ZIP	4	19,997	68%	0.92	0.64	23%	5
Common Murre	summer	6,533	293,713	0.64	45.0	ZIP	4	17,968	76%	0.93	0.75	19%	5
Common Murre	winter	405	6,516	0.33	16.1	ZIP	5	1,853	59%	0.86	0.63	28%	4
Black-footed Albatross	summer	421	3,008	0.04	7.1	ZINB	4	15,378	66%	0.96	0.45	12%	5
Black-footed Albatross	winter	87	162	0.07	1.9	ZINB	5	15,084	67%	0.97	0.50	43%	5
Northern Fulmar	summer	463	2,916	0.05	6.3	ZINB	4	17,773	68%	0.97	0.62	16%	5
Pink-footed Shearwater	summer	611	3,977	0.06	6.5	ZINB	5	17,996	58%	0.96	0.48	20%	5
Sooty Shearwater	summer	2,586	249,380	0.27	96.4	ZIP	5	17,290	83%	0.88	0.56	6%	5
Steller sea lion	summer	221	330	0.02	1.5	ZINB	4	20,000	38%	0.93	0.40	61%	4
harbor seal	summer	563	977	0.04	1.7	ZINB	5	20,000	42%	0.90	0.47	47%	4
humpback whale	summer	430	904	0.03	2.1	ZINB	5	15,777	35%	0.92	0.26	92%	4
gray whale	summer	118	182	0.01	1.5	ZINB	4	19,999	42%	0.96	0.38	63%	4
harbor porpoise	summer	1,673	4,092	0.11	2.4	ZINB	4	17,993	36%	0.87	0.35	36%	4
Dall's porpoise	summer	237	857	0.02	3.6	ZIP	4	8,654	24%	0.89	0.32	81%	3

Results and Discussion

USES OF MODELS AND MAPS

The spatial models and associated maps and tables presented in this report provide information on the long-term spatial distribution of eight seabird species (Marbled Murrelet, Rhinoceros Auklet, Tufted Puffin, Common Murre, Black-footed Albatross, Northern Fulmar, Pink-footed Shearwater and Sooty Shearwater), two pinniped species (Steller sea lion and harbor seal), and four cetacean species (humpback whale, gray whale, harbor porpoise and Dall's porpoise) from April to October, and three seabird species (Rhinoceros Auklet, Common Murre and Black-footed Albatross) from November to March. The models and maps are intended to distinguish persistent areas of high relative density from low relative density. It is important to contrast this approach with models and maps that address absolute abundance or density, which require additional parameters such as probability of species detection.



Pink-footed Shearwater (David Pereksta, BOEM)

While this work was completed to support marine spatial planning by the state of Washington and resource characterizations by the sanctuary, these data will benefit other organizations and other purposes including assessments of ecosystem health, coastal hazard impacts, and climate change.

All models show good performance based on model diagnostics (quality levels 5 to 3), and maps have been vetted by expert review; however, users should not assume unqualified accuracy. A model, even a very good one, cannot be a perfect fit in all locations, and corollary maps will be imperfect. In order to understand any specific points of deficiency, we emphasize that relative density maps should be interpreted alongside supporting data. In particular, when using maps to make management decisions, we recommend:

- Evaluating model performance diagnostics to better understand overall model fit and uncertainty,
- Comparing and evaluating spatial and temporal patterns of observations and residuals,
- Interpreting density maps alongside maps of spatially explicit model uncertainty, represented in this report by the CV and the 5% and 95% quantile maps, and
- Confirming model findings using independent data, including expert opinion or independent seabird, pinniped, or cetacean observations.

This report provides information to support many of these recommendations. Model performance diagnostics are provided in Table 9, distributions of observations and residuals are in Appendix D, maps of spatially explicit model uncertainty are provided in Figures 7-39, and this report presents maps which underwent expert review. We did not review model results against independent observation data and recommend these comparisons for follow up work. Menza et al. (2014) and Kracker and Menza (2015) provide a list of seabird, pinniped, and cetacean survey programs; some of which are used in these models, but others offer independent data sets in the study area.

There are also several caveats for supporting data:

- Given the use of zero-inflated distributions, which are inherently complex, certain diagnostics (e.g., residual plots, percent deviance explained) may be different than when used with more common distributions.
- Any biases in species detection, observed habitats or temporal periods that are inherent in observation data are propagated into the model results.
- Expert reviews were focused on coarse scale distributional patterns. Fine-scale expert review will be required for site-specific usage.

Results and Discussion

INFORMATION GAPS

The collection of at-sea sightings used in this report is the largest collection from the study area that we are aware of. Yet, Figure 5 reveals the collection does not exhaustively cover the study area and includes areas of relatively little survey effort. The limited amount of offshore data likely accounts for greater uncertainty in predictions of relative density in deeper water and poorer model performance for more pelagic species such as Black-footed Albatross, Pink-footed Shearwater, humpback whale, and Dall's porpoise. Given the limited number of sightings, four year-round resident species (Steller sea lion, harbor seal, harbor porpoise, and Dall's porpoise) were not modeled in the winter season. It is likely that winter distributions for some of these year-round species could be modeled with a moderate level of additional survey effort in the winter season.

The collection of at-sea sightings was also insufficient to model distributions for several species explicitly requested by coastal managers, such as Short-tailed Albatross, sei whale, blue whale, fin whale, southern resident killer whale, and sperm whale. Given their rarity, these species are challenging to model with at-sea data using any modeling framework, and may be more appropriate to model using alternative observation data, such as tracking or passive acoustic information. Models for rare species might be improved by accepting predictions at a coarser spatial resolution, encompassing a larger geographic extent to increase sample size, or combining species into broader taxonomic groups.



Blue whale
(NOAA)

The set of environmental predictors used to model species distributions was more useful for some species and season combinations than others. Additional environmental predictors would likely improve performance. Two predictors expected to improve model performance for several species are fishing fleet distribution and forage fish distribution. In addition, predictors which provide more information on nearshore dynamics such as current flow, salinity, turbidity, and mixing would likely improve model performance for many nearshore species.

NEXT STEPS

There are a number of modeling concepts that would benefit from further research and could improve predictive model performance. The development of predictive models raises many considerations concerning the appropriate spatial and temporal scales of assessment. The models in this report used a climatological approach, where observations are linked to climatological covariates representing long-term environmental patterns (i.e., climatologies). An alternative approach is to link animal observations to contemporaneous covariates (e.g., in situ sea surface temperature, chlorophyll a concentration, prey distribution, etc.; Ainley et al., 2005). Several authors noted that there are important differences in these two approaches, which may affect model performance and change predicted spatial patterns. There is an ongoing discussion among authors and other academic partners comparing results from the two approaches, but current research suggests that neither approach is clearly superior to the other, and which approach is used should depend on model objectives, the sample size of observations, and the quality of environmental predictors (Scales et al., in press).

Understanding that there are large seasonal variations in seabird, pinniped and cetacean spatial distributions, we stratified climatological predictions into two oceanographic seasons. Although seasonal divisions were helpful to separate distinct life history patterns for most species, grouping sightings has the potential to mask important intra-seasonal changes in distribution, especially if they are out of sync with the oceanographic patterns used to partition seasons in this report. For instance, if a species is breeding from April to July and then feeds offshore from August to October, separate models created for the breeding and feeding periods will likely be better than a single model during the time period we refer to as the upwelling season. Evaluating plots of

Results and Discussion

average density per month in Appendix D against known life history patterns can indicate if seasons are unlikely to represent expected species seasonal patterns.

The impact of heterogeneous survey effort is assumed to affect results, yet we did not quantify the spatial or temporal impacts of variable effort on predicted relative density patterns. In addition, it is reasonable to assume that model diagnostic metrics are less accurate when and where there is less survey effort. We present maps of survey effort and marginal and residuals plots to highlight potential biases, but a comparison of model outputs with independent data sets is needed to comprehensively assess model accuracy.

Seasonal species-specific predictive models can be used alone or in combination to identify multi-species areas of relative high and low use. At the time of this publication we understand the Washington Department of Fish and Wildlife has begun to investigate combining maps presented in this report to identify ecologically important areas. This is an obvious next step in transforming species distribution models into products to support marine planning.

The maps and models in this report are valuable for decision makers today and into the future, but they should be considered as part of an adaptive management strategy. New data sources may become available, new modeling approaches will improve fit of relationships between observations and predictors, and new management objectives will dictate the need for new outputs. To encourage adaptive management and integrate environmental change in a timely manner, there is tremendous value in at-sea observation field program investments and exploration of new modeling techniques to integrate data sets. These field programs are immensely helpful to understand population-level distributions across many spatial scales.

In addition to the Washington Department of Fish and Wildlife's effort to use our modeling products for marine planning, we know of at least one additional project which will build off of this work. From 2016 to 2018, NOAA's National Centers for Coastal Ocean Science and other contributors of this modeling work plan to expand seabird models to the entire U.S. continental Pacific coast in support of the Bureau of Ocean Energy Management.

- Adams, J., J. Felis, J.W. Mason and J.Y. Takekawa. 2014. Pacific Continental Shelf Environmental Assessment (PaCSEA): aerial seabird and marine mammal surveys off northern California, Oregon, and Washington, 2011-2012. U.S. Dept. of the Interior, Bureau of Ocean Energy Management, Pacific OCS Region, Camarillo, CA. OCS Study BOEM 2014-003. 266 pp.
- Ainley, D.G., L.B. Spear, C.T. Tynan, J.A. Barth, S.D. Pierce, R.G. Ford and T.J. Cowles. 2005. Physical and biological variables affecting seabird distributions during the upwelling season of the northern California Current. *Deep-Sea Research II* 52: 123-143.
- Appler, J., J. Barlow and S. Rankin. 2004. Marine Mammal Data Collected During the Oregon, California and Washington Line-Transect Expedition (ORCAWALE) Conducted Aboard the NOAA Ships *McArthur* and *David Starr Jordan*, July - December 2001. NOAA Technical Memorandum NOAA-TM-NMFS-SWFSC-359.
- Barlow, J. 2015. Inferring trackline detection probabilities, $g(0)$, for cetaceans from apparent densities in different survey conditions. *Marine Mammal Science* 31:923-943.
- Barlow, J., A. Henry, J.V. Redfern, T. Yack, A. Jackson, C. Hall, E. Archer and L. Ballance. 2010. Oregon, California and Washington line-transect and ecosystem (ORCAWALE) 2008 cruise report. NOAA Technical Memorandum NOAA-TM-NMFS-SWFSC-465.
- Becker, E.A., K.A. Forney, M.C. Ferguson, D.G. Foley, R.C. Smith, J. Barlow and J.V. Redfern. 2010. Comparing California Current cetacean-habitat models developed using in situ and remotely sensed sea surface temperature data. *Marine Ecology Progress Series* 413:163-183.
- Benson, S.R. and J. Seminoff. 2011. 2011 Aerial survey of distribution and abundance of western Pacific leatherback turtles (*Dermochelys coriacea*) in coastal waters of Oregon and Washington. Unpublished report.
- Bodenhofer, U., M. Krone and F. Klawonn. 2013. Testing noisy numerical data for monotonic association. *Information Sciences* 245:21-37.
- Boudt, K., J. Cornelissen, and C. Croux. 2012. The Gaussian rank correlation estimator: robustness properties. *Statistics and Computing* 22:471-483.
- Bowen W.D. 1997. Role of marine mammals in aquatic ecosystems. *Marine Ecology Progress Series* 158:267-274.
- Buckland, S.T., D.R. Anderson, K.P. Burnham, J.L. Laake, D.L. Borchers and L. Thomas. 2001. Introduction to Distance Sampling: Estimating Abundance of Biological Populations. Oxford University Press, Oxford, UK.
- Bühlmann, P. and T. Hothorn. 2007. Boosting algorithms: regularization, prediction and model fitting. *Statistical Science* 22(4):477-505.
- Burger, A.E. 2003. Effects of the Juan de Fuca Eddy and upwelling on densities and distributions of seabirds off southwest Vancouver Island, British Columbia. *Marine Ornithology* 31:113-122.
- Calambokidis, J., G.H. Steiger, D.K. Ellifrit, B.L. Troutman and C.E. Bowlby. 2004. Distribution and abundance of humpback whales (*Megaptera novaeangliae*) and other marine mammals off the northern Washington coast. *Fishery Bulletin* 102:563-580.

References

- Carretta, J.V., S.M. Wilkin, M.M. Muto and K. Wilkinson. 2013. Sources of human-related injury and mortality for U.S. Pacific west coast marine mammal stock assessments, 2007-2011. NOAA Technical Memorandum NOAA-TM-NMFS-SWFSC-514.
- Chandler, T. and J. Calambokidis. 2003. Contract report: 2003 aerial surveys for harbor porpoise and other marine mammals off Oregon, Washington and British Columbia. Prepared for the National Marine Mammal Laboratory. Online: <http://www.cascadiaresearch.org/reports/Rep-HP-2003.pdf> (Accessed 8 March 2016)
- Cotté, C., Y.H. Park, C. Guinet and C.A. Bost. 2007. Movements of foraging king penguins through marine mesoscale eddies. *Proceedings of the Royal Society B: Biological Sciences* 274(1624):2385-2391.
- Croll, D.A., B.R. Tershy, R. Hewitt, D. Demer, S. Hayes, P. Fiedler, J. Popp and V.L. Lopez. 1998. An integrated approach to the foraging ecology of marine birds and mammals. *Deep-Sea Research Part II: Topical Studies in Oceanography* 45:1353-1371.
- Croxall, J.P., S. H.M. Butchart, B. Lascelles, A.J. Stattersfield, B. Sullivan, A. Symes and P. Taylor. 2012. Seabird conservation status, threats and priority actions: a global assessment. *Bird Conservation International* 22:1-34.
- Ehler C. and F. Douvère. 2009. Marine spatial planning: a step-by-step approach toward ecosystem-based management. Intergovernmental Oceanographic Commission and Man and the Biosphere Programme. IOC Manual and Guides No. 53, IOCAM Dossier No. 6. Paris: UNESCO.
- Etheridge L., T. Bowling, and S. Showalter Otts. 2010. The Adaptive Management Experience of the National Marine Sanctuaries Program. *Sea Grant Law and Policy Journal* 3(1):9-18.
- Kracker, L. and C. Menza. 2015. An Evaluation of Marine Mammal Surveys to Support Washington State's Marine Spatial Planning Process. NOAA Technical Memorandum NOS NCCOS 195. Silver Spring, MD. 37 pp.
- Falxa, G., J. Baldwin, M. Lance, D. Lynch, S.K. Nelson, S. F. Pearson, M.G. Raphael, C. Strong, and R. Young. 2014. Marbled Murrelet effectiveness monitoring, Northwest Forest Plan: 2013 summary report. 20 pp.
- Forney, K.A. 2007. Preliminary Estimates of Cetacean Abundance along the U.S. West Coast and Within Four National Marine Sanctuaries During 2005. NOAA Technical Memorandum NOAA-TM-NMFS-SWFSC-406.
- Friedman, J.H. 2002. Stochastic gradient boosting. *Computational Statistics & Data Analysis* 38:367-378.
- Furness, R.W. and C.J. Camphuysen. 1997. Seabirds as monitors of the marine environment. *Ices Journal of Marine Science* 54(4):726-737.
- Gneiting, T. and A.E. Raftery. 2007. Strictly Proper Scoring Rules, Prediction, and Estimation. *Journal of the American Statistical Association* 102:359-378.
- Hanson, M.B., D.P. Noren, T.F. Norris, C.A. Emmons, M.M. Holt, E. Phillips, J. Zamon and J. Menkel. 2010. Pacific Orca Distribution Survey (PODS) conducted aboard the NOAA ship *McArthur II* in March-April 2009. (State Department Cruise No: 2009-002) Unpublished report, NWFSC, Seattle, WA.
- Hickey, B.M. and N.S. Banas. 2003. Oceanography of the US Pacific Northwest Coastal Ocean and estuaries with application to coastal ecology. *Estuaries* 26(4B):1010-1031.

References

- Hoefler, C.J. 2000. Marine bird attraction to thermal fronts in the California current system. *The Condor* 102(2):423-427.
- Hofner, B., A. Mayr, N. Robinzonov and M. Schmid. 2012. Model-based boosting in R: a hands-on tutorial using the R package mboost. Technical Report 120, Department of Statistics, University of Munich, Germany.
- Hothorn, T., P. Buehlmann, T. Kneib, M. Schmid and B. Hofner. 2015. mboost: Model-Based Boosting, R package version 2.4-2. Online: <http://CRAN.R-project.org/package=mboost> (Accessed 8 March 2016)
- Hoyt, E. 2001. Whale Watching 2001: Worldwide tourism numbers, expenditures, and expanding socioeconomic benefits. International Fund for Animal Welfare, Yarmouth Port, MA, USA. 1-158 pp.
- Kinlan, B.P., R. Rankin, A. Winship and C. Caldow. 2014. Modeling At-Sea Occurrence and Abundance of Marine Birds to Support Mid-Atlantic Marine Renewable Energy Planning. U.S. Department of the Interior, Bureau of Ocean Energy Management, Herndon, VA. OCS Study BOEM 2014. NOAA Technical Memorandum NOS NCCOS. In review.
- Lopez, J. 2011. Seabird density in the Olympic Coast National Marine Sanctuary. Online: http://olympiccoast.noaa.gov/science/surveycruises/2011/seabird_density1995-2007.pdf (Accessed 8 March 2016)
- Mann, K.H. and J.R.N. Lazier. 2005. Vertical Structure in Coastal Waters: Coastal Upwelling Regions, in Dynamics of Marine Ecosystems, Third Edition. Blackwell Publishing Ltd., Malden, MA, USA. 512 pp.
- Mayr, A., N. Fenske, B. Hofner, T. Kneib and M. Schmid. 2012. Generalized additive models for location, scale and shape for high dimensional data---a flexible approach based on boosting. *Applied Statistics* 61(3):403-427.
- McGillicuddy, D.J., A.R. Robinson, D.A. Siegel, H.W. Jannasch, R. Johnson, T.D. Dickey, J. McNeil, A.F. Michaels and A.H. Knap. 1998. Influence of mesoscale eddies on new production in the Sargasso Sea. *Nature* 394:263-266.
- Menza, C., T. Battista, and D. Dorfman. 2014. Technical and Mapping Support for Washington State Marine Spatial Planning. NOAA Technical Memorandum NOS NCCOS 181. Silver Spring, MD. 37 pp.
- Menza C., J. Leirness, T. White, A. Winship, B. Kinlan, J.E. Zamon, L. Ballance, E. Becker, K. Forney, J. Adams, D. Pereksta, S. Pearson, J. Pierce, L. Antrim, N. Wright and E. Bowlby. 2015. Modeling Seabird Distributions off The Pacific Coast of Washington. Final report to Washington State Department of Natural Resources. 63 pp.
- Miller, D.L. 2015. Distance: Distance Sampling Detection Function and Abundance Estimation. R package version 0.9.4. Online: <http://CRAN.R-project.org/package=Distance> (Accessed 8 March 2016)
- Morgan, C.A., A. De Robertis and R.W. Zabel. 2005. Columbia River plume fronts. I. Hydrography, zooplankton distribution, and community composition. *Marine Ecology Progress Series* 299:19-31.
- National Oceanic and Atmospheric Administration (NOAA). 1993. Olympic Coast National Marine Sanctuary. Final Environmental Impact Statement/ Management Plan. Volumes 1 and 2. U.S. Department of Commerce, National Oceanic and Atmospheric Administration, Sanctuaries and Reserves Division. Washington, D.C.

References

Nur, N., J. Jahncke, M.P. Herzog, J. Howar, K.D. Hyrenbach, J.E. Zamon, D.G. Ainley, J.A. Wiens, K. Morgan, L.T. Balance and D. Stralberg. 2011. Where the wild things are: predicting hotspots of seabird aggregations in the California Current System. *Ecological Applications* 21(6):2241-2257.

Office of National Marine Sanctuaries. 2008. Olympic Coast National Marine Sanctuary Condition Report 2008. U.S. Department of Commerce, National Oceanic and Atmospheric Administration, National Ocean Service, Office of National Marine Sanctuaries, Silver Spring, MD. 72 pp.

Office of National Marine Sanctuaries. 2011. Olympic Coast National Marine Sanctuary Final Management Plan and Environmental Assessment. U.S. Department of Commerce, National Oceanic and Atmospheric Administration, National Ocean Service, Office of National Marine Sanctuaries. Silver Spring, MD. 352 pp.

Olson, D.B., G.L. Hitchcock, A.J. Mariano, C.J. Ashjian, G. Peng, R.W. Nero and G.P. Podesta. 1994. Life on the edge: marine life and fronts. *Oceanography* 7(2):52-60.

Paleczny M., E. Hammill, V. Karpouzi and D. Pauly. 2015. Population Trend of the World's Monitored Seabirds, 1950-2010. *PLoS ONE* 10(6):e0129342.

R Core Team. 2015. R: a language and environment for statistical computing. R Foundation for Statistical Computing, Vienna, Austria.

Roberts, J.J., B.D. Best, D.C. Dunn, E.A. Trembl and P.N. Halpin. 2010. Marine Geospatial Ecology Tools: An integrated framework for ecological geoprocessing with ArcGIS, Python, R, MATLAB, and C++. *Environmental Modelling & Software* 25:1197-1207.

Sbrocco, E.J. and P.H. Barber. 2013. MARSPEC: ocean climate layers for marine spatial ecology. *Ecology* 94(4):979-979.

Scales, K.L., E.L. Hazen, M.G. Jacox, C.A. Edwards, A.M. Boustany, M.J. Oliver and S.J. Bograd. In press. Scales of inference: On the sensitivity of habitat models for wide-ranging marine predators to the resolution of environmental data. Submitted to *Ecography*.

Schmid, M., S. Potapov, A. Pfahler and T. Hothorn. 2008. Estimation and regularization techniques for regression models with multidimensional prediction functions. Technical Report 42, Department of Statistics, University of Munich, Germany.

Schneider, D.C. 1990. Seabirds and fronts: a brief overview. *Polar Research* 8:17-21.

Schreiber, E.A. and J. Burger. 2001. *Biology of Marine Birds*. CRC Press, Boca Raton, FL, USA. 740 pp.

Spear, L.B., D.G. Ainley and P. Pyle. 1999. Seabirds in southeastern Hawaiian waters. *Western Birds* 30:1-32.

Suryan, R. M., J. A. Santora, and W. J. Sydeman. 2012. New approach for using remotely-sensed chlorophyll a to identify seabird hotspots. *Marine Ecology Progress Series* 451:213-225.

U.S. Department of the Navy. 2006. Marine Resources Assessment for the Pacific Northwest Operating Area. Pacific Division, Naval Facilities Engineering Command, Pearl Harbor, Hawaii. Contract # N62470-02-D09997, CTO 0029. Prepared by Geo-Marine, Inc. Plano, Texas.

References

- U.S. Fish and Wildlife Service. 2005. Regional Seabird Conservation Plan, Pacific Region. U.S. Fish and Wildlife Service, Migratory Birds and Habitat Programs, Pacific Region, Portland, OR.
- U.S. Fish and Wildlife Service. 2013. Birding in the United States: A Demographic and Economic Analysis. Report 2011-1. U.S. Fish and Wildlife Service Division of Economics, Arlington, VA.
- Ware, D. M. and R. E. Thomson. 2005. Bottom-up ecosystem trophic dynamics determine fish production in the Northeast Pacific. *Science* 308(5726):1280-1284.
- Washington Department of Ecology. 2014. Marine Spatial Plan for Washington's Pacific Coast: Summary of SEPA Scoping and Response to Comments. Washington State Department of Ecology. 62 pp.
- Washington Department of Fish and Wildlife. 2013. Threatened and Endangered Wildlife in Washington: 2012 Annual Report. Listing and Recovery Section, Wildlife Program, Washington Department of Fish and Wildlife, Olympia. 251 pp.
- Washington Department of Fish and Wildlife. 2015a. Washington Department of Fish and Wildlife 2015-2017 Strategic Plan. Online: <http://wdfw.wa.gov/publications/01765/wdfw01765.pdf> (Accessed 8 March 2016)
- Washington Department of Fish and Wildlife. 2015b. List of Species of Concern in Washington State. Online: <http://wdfw.wa.gov/conservation/endangered/All/> (Accessed 8 March 2016)
- Wiebe, P.H., E.M. Hulburt, E.J. Carpenter, A.E. Jahn, G.P. Knapp III S.H. Boyd, P.B. Ortner and J.L. Cox. 1976. Gulf Stream cold core rings: large-scale interaction sites for open ocean plankton communities. *Deep Sea Research and Oceanographic Abstracts* 23(8):695-710.
- Yen, P.P.W., W.J. Sydeman and K.D. Hyrenbach. 2004. Marine bird and cetacean associations with bathymetric habitats and shallow-water topographies: implications for trophic transfer and conservation. *Journal of Marine Systems* 50:79-99.

Appendices

Appendix A: Survey Program Information

Survey name	Collector(s)	Platform type	Years	Geographic coverage	Reference	Notes
Harbor porpoise surveys	Cascadia Research Collective, NOAA AFSC	High-altitude fixed-wing aircraft	2002-2003	Coastal and inland waters of Washington and southern British Columbia, 0-200 m	Chandler and Calambokidis, 2003	
Leatherback turtle aerial survey	NOAA SWFSC	High-altitude fixed-wing aircraft	2010, 2011, 2014	Offshore and coastal waters of Washington and Oregon	Benson and Seminoff, 2011	
Pacific Continental Shelf Environmental Assessment (PaCSEA)	USGS WERC, BOEM	Low-altitude fixed-wing aircraft	2011-2012	Offshore and coastal waters of Washington Oregon, and northern California; finer scale information collected in selected areas	Adams et al., 2014	
California Current Ecosystem Surveys (includes ORCAWALE and CSCAPE surveys)	NOAA SWFSC	Large ship	1996, 2001, 2005, 2008	Offshore and coastal waters of U.S. west coast; finer scale information collected in National Marine Sanctuaries	Barlow et al., 2010 Appler et al., 2004 Forney, 2007	Data from 1996 not used in seabird models
Northwest Fisheries Science Center Northern California Current Seabird Surveys	NOAA NWFSC (Conservation Biology, Fish Ecology)	Large ship	2008, 2009, 2012	Offshore and coastal waters of Washington Oregon, and northern California	Hanson et al., 2010	Some seabird observations included in this data set were collected on PODS cruises
Olympic Coast National Marine Sanctuary Seabird and Marine Mammal Surveys	Cascadia Research Collective, OCNMS, SWFSC	Large ship	1995-2008	Coastal waters of Southern British Columbia, Washington and Oregon	Calambokidis et al., 2004 Lopez, 2011	
Pacific Coast Winter Seaduck Survey	Sea Duck Joint Venture, WDFW	Large ship	2011	Coastal waters of Washington and Oregon	Contact: Tim Bowman (USFWS)	
Pacific Orcinus Distribution Survey (PODS)	NOAA NWFSC	Large ship	2004-2012	Coastal waters of Washington and Oregon	Hanson et al., 2010	
Large whale surveys off Washington and Oregon	Cascadia Research Collective, WDFW, ODFW	Small boat	2011-2013	Coastal waters of Washington and Oregon	Contact: John Calambokidis (Cascadia)	
Northwest Forest Plan Marbled Murrelet Effectiveness Monitoring Program	USFS, USFWS, WDFW	Small boat	2004-2013	Coastal waters of Washington Oregon, and northern California	Falxa et al., 2014	
Seasonal Olympic Coast National Marine Sanctuary seabird surveys	NOAA OCNMS	Small boat	2006-2012	Offshore waters of Washington; La Push to Juan de Fuca Canyon	Online report: http://olympiccoast.noaa.gov/science/surveycruises/2012/marinebirds.html	

Appendix B: Processing Steps for Environmental Predictors

CLIMATE INDICES

The North Pacific Gyre Oscillation Index, Pacific Decadal Oscillation Index, and upwelling index were processed by calculating a three-month moving average (using the values of the current month plus the previous two months) prior to analyses. A three-month moving average was not calculated for Multivariate El Niño-Southern Oscillation Index, as these data had already been ‘smoothed’ using a two-month moving average prior to obtaining them. For each climate index, two values were included as predictor variables: the value for the month and year of a given transect segment and the value for the same month one year previous (i.e., 12 month lag).

DISTANCE TO 200 METER ISOBATH

The 200 m isobath was derived from the MARSPEC depth layer and distance to the 200 m isobath was calculated using the Spatial Analyst toolbox in ArcGIS 10.2 across the entire study area at a resolution of 100 m.

DISTANCE TO COLONIES, NESTING HABITAT, AND HAUL-OUTS

Locations of Common Murre and Tufted Puffin colonies were extracted from the Washington Seabird Catalog (http://wdfw.wa.gov/conservation/research/projects/seabird/seabird_catalog/) and converted to shapefiles as points. The locations of Marbled Murrelet nesting habitat were taken from the Final Revised Marbled Murrelet Critical Habitat Designation which can be downloaded from the USFWS Washington Fish and Wildlife Office (<http://www.fws.gov/wafwo/mamu.html>). Distance to the nearest colony and critical habitat were calculated using the Spatial Analyst toolbox in ArcGIS 10.2.

The seal and sea lion haul-out database maintained by the Washington Department of Fish and Wildlife was used to identify the locations of harbor seal and Steller sea lion haul-outs and population counts among haul-outs. The database comprises generalized polygons and survey data collected during aerial, ground, and boat surveys conducted by personnel from the Washington Department of Fish and Wildlife, the National Marine Fisheries Service, and Cascadia Research from 1998 to 2013. The distance to nearest haul-out was first tested as a predictor, but during technical review the predictor was found to be ineffectual at predicting pinniped distributions. The average distance to haul-outs weighted by haul-out population was then investigated and found to be a better predictor. The average weighted distance predictor improved predictions by aggregating contributions from multiple haul-outs and by increasing the relative contributions of haul-outs with more individuals.

DEPTH AND PREDICTORS DERIVED FROM DEPTH

Seafloor topography has strong direct effects on marine ecosystems by steering the flow field and providing habitat for marine organisms. Discrete topographic features are important spatial predictors of seabird distribution and abundance, and influence foraging distributions of seabirds across a variety of spatial scales (e.g., continental shelf breaks / shelf slopes, submarine canyons, ledges, and shoals; Croll et al., 1998; Yen et al., 2004; Nur et al., 2011).

Depth, topographic slope, and planform and profile curvature data were taken from MARSPEC, a high-resolution GIS database of ocean climate layers intended for marine ecological niche modeling and other applications in marine spatial ecology (<http://www.marspec.org>; Sbrocco and Barber, 2013). MARSPEC uses the SRTM30 Plus Bathymetry version 6.0 data set for bathymetry (accessed from http://topex.ucsd.edu/WWW_html/srtm30_plus.html). Bathymetric slope was measured in degrees ranging from 0° (flat surface) to 90° (vertical slope). Curvature layers are used to infer flow-field dynamics. Positive/negative values of planform curvature

Appendices

may indicate divergent/convergent flow, whereas, positive/negative values of profile curvature may indicate acceleration/deceleration of the flow field (Sbrocco and Barber, 2013).

The bathymetric position index (BPI) is a measure of depth relative to a surrounding neighborhood. The bathymetric position index was calculated for two spatial scales (3 km and 20 km) to capture topographic features and complexity of the seafloor (e.g., flat bottom, trough, and steep wall) at moderate and coarse spatial scales. BPI for both scales was calculated with the Spatial Analyst toolbox in ArcGIS 10.2 using an annulus neighborhood with an inner radius of one cell and outer radius approximately half the corresponding scale.

PROBABILITY OF CYCLONIC AND ANTICYCLONIC EDDY RINGS

Oceanic eddies are large circular currents with scales ranging from tens to hundreds of kilometers. Eddies can transfer nutrients across water masses and elevate primary production in upwelling cores (McGillicuddy et al., 1998), retain zooplankton (Wiebe et al., 1976), and enhance top predator densities (Burger, 2003; Yen et al., 2004; Cotté et al., 2007). Rotational patterns of mesoscale eddies are cyclonic or anticyclonic. In the northern hemisphere, centers of anticyclonic eddies are warmer and higher (by a few tens of centimeters) than outer waters and are referred to as downwelling eddies or warm-core rings. Cyclonic eddies exhibit an opposite rotational pattern are likely cooler and lower in height (by a few tens of centimeters) than outer lying waters and are referred to as upwelling eddies or cold-core rings.

Oceanic eddy climatologies were derived from a 21-year dataset (1993-2014) of daily AVISO sea surface height (SSH) imagery, specifically Mean Absolute Dynamic Topography (MADT). The AVISO website (<http://www.aviso.altimetry.fr/en/data/products/sea-surface-height-products/global/madt.html>) provides additional information for MADT and geospatial data layers in NetCDF format. The spatial resolution of AVISO SSH data is 0.25 degrees or approximately 25 km. The Okubo-Weiss Algorithm was applied to MADT using the Marine Geospatial Ecology Tools (MGET) geoprocessing ArcGIS toolbox (<http://mgel.env.duke.edu/mget>; Roberts et al., 2010) to identify anticyclonic and cyclonic eddies. The Okubo-Weiss algorithm parameter, “Minimum area-to-perimeter ratio of eddy cores” was modified to 0.45 in order to select for circular eddies; however, all other parameters remained set at default levels (Okubo-Weiss parameter threshold type = -0.2; Minimum area of eddy cores = 4; Minimum duration of eddy cores = 28 days).

Eddy climatologies are probability layers that estimate the probability of anticyclonic or cyclonic eddies in two seasons: April to October and November to March. Eddy probabilities were calculated at coincident pixels using the native resolution of MADT by summing the number of times each pixel was classified as an eddy, divided by the number of pixels with SSH data at the scale of the pixel frame.

SEA SURFACE SALINITY

Monthly sea surface salinity climatologies were extracted from the MARSPEC monthly climatological dataset (Sbrocco and Barber, 2013). The average of monthly climatologies from April to October and November to March were used to produce two seasonal climatologies.

SEASONAL SEA SURFACE TEMPERATURE

Sea surface temperature data was derived from Aqua MODIS, processed to a level 3 monthly composite for years 2002-12. Monthly composites were averaged into two seasonal climatologies: April to October and November to March.

PROBABILITY OF SEA SURFACE TEMPERATURE FRONT

Hydrographic fronts manifest across a wide variety of spatial and temporal scales and some may facilitate trophic energy transfer, where high concentrations of prey associated with fronts attract marine predators searching for food (Schneider, 1990; Olson et al., 1994; Hoefler, 2000).

A 13-year dataset of monthly sea surface temperature front probability composites (accessed from <http://coastwatch.pfeg.noaa.gov/erddap/griddap/erdGATfntmday.html>) was used to create seasonal climatologies for two modeled time periods: April to October and November to March. The CoastWatch Oceanic Front Probability Index measures the probability of sea surface temperature front formation based on data from NOAA's GOES satellites. For each time period, front probabilities layers were averaged using the native resolution of the data (0.05 degrees; ~5.5 km) in order to calculate each seasonal climatological mean.

SURFACE CHLOROPHYLL A CONCENTRATION

Chlorophyll *a* data was derived from Aqua MODIS, processed to a level 3 monthly composite for years 2002-12. Monthly composites were averaged to create two seasonal climatologies: April to October and November to March.

FREQUENCY OF CHLOROPHYLL PEAKS INDEX (FCPI)

Chlorophyll *a* data for this climatology was derived from the SeaWiFS satellite, unlike the mean climatologies derived from the MODIS sensor. FCPI is a 9-year index that represents chlorophyll *a* intensity above a modeled mean of chlorophyll *a* concentration across all months (January 1998 through December 2006). The index is not seasonal, so the same climatological values are used for both upwelling and downwelling seasons. See Suryan et al. (2012) for details.

Appendices

Appendix C: Model Performance Metrics (Full Model Assemblage)

Performance metrics for all models of each species-season combination. Models are sorted in descending order of performance in terms of percent deviance explained (PDE) for each species-season combination, with the final selected model shown in bold font.

Species	Season	Model type	Max. tree depth	No. boosting iterations	PDE	AUC	<i>r</i>	% error
Marbled Murrelet	summer	ZINB	4	20,000	52%	0.92	0.64	32%
Marbled Murrelet	summer	ZINB	5	19,999	52%	0.92	0.64	32%
Marbled Murrelet	summer	ZIP	4	20,000	47%	0.92	0.50	32%
Marbled Murrelet	summer	ZIP	5	17,999	36%	0.88	0.39	36%
Rhinoceros Auklet	summer	ZIP	4	12,769	74%	0.86	0.69	20%
Rhinoceros Auklet	summer	ZIP	5	13,214	74%	0.86	0.70	20%
Rhinoceros Auklet	summer	ZINB	5	18,999	53%	0.85	0.67	23%
Rhinoceros Auklet	summer	ZINB	4	17,999	50%	0.84	0.63	29%
Rhinoceros Auklet	winter	ZIP	4	12,393	52%	0.89	0.49	26%
Rhinoceros Auklet	winter	ZIP	5	9,724	51%	0.88	0.48	29%
Rhinoceros Auklet	winter	ZINB	5	8,319	44%	0.88	0.53	32%
Rhinoceros Auklet	winter	ZINB	4	7,879	43%	0.87	0.52	32%
Tufted Puffin	summer	ZIP	4	19,997	68%	0.92	0.64	23%
Tufted Puffin	summer	ZIP	5	17,998	60%	0.89	0.58	28%
Tufted Puffin	summer	ZINB	5	20,000	57%	0.91	0.64	23%
Tufted Puffin	summer	ZINB	4	20,000	57%	0.91	0.63	23%
Common Murre	summer	ZIP	4	17,968	76%	0.93	0.75	19%
Common Murre	summer	ZIP	5	17,897	74%	0.92	0.75	19%
Common Murre	summer	ZINB	4	18,999	61%	0.92	0.72	22%
Common Murre	summer	ZINB	5	17,999	57%	0.91	0.70	27%
Common Murre	winter	ZIP	5	1,853	59%	0.86	0.63	28%
Common Murre	winter	ZIP	4	1,554	59%	0.87	0.64	27%
Common Murre	winter	ZINB	5	17,978	54%	0.88	0.72	19%
Common Murre	winter	ZINB	4	17,383	53%	0.87	0.71	18%
Black-footed Albatross	summer	ZIP	4	8,375	83%	0.92	0.25	12%
Black-footed Albatross	summer	ZIP	5	2,443	83%	0.91	0.33	12%
Black-footed Albatross	summer	ZINB	4	15,378	66%	0.96	0.45	12%
Black-footed Albatross	summer	ZINB	5	15,540	65%	0.96	0.44	12%
Black-footed Albatross	winter	ZINB	5	15,084	67%	0.97	0.50	43%
Black-footed Albatross	winter	ZINB	4	15,553	66%	0.97	0.53	45%
Black-footed Albatross	winter	ZIP	4	17,950	64%	0.98	0.43	45%
Black-footed Albatross	winter	ZIP	5	17,976	64%	0.98	0.43	42%
Northern Fulmar	summer	ZIP	5	16,636	75%	0.97	0.56	17%
Northern Fulmar	summer	ZIP	4	16,200	74%	0.97	0.56	18%
Northern Fulmar	summer	ZINB	4	17,773	68%	0.97	0.62	16%
Northern Fulmar	summer	ZINB	5	17,957	68%	0.97	0.60	16%
Pink-footed Shearwater	summer	ZINB	5	17,996	58%	0.96	0.48	20%
Pink-footed Shearwater	summer	ZINB	4	17,997	57%	0.96	0.44	20%
Pink-footed Shearwater	summer	ZIP	4	17,932	53%	0.96	0.44	19%
Pink-footed Shearwater	summer	ZIP	5	17,972	52%	0.96	0.45	20%

Appendices

Species	Season	Model type	Max. tree depth	No. boosting iterations	PDE	AUC	<i>r</i>	% error
Sooty Shearwater	summer	ZIP	5	17,290	83%	0.88	0.56	6%
Sooty Shearwater	summer	ZIP	4	17,819	82%	0.88	0.54	6%
Sooty Shearwater	summer	ZINB	4	18,998	59%	0.92	0.57	8%
Sooty Shearwater	summer	ZINB	5	17,999	56%	0.91	0.53	8%
Steller sea lion	summer	ZINB	4	20,000	38%	0.93	0.40	61%
Steller sea lion	summer	ZINB	5	20,000	38%	0.93	0.39	61%
Steller sea lion	summer	ZIP	4	20,000	30%	0.91	0.25	61%
Steller sea lion	summer	ZIP	5	20,000	30%	0.91	0.27	60%
harbor seal	summer	ZINB	5	20,000	42%	0.90	0.47	47%
harbor seal	summer	ZINB	4	19,999	42%	0.90	0.47	47%
harbor seal	summer	ZIP	5	20,000	40%	0.89	0.35	47%
harbor seal	summer	ZIP	4	19,999	39%	0.89	0.34	47%
humpback whale	summer	ZINB	5	15,777	35%	0.92	0.26	92%
humpback whale	summer	ZINB	4	10,266	35%	0.91	0.27	92%
humpback whale	summer	ZIP	4	1,225	23%	0.89	0.22	93%
humpback whale	summer	ZIP	5	1,246	23%	0.89	0.22	93%
gray whale	summer	ZINB	4	19,999	42%	0.96	0.38	63%
gray whale	summer	ZINB	5	20,000	41%	0.96	0.38	63%
gray whale	summer	ZIP	4	18,999	29%	0.94	0.25	63%
gray whale	summer	ZIP	5	17,999	27%	0.94	0.25	63%
harbor porpoise	summer	ZINB	4	17,993	36%	0.87	0.35	36%
harbor porpoise	summer	ZINB	5	17,999	36%	0.87	0.34	36%
harbor porpoise	summer	ZIP	4	17,995	29%	0.87	0.26	37%
harbor porpoise	summer	ZIP	5	17,999	29%	0.87	0.25	36%
Dall's porpoise	summer	ZIP	4	8,654	24%	0.89	0.32	81%
Dall's porpoise	summer	ZIP	5	5,337	23%	0.89	0.34	81%
Dall's porpoise	summer	ZINB	4	4,470	21%	0.89	0.30	80%
Dall's porpoise	summer	ZINB	5	4,496	21%	0.89	0.30	80%

Appendices

Appendix D: Select Marginal and Residual Plots

Figures D1-17: Select marginal and residual plots for the final selected model of each species-season combination. Panels from left to right, top to bottom are: 1) observed monthly average density (individuals per sq. km) per segment; 2) marginal plot of $\text{logit}(1-p)$ versus Julian day; 3) marginal plot of $\log(\mu)$ versus Julian day; 4) blank; 5) marginal plot of $\text{logit}(1-p)$ versus year; 6) marginal plot of $\log(\mu)$ versus year; 7) scatterplot of deviance residuals versus latitude; 8) scatterplot of deviance residuals versus longitude; 9) scatterplot of deviance residuals versus date; 10) histogram of predicted relative densities with horizontal axis labels showing color gradient class divisions (see Figures 6-39) as multiples of the minimum predicted relative density value. Marginal plots show patterns in the functional relationship between transformed versions of the zero-inflation and count model components and Julian day and year, after accounting for the effects of all other predictors in the model. Gray shading represents ± 1 standard deviation from the mean. Absent marginal plots indicate either Julian day or year was not selected as an important predictor in the final model. To calculate deviance residuals, the saturated likelihood was assumed to be the maximum possible likelihood value (unpublished).

1	2	3
4	5	6
7	8	9
10		

Marbled Murrelet (*Brachyramphus marmoratus*): April to October

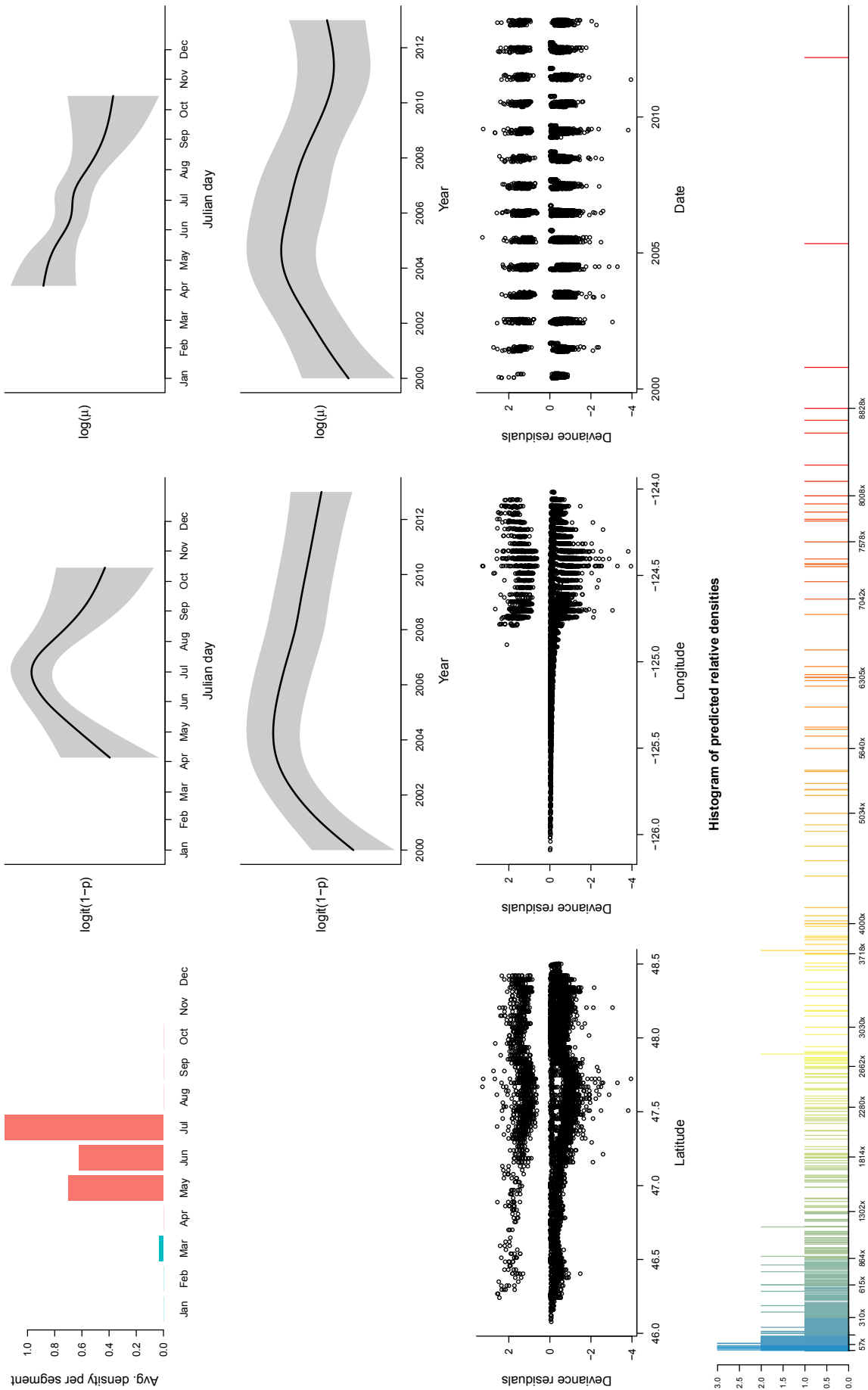


Figure D1. Marginal and residual plots for Marbled Murrelet (*Brachyramphus marmoratus*) during the months of April to October.

Appendices

Rhinoceros Auklet (*Cerorhinca monocerata*): April to October

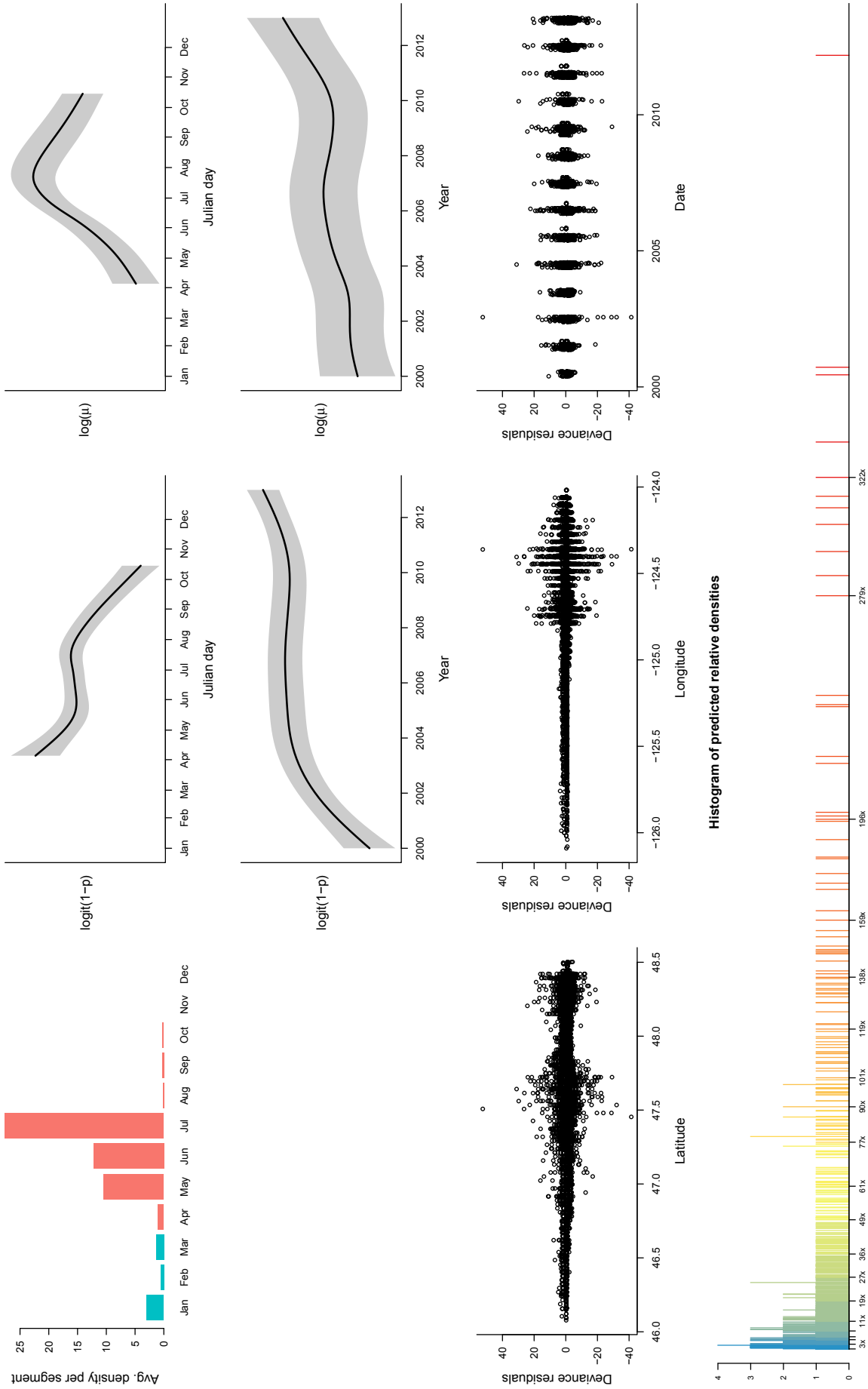


Figure D2. Marginal and residual plots for Rhinoceros Auklet (*Cerorhinca monocerata*) during the months of April to October.

Rhinoceros Auklet (*Cerorhinca monocerata*): November to March

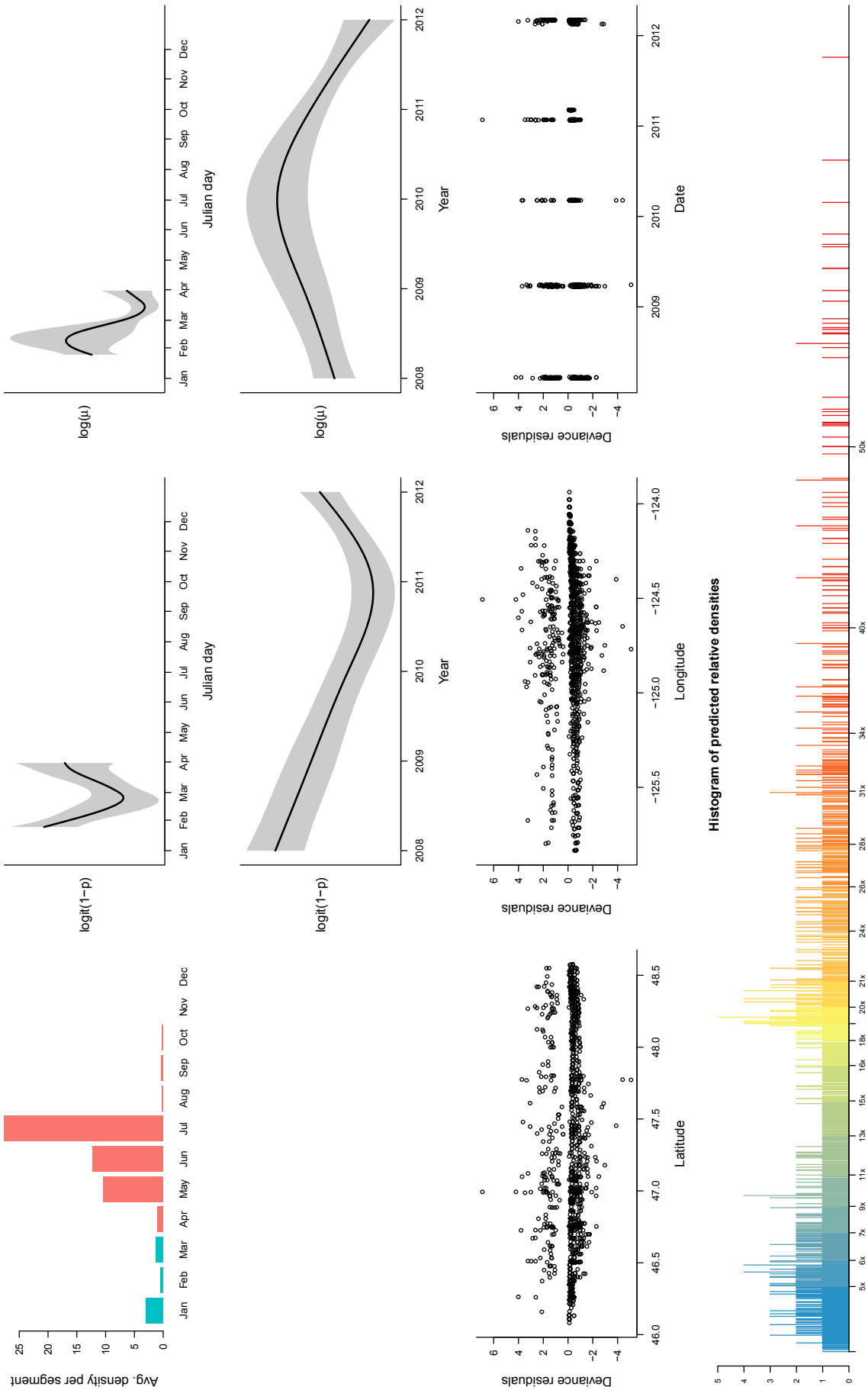


Figure D3. Marginal and residual plots for Rhinoceros Auklet (*Cerorhinca monocerata*) during the months of November to March.

Tufted Puffin (*Fratercula cirrhata*): April to October

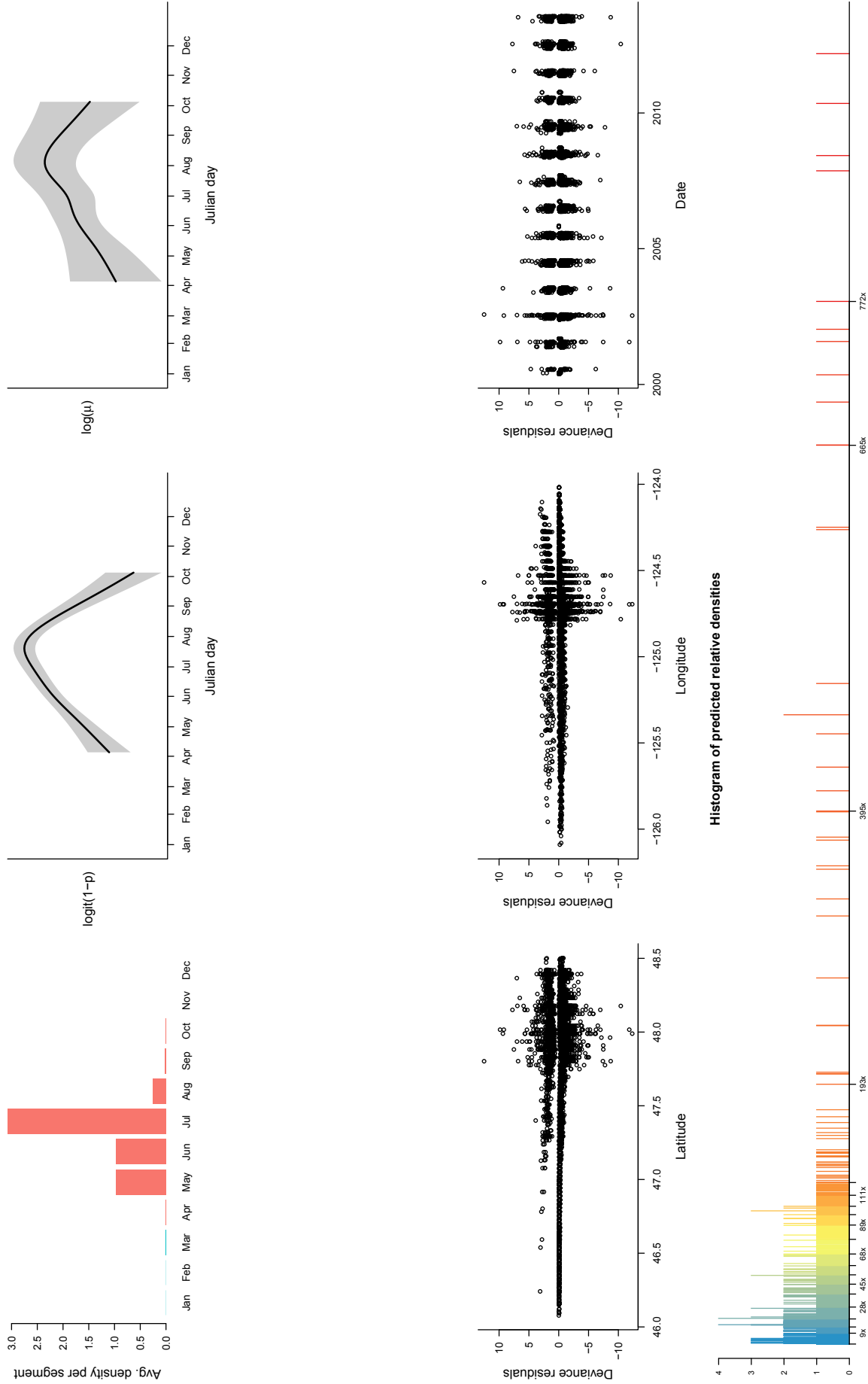


Figure D4. Marginal and residual plots for Tufted Puffin (*Fratercula cirrhata*) during the months of April to October.

Common Murre (Uria aalge): April to October

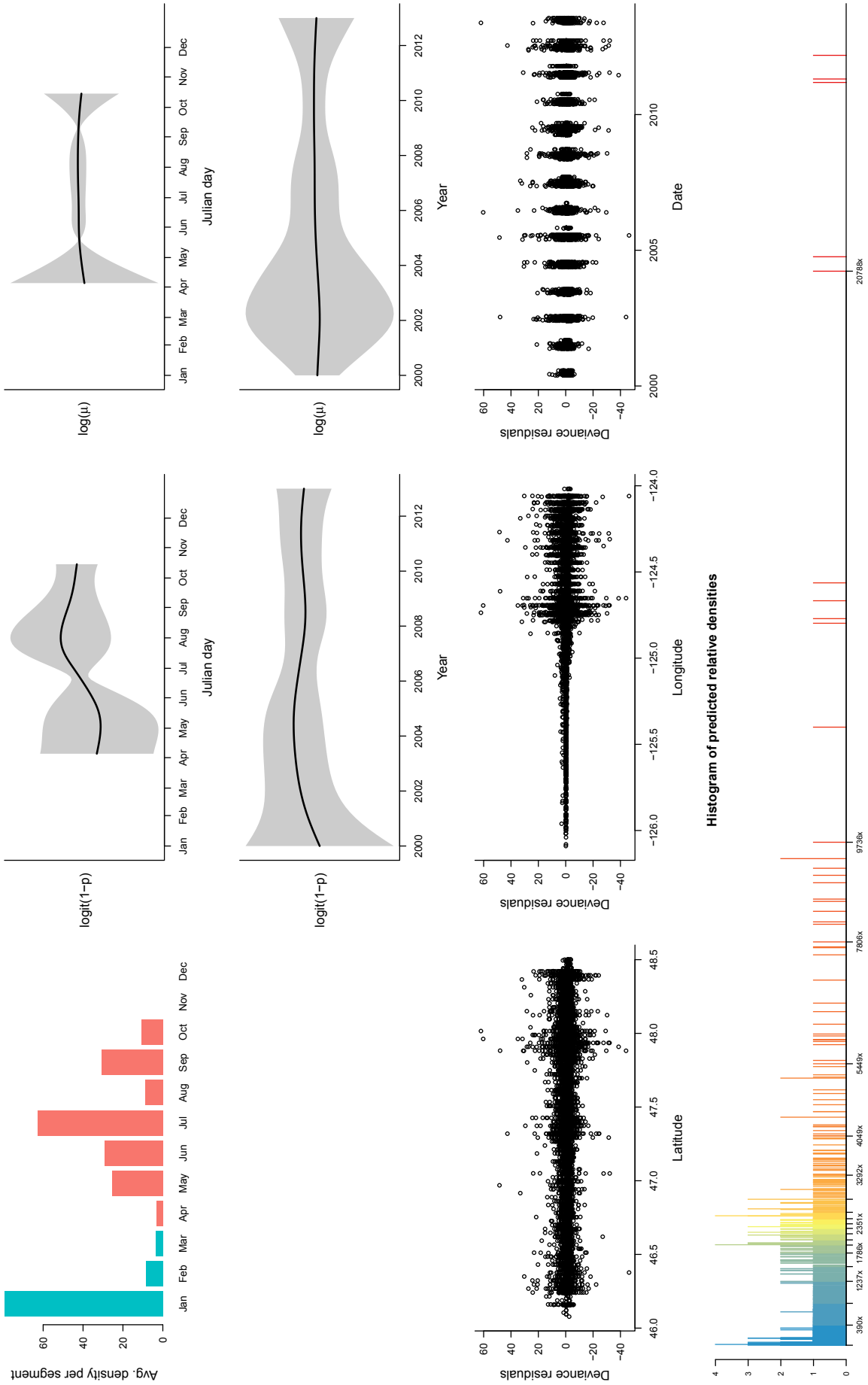


Figure D5. Marginal and residual plots for Common Murre (Uria aalge) during the months of April to October.

Appendices

Common Murre (*Uria aalge*): November to March

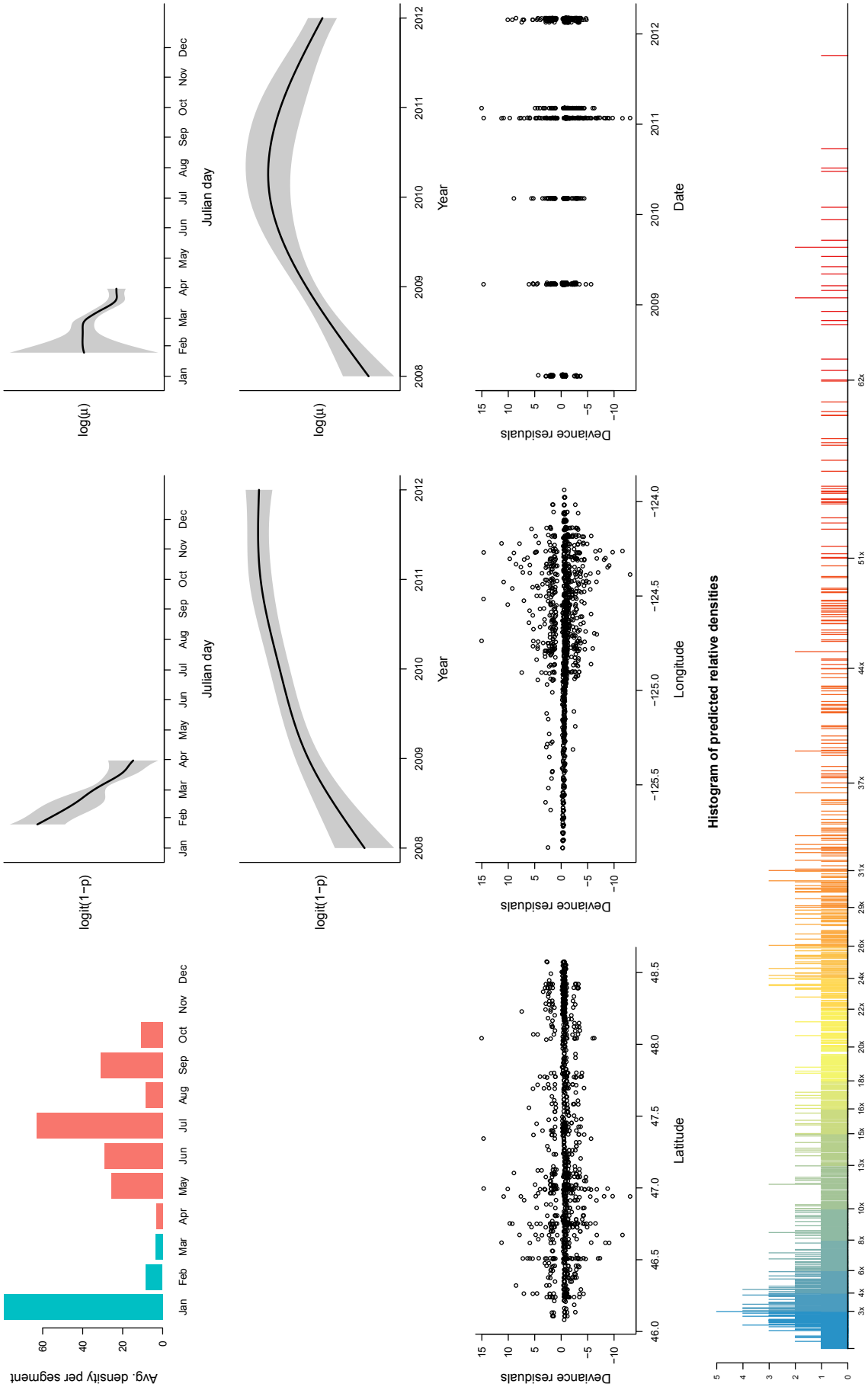
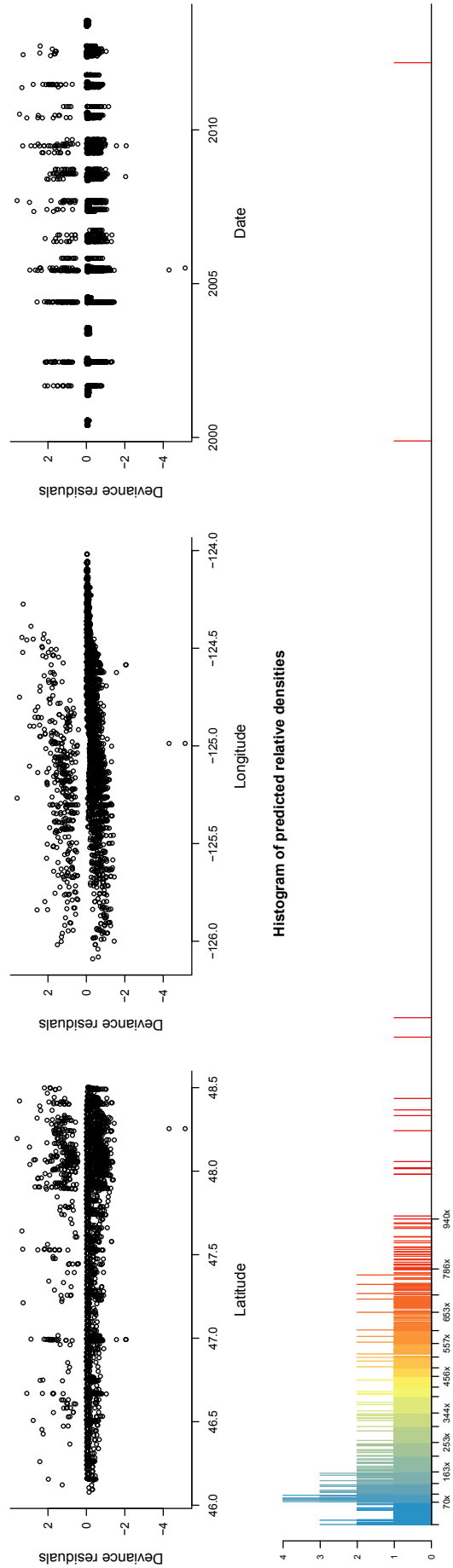
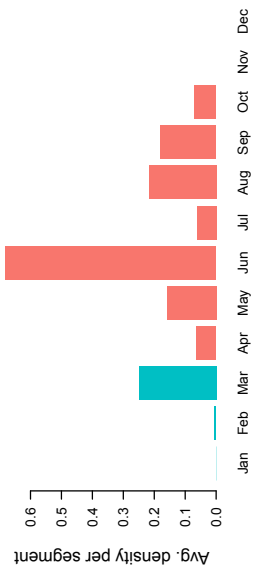


Figure D6. Marginal and residual plots for Common Murre (*Uria aalge*) during the months of November to March.

Black-footed Albatross (*Phoebastria nigripes*): April to October



*Figure D7. Marginal and residual plots for Black-footed Albatross (*Phoebastria nigripes*) during the months of April to October.*

Appendices

Black-footed Albatross (*Phoebastria nigripes*): November to March

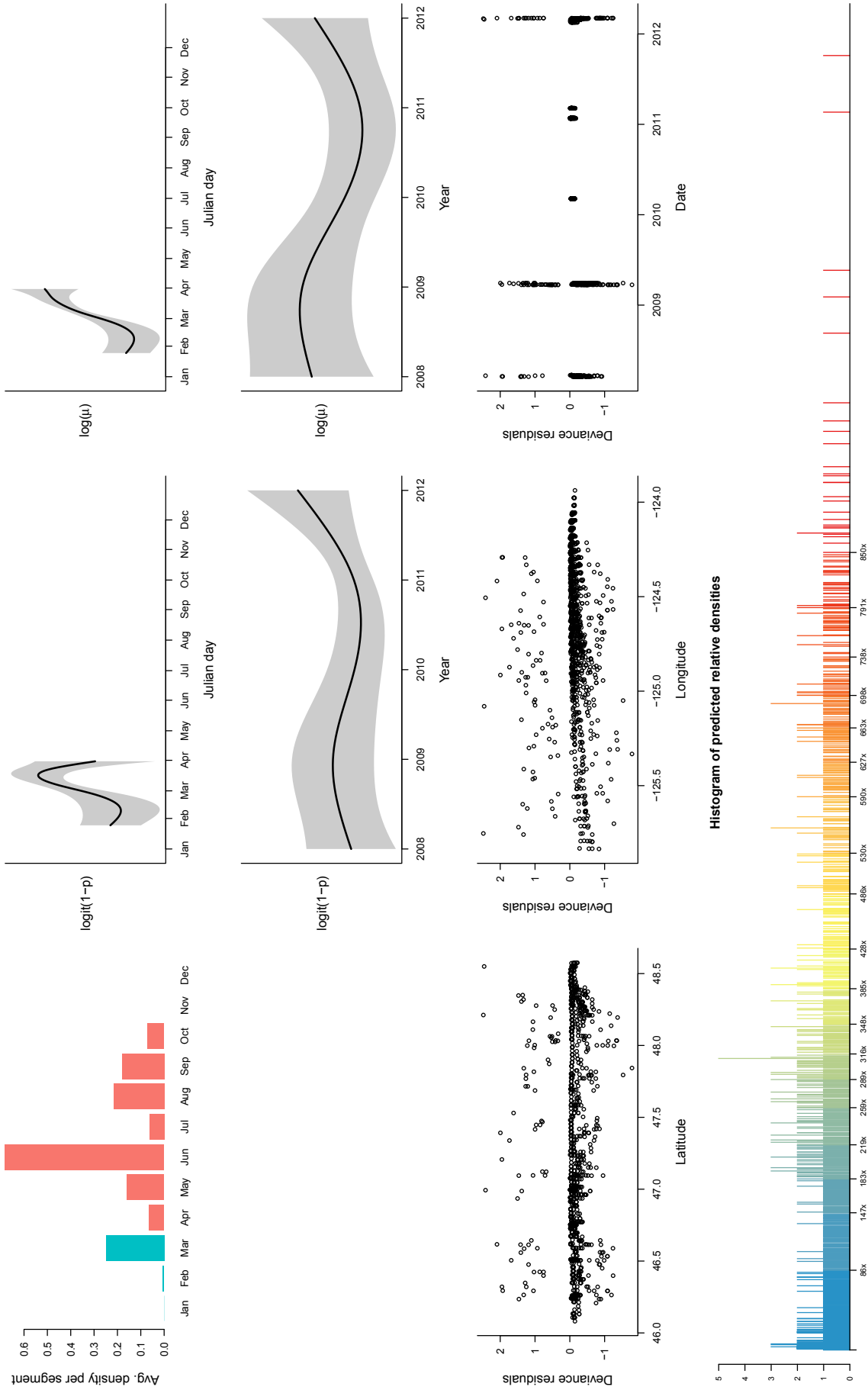


Figure D8. Marginal and residual plots for Black-footed Albatross (*Phoebastria nigripes*) during the months of November to March.

Northern Fulmar (Fulmarus glacialis): April to October

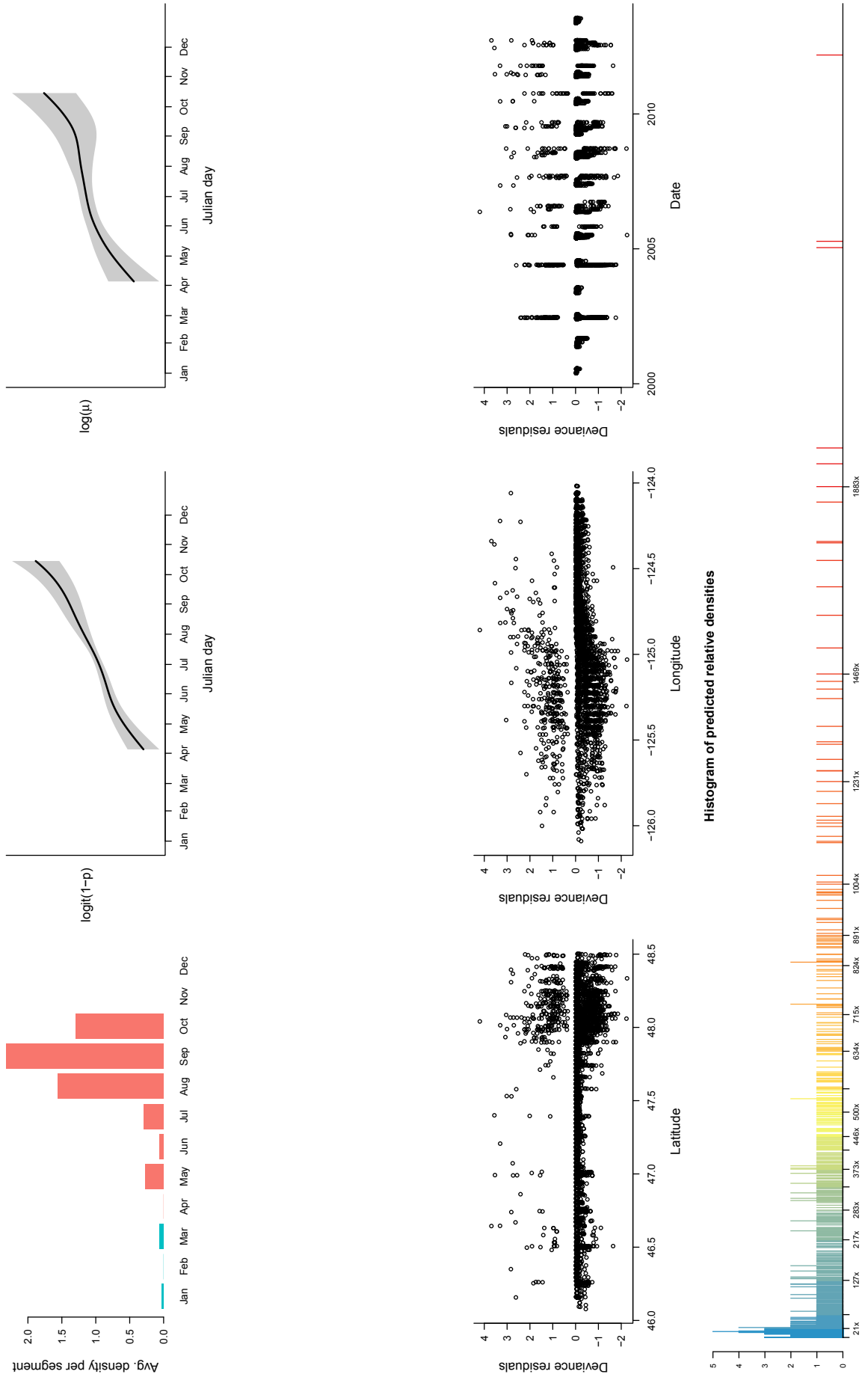
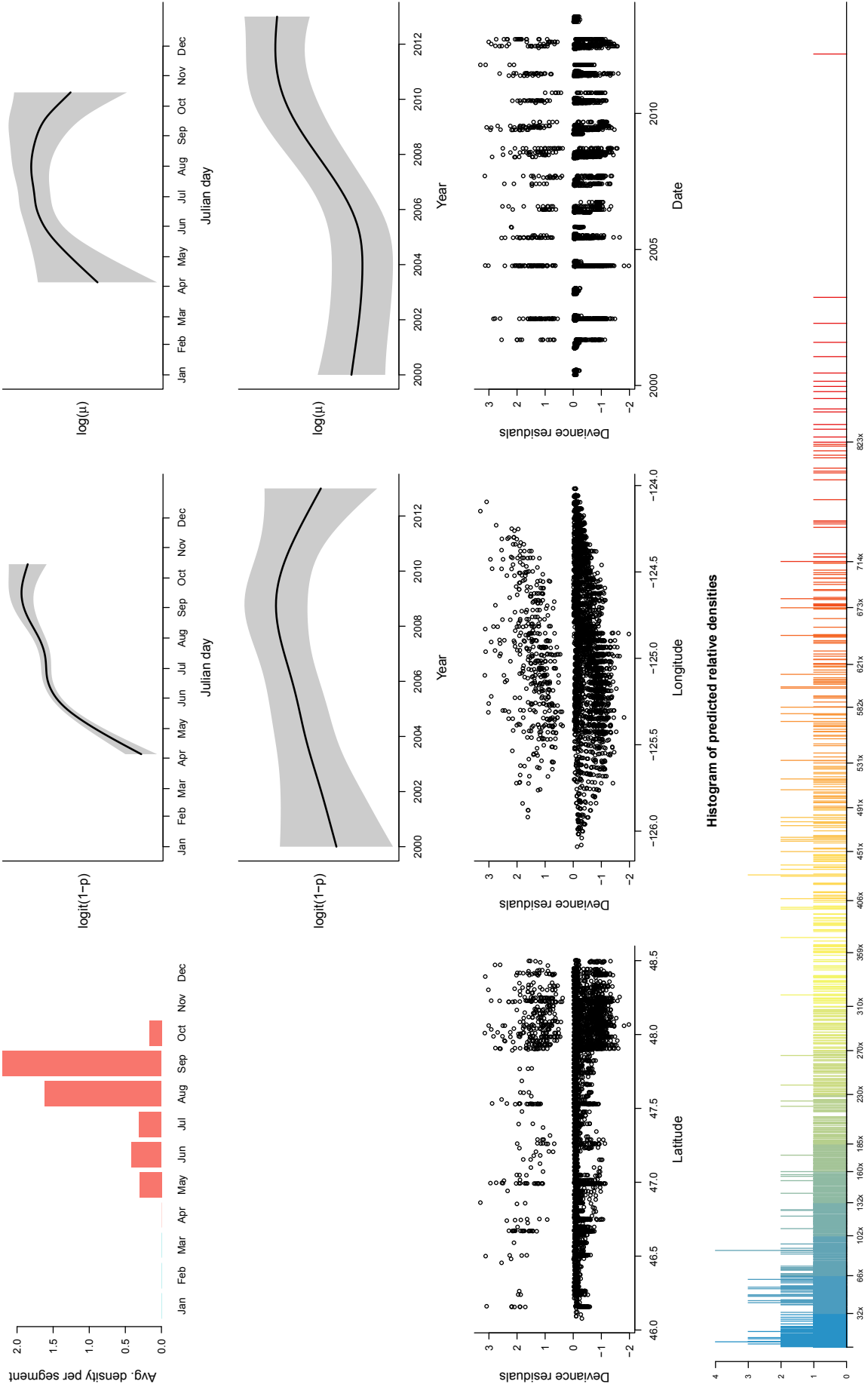


Figure D9. Marginal and residual plots for Northern Fulmar (*Fulmarus glacialis*) during the months of April to October.

Appendices

Pink-footed Shearwater (*Puffinus creatopus*): April to October



*Figure D10. Marginal and residual plots for Pink-footed Shearwater (*Puffinus creatopus*) during the months of April to October.*

Sooty Shearwater (*Puffinus griseus*): April to October

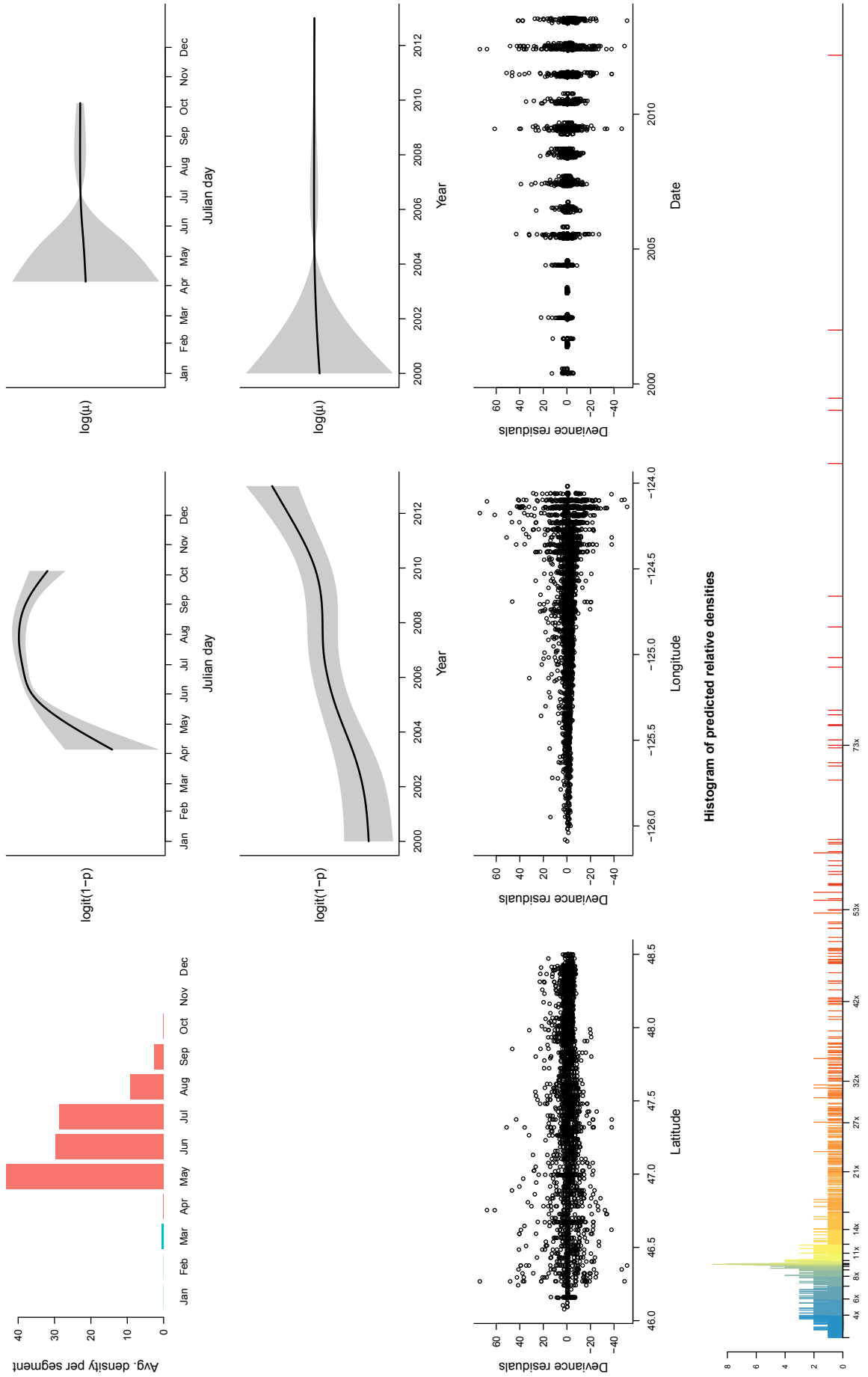


Figure D11. Marginal and residual plots for Sooty Shearwater (*Puffinus griseus*) during the months of April to October.

Steller sea lion (*Eumetopias jubatus*): April to October

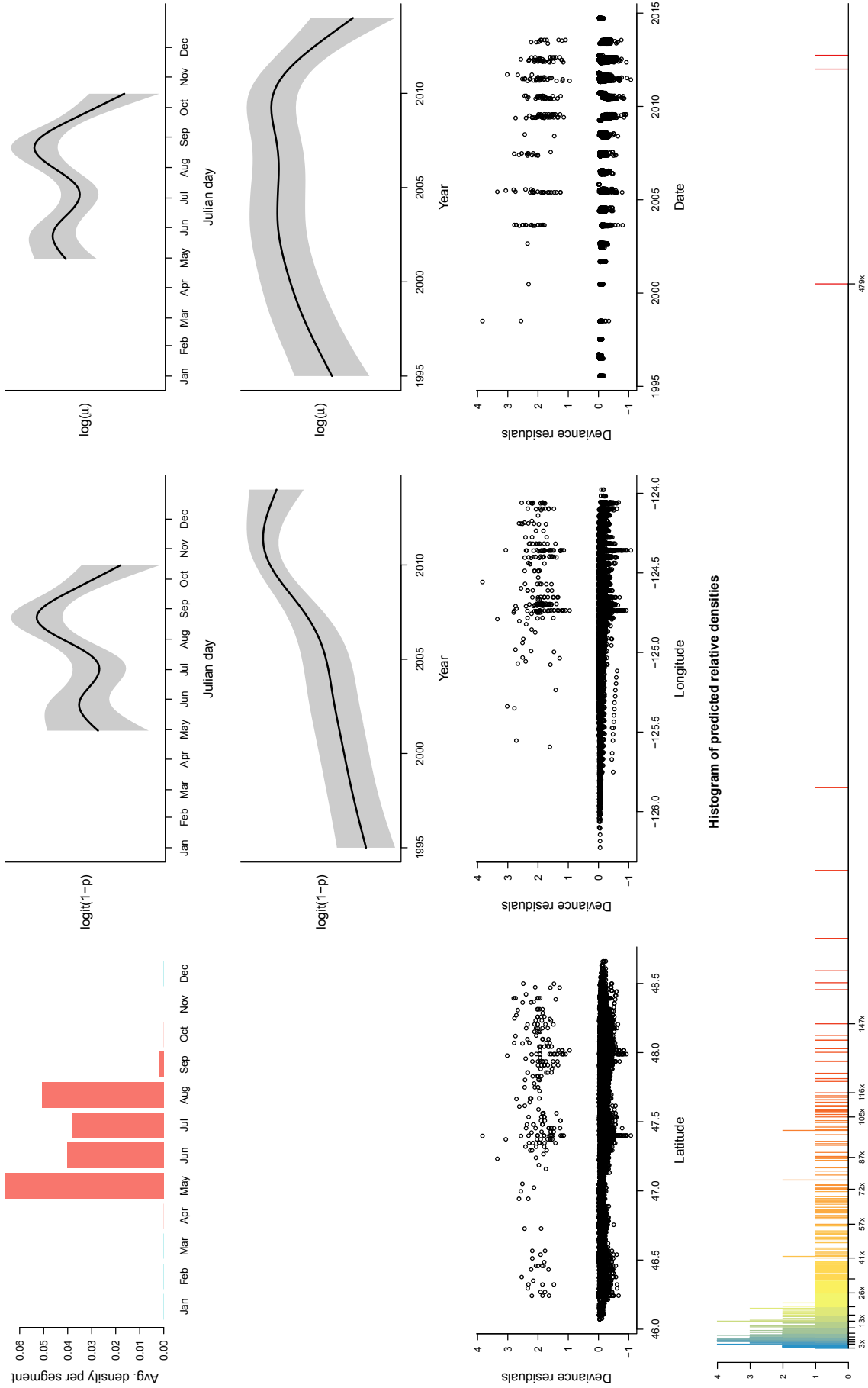


Figure D12. Marginal and residual plots for Steller sea lion (*Eumetopias jubatus*) during the months of April to October.

Harbor seal (*Phoca vitulina*): April to October

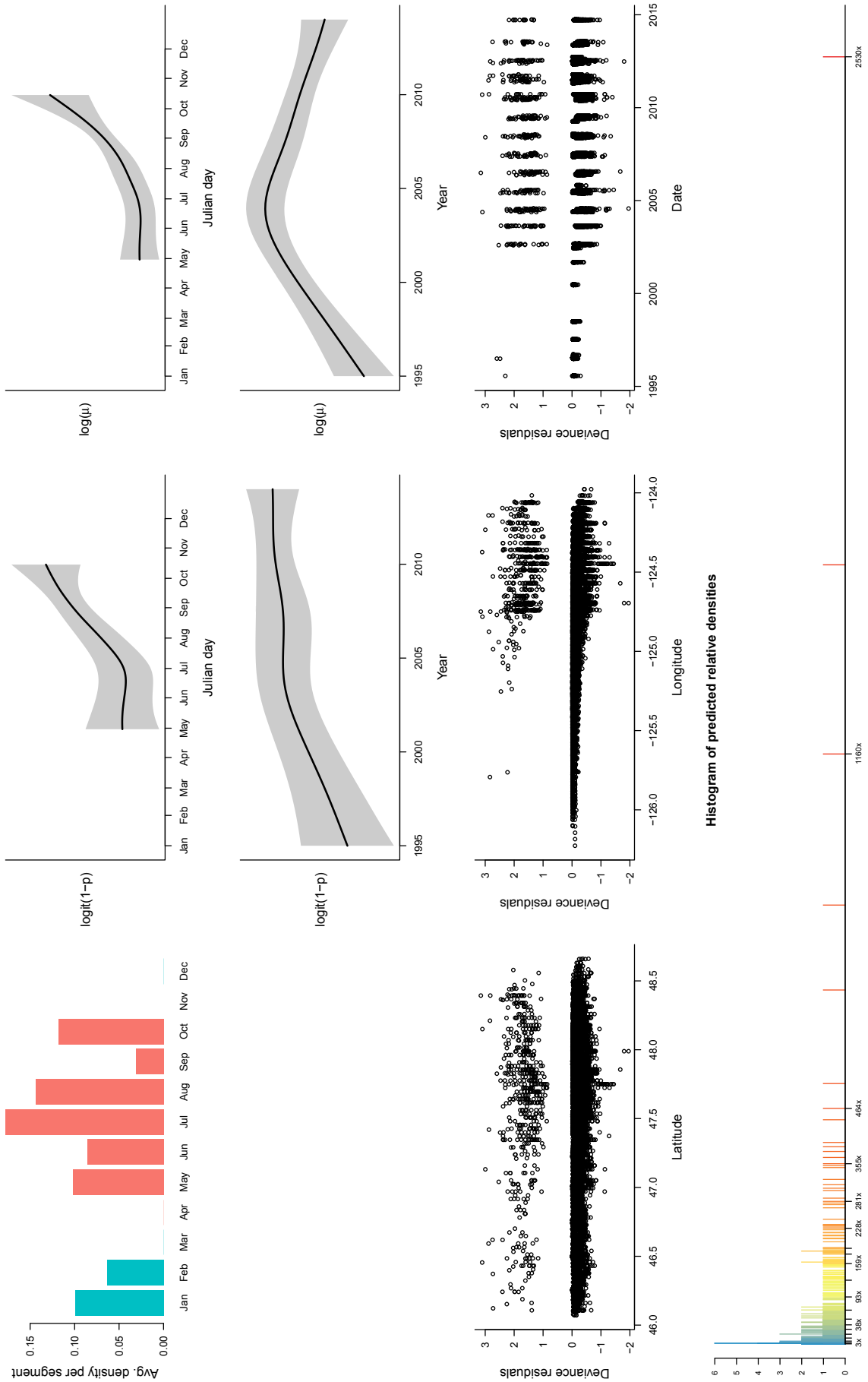


Figure D13. Marginal and residual plots for harbor seal (*Phoca vitulina*) during the months of April to October

Appendices

Humpback whale (*Megaptera novaeangliae*): April to October

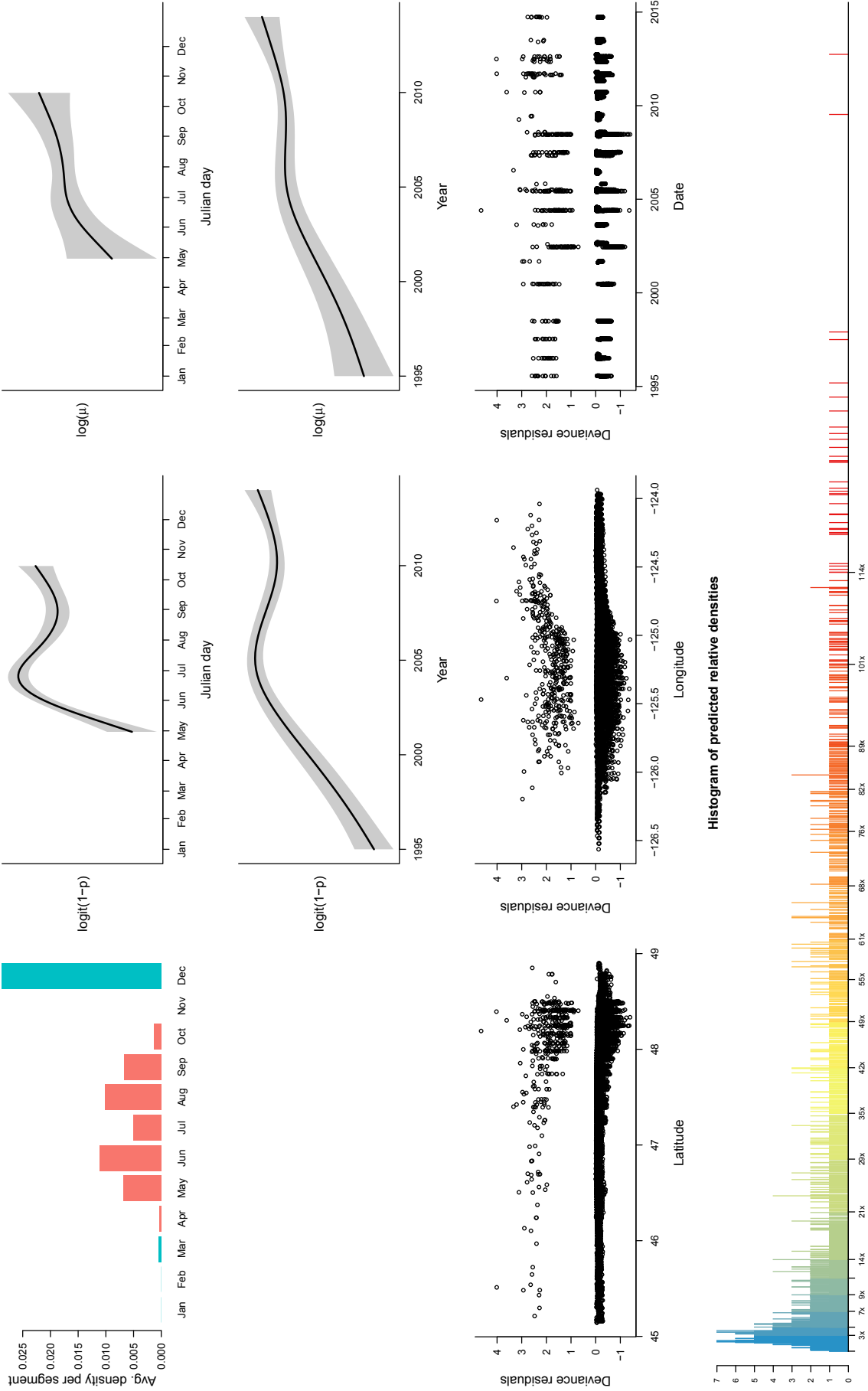


Figure D14. Marginal and residual plots for humpback whale (*Megaptera novaeangliae*) during the months of April to October.

Gray whale (*Eschrichtius robustus*): April to October

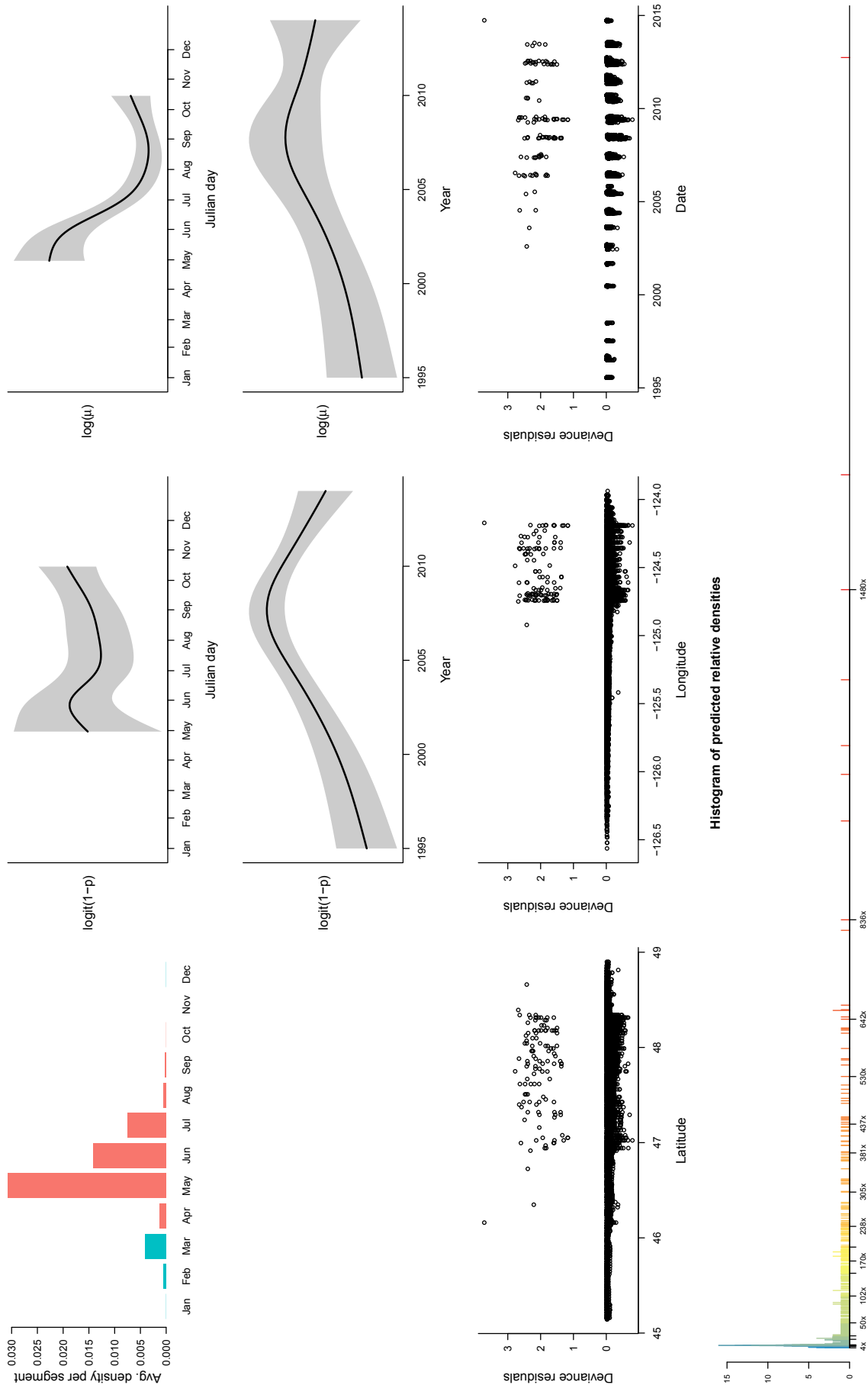


Figure D15. Marginal and residual plots for gray whale (*Eschrichtius robustus*) during the months of April to October.

Appendices

Harbor porpoise (*Phocoena phocoena*): April to October

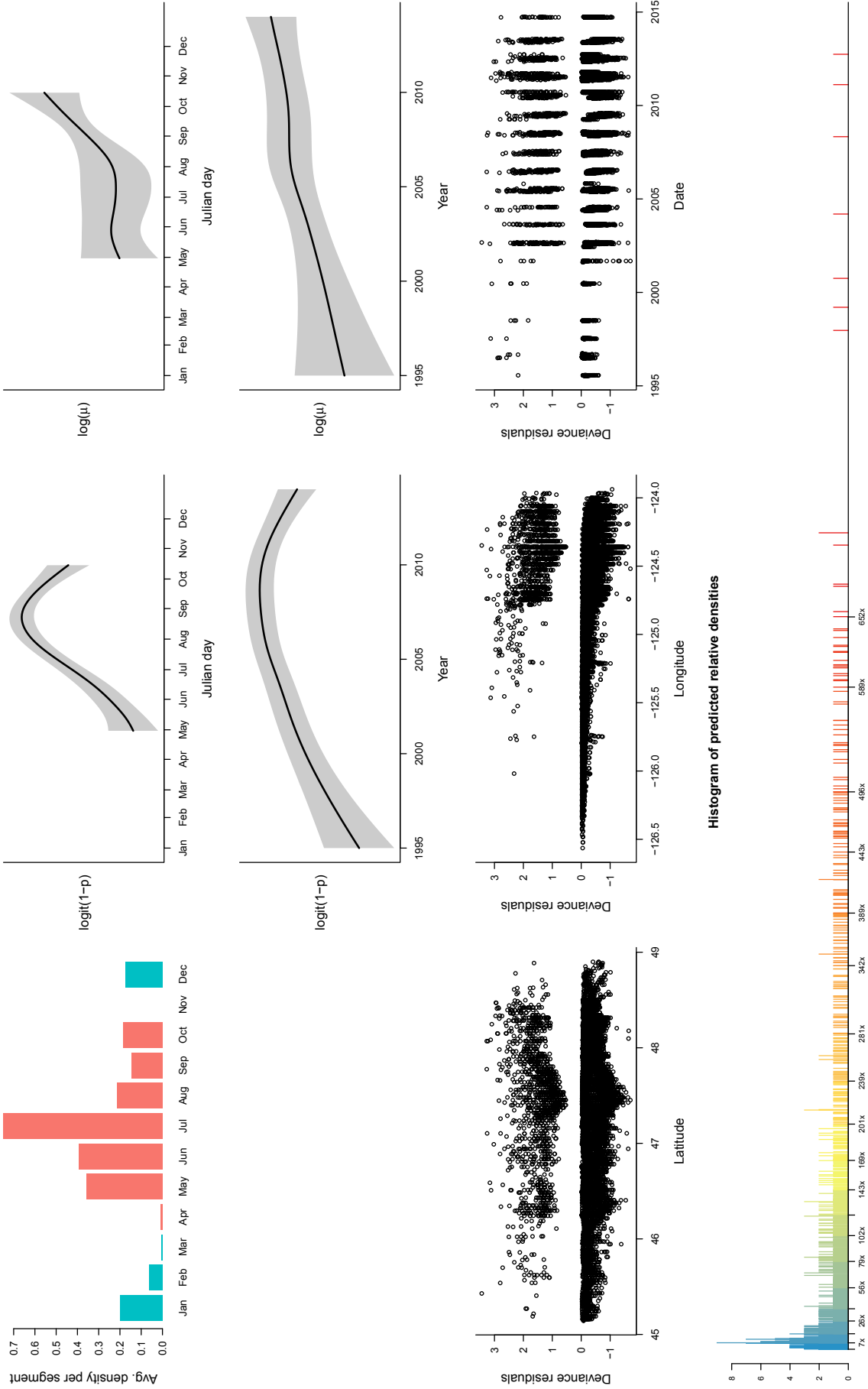


Figure D16. Marginal and residual plots for harbor porpoise (*Phocoena phocoena*) during the months of April to October.

Dall's porpoise (*Phocoenoides dalli*): April to October

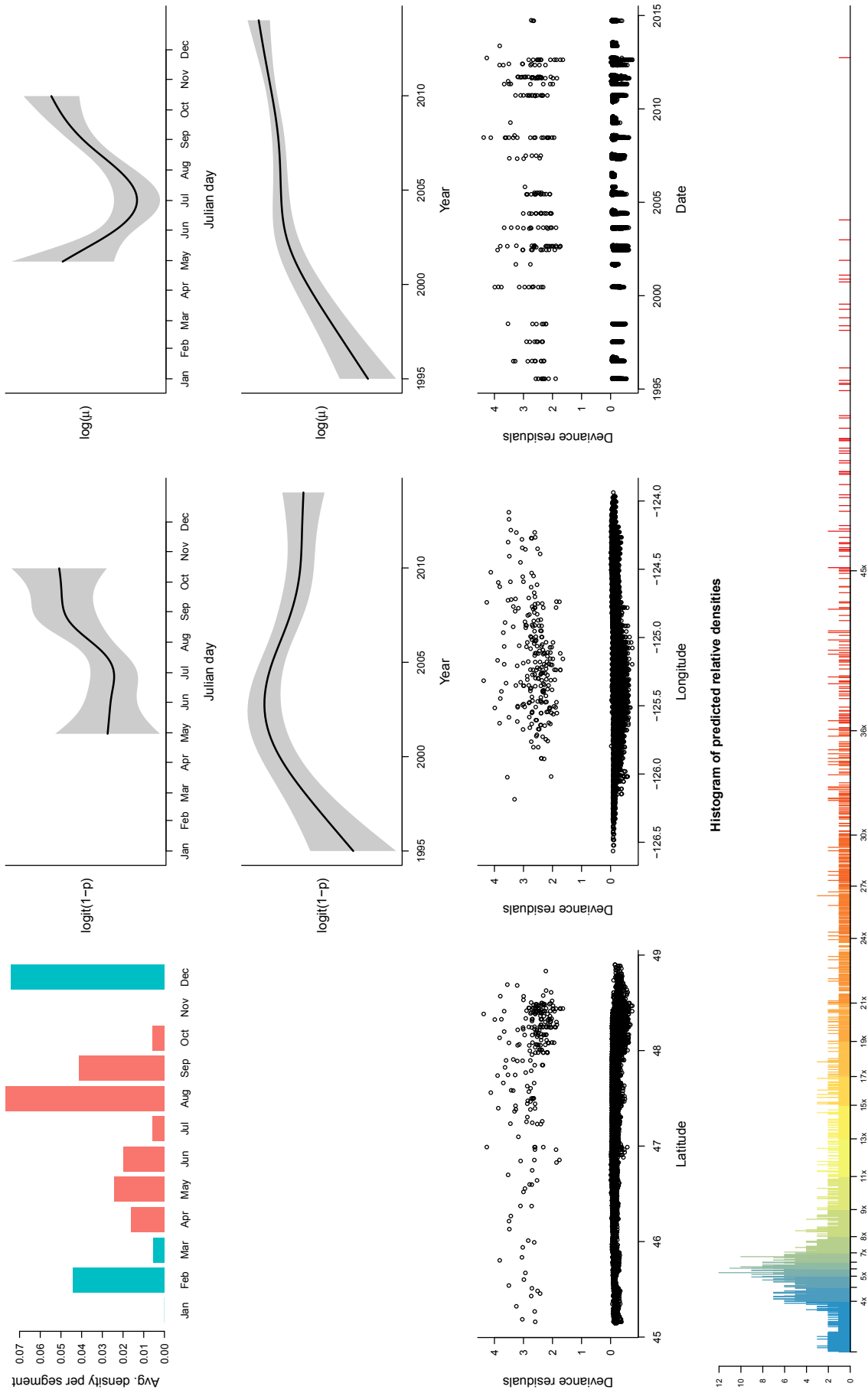


Figure D17. Marginal and residual plots for Dall's porpoise (*Phocoenoides dalli*) during the months of April to October.

Appendices

Appendix E: Variable Importance Figures

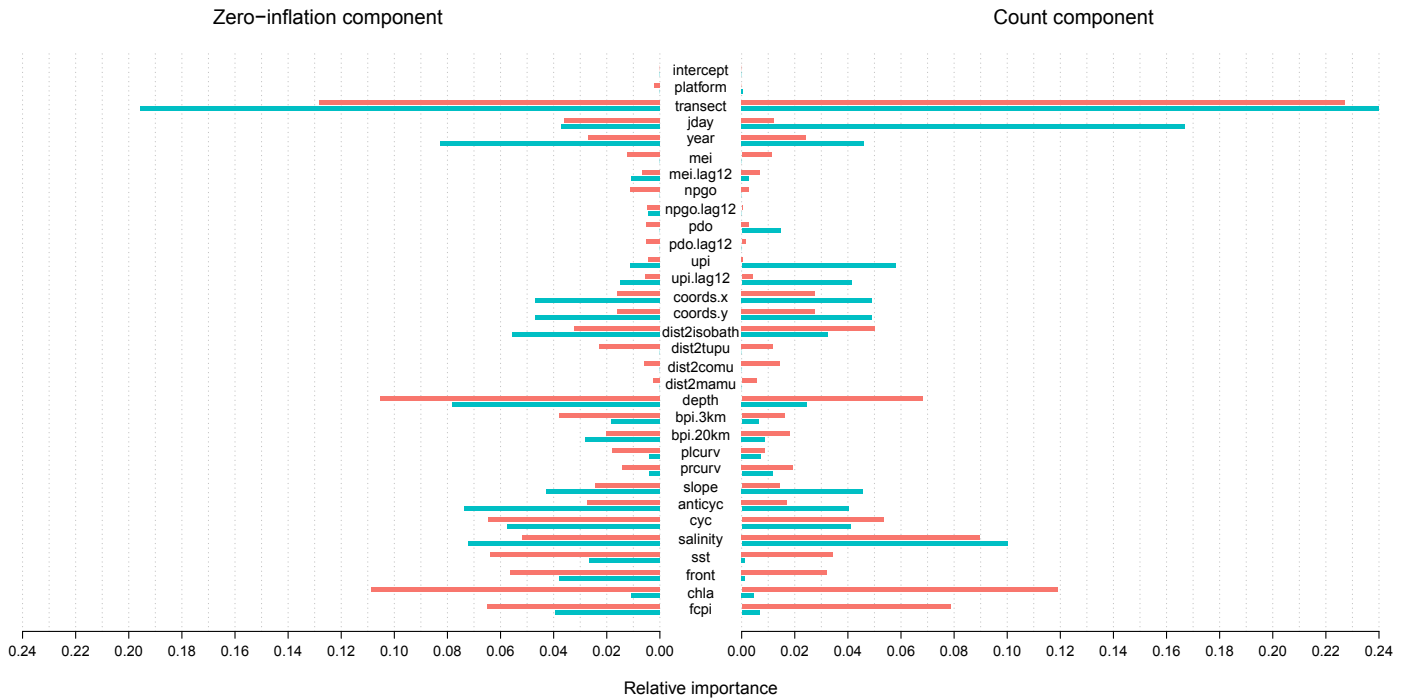


Figure E1. Mean relative importance of predictor variables for seabird species in the months of April to October (red) and November to March (cyan), calculated by averaging across species within the zero-inflation (p) and count (μ) components of the selected models.

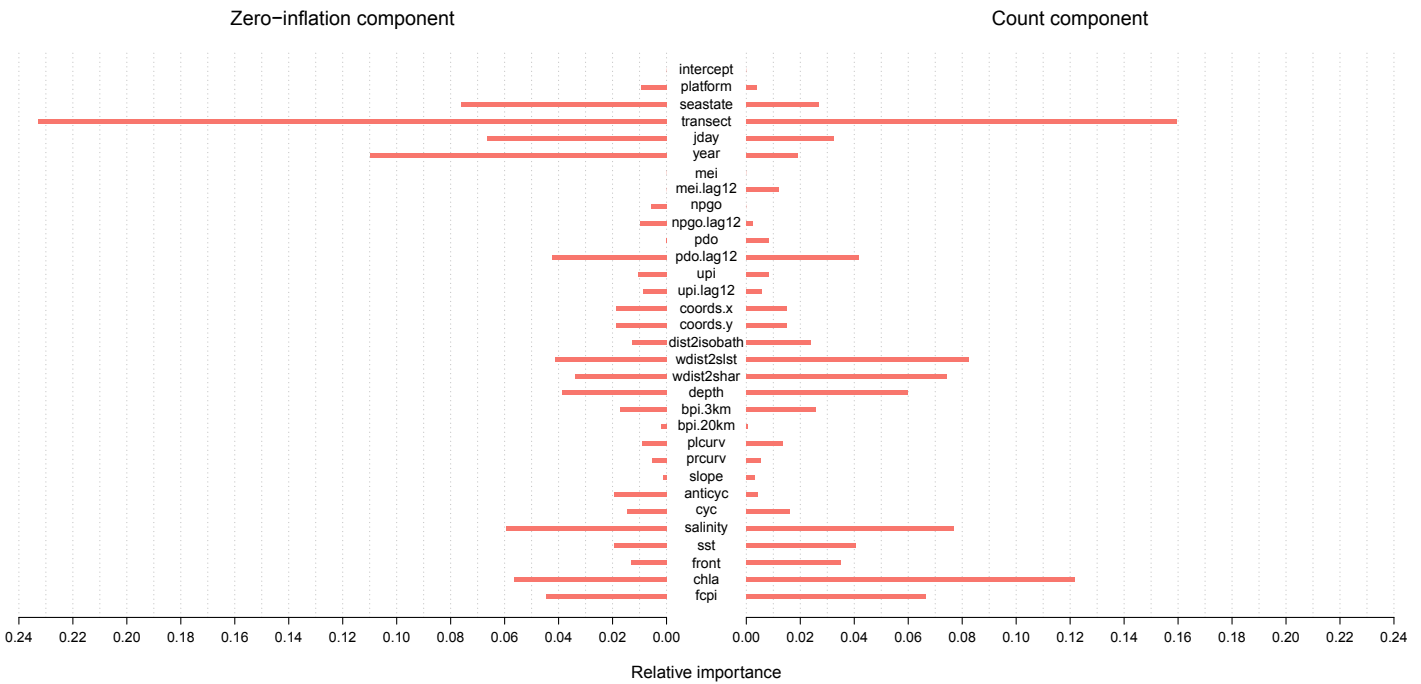


Figure E2. Mean relative importance of predictor variables for pinniped species in the months of April to October, calculated by averaging across species within the zero-inflation (p) and count (μ) components of the selected models.

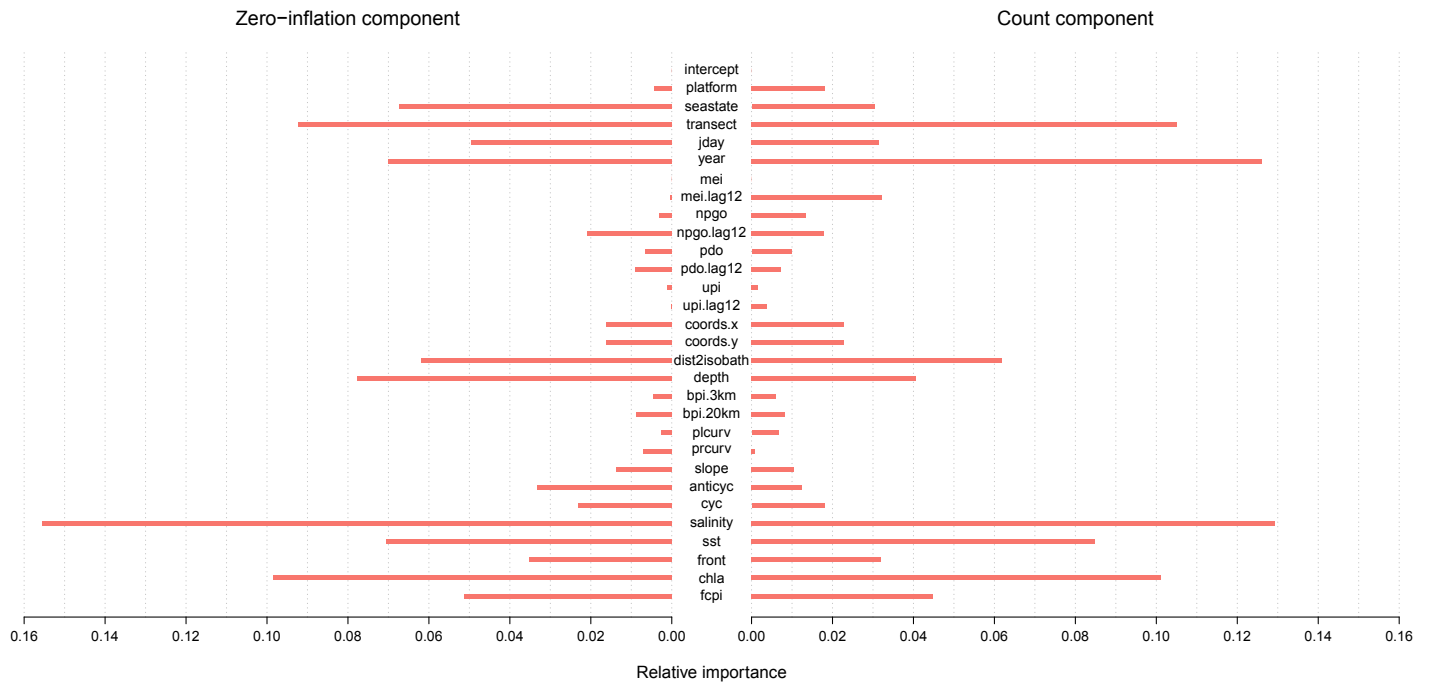


Figure E3. Mean relative importance of predictor variables for cetacean species in the months of April to October, calculated by averaging across species within the zero-inflation (p) and count (μ) components of the selected models.

Appendices

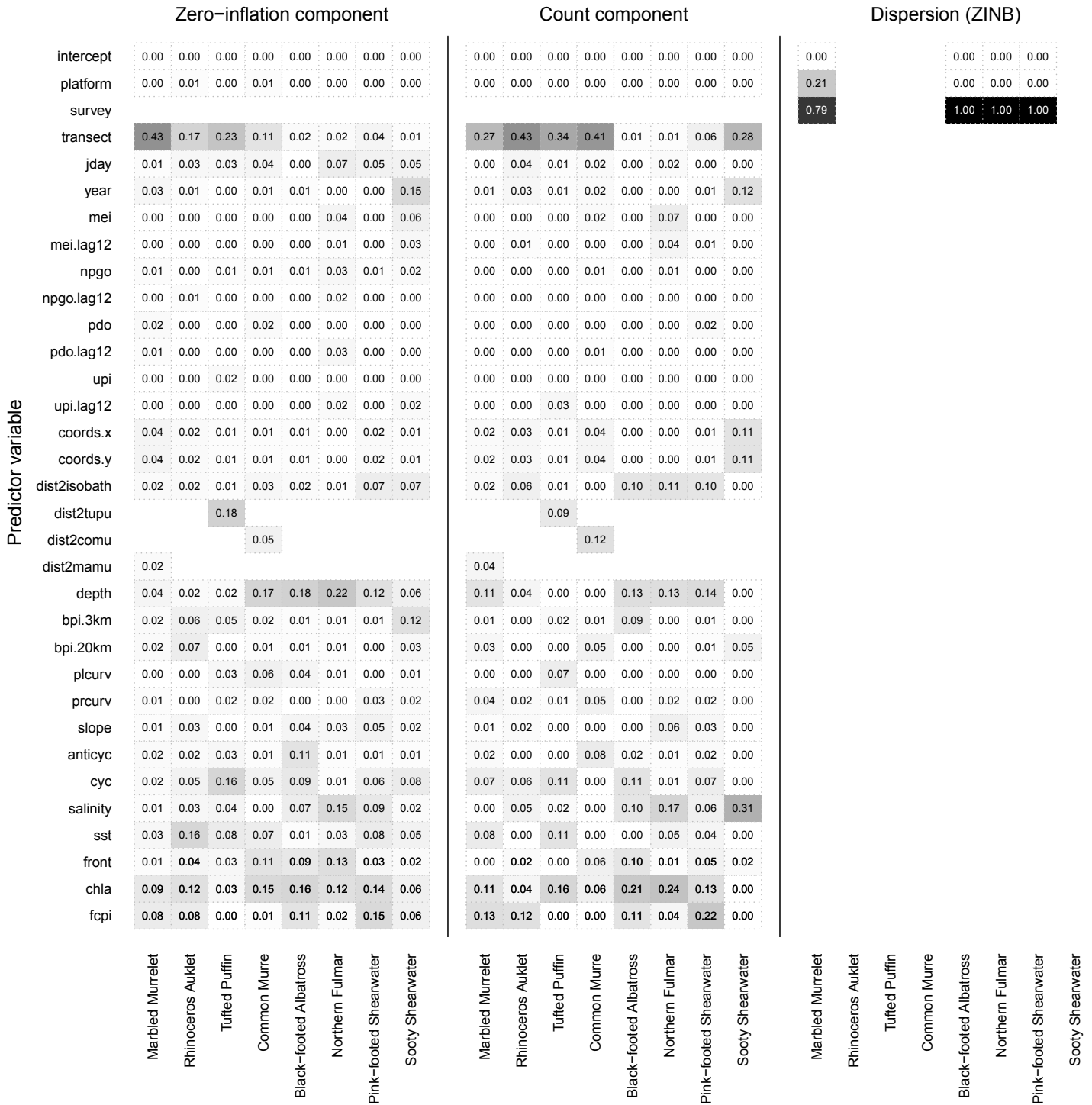


Figure E4. Relative importance of predictor variables for the selected model of each seabird species during the months of April to October. Empty cells represent predictors that were not modeled for a given species. When all cells of the dispersion (ZINB) model component are empty for a given species, the final fitted model assumed a zero-inflated Poisson distribution.

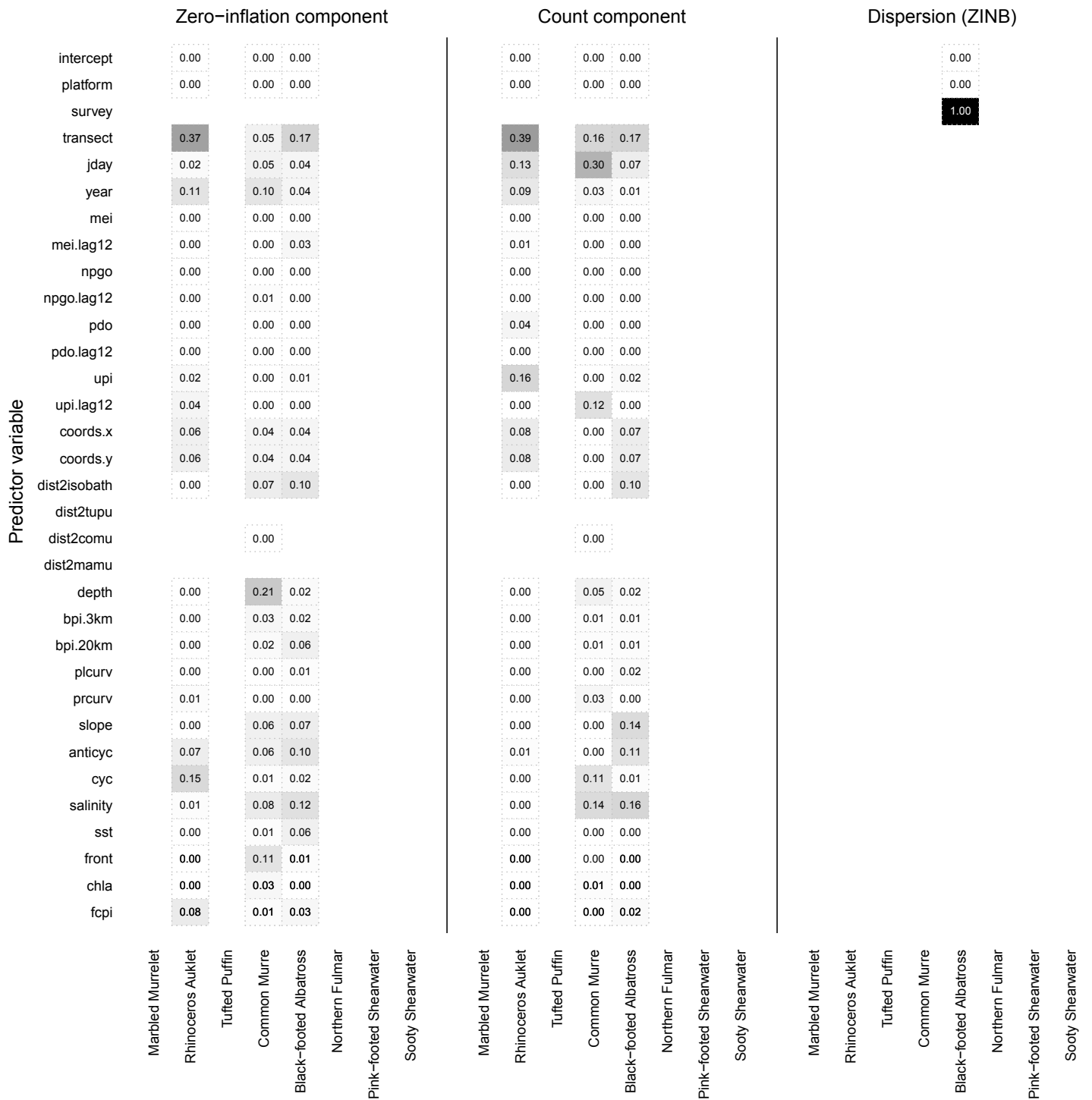


Figure E5. Relative importance of predictor variables for the selected model of each seabird species during the months of November to March. Empty cells represent predictors that were not modeled for a given species. When all cells of the dispersion (ZINB) model component are empty for a given species, the final fitted model assumed a zero-inflated Poisson distribution.

Appendices

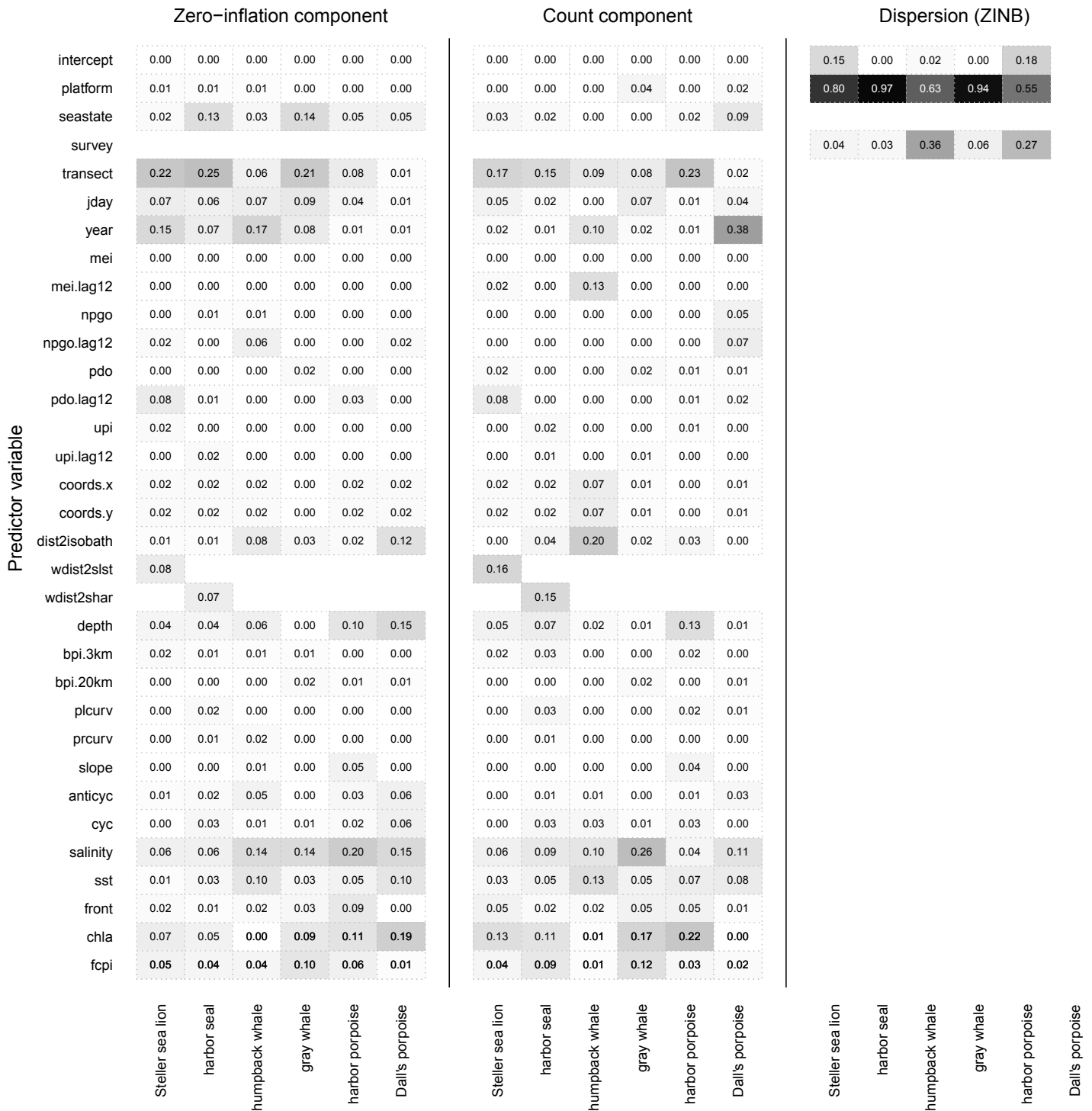


Figure E6. Relative importance of predictor variables for the selected model of each pinniped and cetacean species during the months of April to October. Empty cells represent predictors that were not modeled for a given species. When all cells of the dispersion (ZINB) model component are empty for a given species, the final fitted model assumed a zero-inflated Poisson distribution.



U.S. Department of Commerce

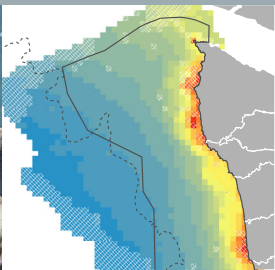
Penny Pritzker, *Secretary*

National Oceanic and Atmospheric Administration

Kathryn Sullivan, *Under Secretary for Oceans and Atmosphere*

National Ocean Service

Russell Callender, *Assistant Administrator for National Ocean Service*



The mission of the National Centers for Coastal Ocean Science is to provide managers with scientific information and tools needed to balance society's environmental, social and economic goals. For more information, visit: <http://www.coastalscience.noaa.gov/>.

